

University of Windsor

## Scholarship at UWindor

---

Electronic Theses and Dissertations

Theses, Dissertations, and Major Papers

---

2018

# Green and Low Cost Mechanochemical Synthesis of 3,3',5,5'-Azobenzene Tetracarboxylic Acid

Sarah Salloum  
*University of Windsor*

Follow this and additional works at: <https://scholar.uwindsor.ca/etd>

---

### Recommended Citation

Salloum, Sarah, "Green and Low Cost Mechanochemical Synthesis of 3,3',5,5'-Azobenzene Tetracarboxylic Acid" (2018). *Electronic Theses and Dissertations*. 7394.  
<https://scholar.uwindsor.ca/etd/7394>

This online database contains the full-text of PhD dissertations and Masters' theses of University of Windsor students from 1954 forward. These documents are made available for personal study and research purposes only, in accordance with the Canadian Copyright Act and the Creative Commons license—CC BY-NC-ND (Attribution, Non-Commercial, No Derivative Works). Under this license, works must always be attributed to the copyright holder (original author), cannot be used for any commercial purposes, and may not be altered. Any other use would require the permission of the copyright holder. Students may inquire about withdrawing their dissertation and/or thesis from this database. For additional inquiries, please contact the repository administrator via email ([scholarship@uwindsor.ca](mailto:scholarship@uwindsor.ca)) or by telephone at 519-253-3000ext. 3208.

# **Green and Low Cost Mechanochemical Synthesis of 3,3',5,5'-Azobenzene Tetracarboxylic Acid**

by  
Sarah Salloum

A Thesis  
Submitted to the Faculty of Graduate Studies  
Through the Department of Chemistry and Biochemistry  
in Partial Fulfillment of the Requirements for  
the Degree of Master of Science at the  
University of Windsor

Windsor, Ontario, Canada

© 2017 Sarah Salloum

***Green and Low Cost Mechanochemical Synthesis of 3,3',5,5'-Azobenzene  
Tetracarboxylic Acid***

by

Sarah Salloum

APPROVED BY:

---

A. Alpas  
Mechanical, Automotive & Materials Engineering

---

S. Loeb  
Department of Chemistry & Biochemistry

---

H. Eichhorn, Advisor  
Department of Chemistry & Biochemistry

October 16, 2017

# **DECLARATION OF ORIGINALITY**

I hereby certify that I am the sole author of this thesis and that no part of this thesis has been published or submitted for publication.

I certify that, to the best of my knowledge, my thesis does not infringe upon anyone's copyright nor violate any proprietary rights and that any ideas, techniques, quotations, or any other material from the work of other people included in my thesis, published or otherwise, are fully acknowledged in accordance with the standard referencing practices. Furthermore, to the extent that I have included copyrighted material that surpasses the bounds of fair dealing within the meaning of the Canada Copyright Act, I certify that I have obtained a written permission from the copyright owner(s) to include such material(s) in my thesis and have included copies of such copyright clearances to my appendix.

I declare that this is a true copy of my thesis, including any final revisions, as approved by my thesis committee and the Graduate Studies office, and that this thesis has not been submitted for a higher degree to any other University or Institution.

## ABSTRACT

Objective of this thesis is the development of a green, low cost, and scalable synthesis of 3,3',5,5'-azobenzene tetracarboxylic acid, which is the organic building block for PCN-250. PCN-250( $\text{Fe}_3$ ) is an important metal-organic framework that has excellent stability and gas adsorption properties and has been commercialized by Framergy, a start-up out of Texas A&M. All reported syntheses of 3,3',5,5'-azobenzene tetracarboxylic acid are based on a one-step reductive coupling of commercially available 5-nitroisophthalic acid in alkaline aqueous or alcoholic solutions with either zinc or D-glucose as reducing agent.

The first part of this thesis focuses on the optimization of the reported procedures in solution but the highest obtained yield of 45% remained well below the reported yields of 70%. In order to further reduce the amount of used solvent and potentially increase the yield, the reactions described above were subsequently conducted mechanochemically in a laboratory-scale ball milling unit. Optimization of the milling time, size and number of milling balls, amount and type of reducing agent, and solvent content improved the conversion to >70% but the formation of hydrazo and N-oxide side-products could not be avoided. Unexpectedly, these mixtures of compounds were advantageous in the formation of the azo product under specific workup conditions. When the crude mixture was directly immersed in alkaline solution for a period of 48 hours under atmospheric conditions, the unreacted starting material and aniline, hydrazo and N-oxide side-products convert to 3,3',5,5'-azobenzene tetracarboxylic acid, most likely by redox reactions between the side-products and with oxygen. These optimized conditions for the ball milling process and workup protocol furnish the desired 3,3',5,5'-azobenzene tetracarboxylic acid in 90% yield and >95% purity by using a green solvent assisted ball milling method and crystallization from aqueous solution as the sole purification step.

## ACKNOWLEDGEMENTS

I am beyond excited that after two full years of my master's program, I am finally writing my acknowledgments page! Thank you to all the people who had helped me along this long journey of hard work and fruitful accomplishments.

Most importantly, I would like to thank my advisor, Dr. Holger Eichhorn, for all his guidance and help throughout my years of research and university studies. His leadership, patience and understanding mean a lot to me. *Thank you!*

I would like to thank Dr. Matt Revington for his patience and help with the NMR experiments. I also send great thanks to Janeen Auld for taking the time to run MS experiments for my compounds. Thanks to Manar Shoshani for performing single crystal measurements. I would like to thank Marlene Bezaire for her warm heart and care for students, as well as for her help in arranging my defense. I am also grateful to our former and current members of the Eichhorn group. I would like to thank undergraduate students, Nadia Albano and Ezzat Makawi, for their contribution and effort in the making of this project. Sincere thanks to Sarah Youssef for her continuous support, and to the rest of my friends and colleagues at the University of Windsor.

At last but not least, the special thanks are due to my wonderful family for their continuous support and care. I don't think I would have been able to continue without my parents' blessings and their encouragement to keep moving forward. I would like to thank my beautiful sisters, Carmen and Lamis, as well as my dear brothers, Daniel and Adam. To my husband, Dr. Mohamed Siblani, a deep thank you for your extreme love and support. I wish for all the happiness and success in our new marriage life.

Despite the successes and challenges, I am truly thankful to God for surrounding me with amazing people and giving me the opportunities for a great learning and research experience.

# TABLE OF CONTENTS

Declaration of Originality	iii
Abstract	iv
Acknowledgments	v
List of Figures	ix
List of Tables	xi
List of Schemes	xii
List of Abbreviations	xiii

## Chapter 1: Introduction

1.1	Properties and Applications of Aromatic Azo Compounds	1
1.2	Methods for the Synthesis of Azobenzenes	2
1.2.1	Azo Coupling Reaction	2
1.2.2	Mills Reaction	3
1.2.3	Oxidation of Anilines	4
1.2.4	Reductive Coupling of Aromatic Nitro Compounds	6
1.2.5	Limitations of Current Methodologies	7
1.3	Mechanochemistry	8
1.4	Solvent-Free Redox Synthesis of Azobenzenes	9
1.5	Reaction Parameters for Ball Milling	12
1.6	Technological Parameters	13
1.6.1	Milling Material	13
1.6.2	Size of Milling Balls	14
1.6.3	Number of Milling Balls	15
1.7	Chemical Parameters	15

1.8	Process Parameters.....	16
1.8.1	Operating Frequency .....	16
1.8.2	Milling Time .....	18
1.9	Background and Scope of Thesis.....	19
1.9.1	Azobenzene Tetracarboxylic Acid: Organic Building Block for PCN-250.....	19
1.9.2	Scope of Thesis .....	20

## Chapter 2: Results and Discussion

2.1	Product Characterization.....	21
2.1.1	Compound <b>3</b> (3,3',5,5'-Azobenzene Tetracarboxylic Acid).....	21
2.1.2	Compound <b>2</b> (3,3',5,5'-Azoxybenzene Tetracarboxylic Acid).....	23
2.1.3	Compound <b>4</b> (3,3',5,5'-Hydrazobenzene Tetracarboxylic Acid).....	24
2.2	Solution-Based Synthesis of 3,3',5,5'-Azobenzene Tetracarboxylic Acid.....	27
2.3	Ball Mill Synthesis of 3,3',5,5'-Azobenzene Tetracarboxylic Acid.....	31
2.4	Optimization of Technological Parameters.....	33
2.4.1	Optimization of Size and Number of Milling Balls .....	33
2.5	Optimization of Process Parameters .....	36
2.5.1	Optimization of Milling Time .....	36
2.6	Optimization of Chemical Parameters .....	40
2.6.1	Optimization of the Amount of Zinc Reducing Agent.....	40
2.6.2	Influence of Wet and Dry Milling Conditions .....	42
2.6.3	Optimization of Type of Reducing Agent.....	43
2.7	Optimization of Workup of Mechanochemical Synthesis of 3,3',5,5'- Azobenzene Tetracarboxylic Acid .....	47
2.8	Is Ball Milling a Better Method for the Synthesis of Azo Compounds? .....	53
2.8.1	Advantages of Ball Mill Chemistry .....	54
2.8.2	Disadvantages of Ball Mill Chemistry .....	55



2.9	Summary and Conclusions.....	56
2.10	Future Work.....	57
<b>Chapter 3: Experimental</b>		
3.1	General Information.....	59
3.2	General Procedures .....	61
3.2.1	Batch Synthesis of compound <b>3</b> with Zinc as Reducing Agent .....	61
3.2.2	Batch Synthesis of compound <b>2</b> with Zinc as Reducing Agent .....	61
3.2.3	Batch Synthesis of compound <b>3</b> with Glucose as Reducing Agent.....	62
3.2.4	General Procedure for the Reduction of 5-nitroisophthlic acid using Zinc under Milling Conditions .....	62
3.2.5	General Procedure for the Reduction of 5-nitroisophthlic acid using Glucose under Milling Conditions .....	63
3.2.6	General Procedure for the Reduction of 5-nitroisophthlic acid using Magnesium under Milling Conditions .....	64
3.2.7	Final Optimized Synthesis of 3,3',5,5'-Azobenzene Tetracarboxylic Acid using Zinc under Milling Conditions .....	64
3.3	Product Characterization and Spectral Data .....	65
<b>REFERENCES</b>		82
<b>APPENDIX</b>		87
<b>VITA AUCTORIS</b>		91

# LIST OF FIGURES

<b>Figure 1:</b> Schematic representation of the milling beaker trajectory on a mixer ball mill.....	17
<b>Figure 2:</b> The structure of PCN-250 .....	20
<b>Figure 3:</b> Molecular structure of 3,3',5,5'-azobenzene tetracarboxylic acid product. ....	20
<b>Figure 4:</b> Photoisomerization process of 3,3',5,5'-azobenzene tetracarboxylic acid. ....	23
<b>Figure 5:</b> UV-Vis absorption spectra of compounds <b>1</b> , <b>2</b> and <b>3</b> in ethanol.....	24
<b>Figure 6:</b> <sup>1</sup> H-NMR spectra for experimental <b>4</b> and commercial 5-aminoisophthalic acid.....	24
<b>Figure 7:</b> <sup>15</sup> N- <sup>1</sup> H HSQC experimental spectra of <b>4</b> . ....	25
<b>Figure 8:</b> Variation with pH of half-peak potentials of azo, azoxy, and hydrazoarenes.....	30
<b>Figure 9:</b> Correlation of the combined yield with the size and number of milling balls. ....	35
<b>Figure 10:</b> Influence of milling time on the product yield and product composition .....	37
<b>Figure 11:</b> Influence of milling time on the product yield and product composition .....	39
<b>Figure 12:</b> Workup procedure for reversible oxidation-reduction process. ....	49
<b>Figure 13:</b> Changes in the UV-Vis absorption spectra for the conversion of <b>4</b> to <b>3</b> . ....	50
<b>Figure 14:</b> Schematic representation and comparison of the synthetic methodologies.. ....	53
<b>Figure 15:</b> <sup>1</sup> H NMR of <b>3</b> recrystallized from DMF (DMSO-d <sub>6</sub> , 300 MHz).....	66
<b>Figure 16:</b> <sup>13</sup> C NMR <b>3</b> recrystallized from DMF (DMSO-d <sub>6</sub> , 300 MHz).....	67
<b>Figure 17:</b> Negative mode MALDI-MS of <b>3</b> . ....	68
<b>Figure 18:</b> UV-Vis absorption spectra of compound <b>3</b> .....	68
<b>Figure 19:</b> IR spectra of <b>3</b> and <b>2</b> .....	69
<b>Figure 20:</b> Single crystal structure of <b>3</b> in trans configuration. ....	69
<b>Figure 21:</b> <sup>1</sup> H NMR of <b>2</b> recrystallized from DMF (DMSO-d <sub>6</sub> , 300 MHz).....	70
<b>Figure 22:</b> <sup>13</sup> C NMR <b>2</b> recrystallized from DMF (DMSO-d <sub>6</sub> , 300 MHz).....	71
<b>Figure 23:</b> UV-Vis absorption spectra of compound <b>2</b> in ethanol. ....	71
<b>Figure 24:</b> <sup>1</sup> H NMR of <b>4</b> and <b>3</b> mixture (DMSO-d <sub>6</sub> , 300 MHz) .....	72

<b>Figure 25:</b> $^{13}\text{C}$ NMR of <b>4</b> and <b>3</b> mixture (DMSO- $d_6$ , 300 MHz) .....	73
<b>Figure 26:</b> UV-Vis absorption spectra of compound <b>4</b> in ethanol .....	73
<b>Figure 27:</b> $^1\text{H}$ DOSY NMR of <b>4</b> and <b>3</b> mixture (MeOD- $d_4$ , 500 MHz).....	74
<b>Figure 28:</b> 2D $^1\text{H}$ - $^1\text{H}$ COSY NMR of <b>4</b> and <b>3</b> mixture (DMSO- $d_6$ , 300 MHz).....	75
<b>Figure 29:</b> $^1\text{H}$ - $^1\text{H}$ NOESY NMR of <b>4</b> and <b>3</b> mixture (DMSO- $d_6$ , 300 MHz).....	76
<b>Figure 30:</b> 1D $^{15}\text{N}$ - $^1\text{H}$ HSQC NMR of <b>4</b> (DMSO- $d_6$ , 300 MHz). .....	77
<b>Figure 31:</b> $^1\text{H}$ NMR of commercial 5-aminoisophthalic acid (DMSO- $d_6$ , 300 MHz). .....	78
<b>Figure 32:</b> $^{13}\text{C}$ NMR of commercial 5-aminoisophthalic acid (DMSO- $d_6$ , 300 MHz). .....	79
<b>Figure 33:</b> $^1\text{H}$ DOSY NMR of 5-aminoisophthalic acid (MeOD- $d_4$ , 500 MHz).....	80
<b>Figure 34:</b> $^1\text{H}$ NMR of commercial 5-nitroisophthalic acid (DMSO- $d_6$ , 300 MHz).....	81

## LIST OF TABLES

<b>Table 1</b> Highest yielding conditions for batch reduction of 5-nitroisophthalic acid .....	27
<b>Table 2</b> Zinc-mediated mechanochemical reduction under single ball milling mode. ....	33
<b>Table 3</b> Zinc-mediated mechanochemical reduction under two-balls milling mode .....	34
<b>Table 4</b> Mechanochemical reduction of 5-nitroisophthalic acid with respect to milling time .....	36
<b>Table 5</b> Mechanochemical reduction of 5-nitroisophthalic acid with various amounts of zinc.....	40
<b>Table 6</b> Mechanochemical reduction of 5-nitroisophthalic acid under dry and wet conditions .....	42
<b>Table 7</b> Standard reduction potentials of selected reducing agents under basic conditions. ....	44
<b>Table 8</b> Mechanochemical reduction of 5-nitroisophthalic acid with different reducing agents .....	44
<b>Table 9</b> Optimization of reaction parameters under for mechanochemical synthesis of azobenzene.....	47

# LIST OF SCHEMES

<b>Scheme 1:</b> Reversible photoisomerization of azobenzenes upon UV-Vis irradiation. ....	1
<b>Scheme 2:</b> Azo coupling reaction for synthesis of asymmetrical azo derivatives.....	2
<b>Scheme 3:</b> Mechanistic scheme for coupling of primary arylamine and nitroso compounds.....	3
<b>Scheme 4:</b> Generation of the nitroso precursor and subsequent formation of the azo product.....	4
<b>Scheme 5:</b> Electrolytic oxidation of aniline with Pt electrode in DMF .....	4
<b>Scheme 6:</b> Oxidation of anilines with 2 equivalents of HgO and I <sub>2</sub> in CH <sub>2</sub> Cl <sub>2</sub> .....	5
<b>Scheme 7:</b> Mechanistic scheme of the radical-mediated dimerization of anilines.....	5
<b>Scheme 8:</b> Catalytic oxidation of aniline with Au/TiO <sub>2</sub> under dioxygen atmosphere.....	6
<b>Scheme 9:</b> Plausible reaction pathway for the reduction of aromatic nitro compounds.....	7
<b>Scheme 10:</b> Chemoselective oxidative coupling of anilines under solvent-free conditions.....	10
<b>Scheme 11:</b> Solvent-free reduction of nitroarenes to azoxy and azoarenes using bismuth shots.....	10
<b>Scheme 12:</b> Proposed pathway for the deoxygenative dimerization of nitroarenes on bismuth.....	11
<b>Scheme 13:</b> AuNP-catalyzed reduction of nitrobenzene under ball milling conditions.....	12
<b>Scheme 14:</b> Generic reaction scheme for ball mill assisted synthesis.....	12
<b>Scheme 15:</b> Synthesis of compounds <b>2</b> , <b>3</b> , <b>4</b> , and <b>5</b> by reduction of 5-nitroisophthalic acid ( <b>1</b> ).....	21
<b>Scheme 16:</b> Proposed redox reaction between azoxybenzene and hydrazobenzene.....	51
<b>Scheme 17:</b> Reductive coupling of 5-nitroisophthalic acid under ball milling conditions.....	65

## LIST OF ABBREVIATIONS

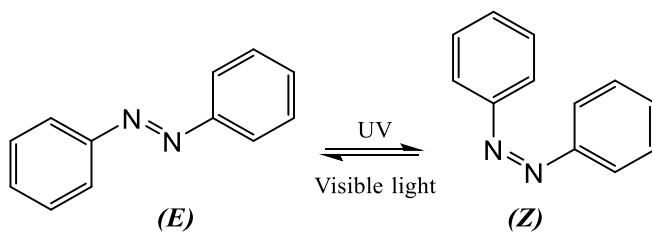
2D	two dimensional
ASAP	atmospheric solids analysis probe
b	broad
COSY	correlation spectroscopy
DCM	dichloromethane
DMSO-d <sub>6</sub>	deuterated dimethylsulfoxide
DMF	dimethylformamide
DOSY	diffusion ordered spectroscopy
DSC	differential scanning calorimetry
EI-MS	electron ionization mass spectrometry
EtOH	ethanol
h	hours
HSQC	hetero-nuclear single quantum coherence spectroscopy
Hz	Hertz
I	moment of inertia
IR	infrared spectroscopy
K	Kelvin
m	multiplet
MALDI	matrix assisted laser desorption ionization
MeOH	methanol
mL	milliliters

mmol	millimoles
MS	mass spectrometry
NMR	nuclear magnetic resonance
NOESY	nuclear Overhauser effect spectroscopy
$\rho$	density
ppm	parts per million
s	singlet
SHE	standard hydrogen electrode
t	triplet
T	temperature
TLC	thin layer chromatography
UV-Vis	visible and ultraviolet spectroscopy
$\nu$	frequency
$\omega$	angular velocity
XRD	X-ray diffraction

# Chapter 1: Introduction

## 1.1 Properties and Applications of Aromatic Azo Compounds

Aromatic azo compounds are typically highly colored molecules composed of two aromatic systems that are linked by an azo group (-N=N-). The term “azobenzene” refers to a wide class of molecules with two phenyl groups linked by an azo group as a core structure. Based on their functionality, azobenzene compounds display unique properties for important applications and are key materials in many areas of science and industry. Azobenzene derivatives are mainly employed as central building blocks in the production of dyes and chemical indicators.<sup>1,2,3</sup> Particularly, azo dyes are used as colorants for digital printing, textile, food, and cosmetic applications.<sup>4, 5</sup> Azobenzenes exist as two isomers: the *E* isomer (or *trans*) and the *Z* isomer (or *cis*) (Scheme 1). Absorbance of UV light (300-400 nm) initiates a  $\pi \rightarrow \pi^*$  transition which easily isomerizes *E* isomers to *Z* isomers. On the other hand, *Z* to *E* isomerization can occur thermally or by exposure to blue light (400-450 nm) to initiate a  $n \rightarrow \pi^*$  transition.<sup>6</sup>



**Scheme 1:** Reversible photoisomerization of azobenzenes upon UV-Vis irradiation.<sup>6</sup>

The *cis-trans* photoisomerization of azobenzene induces a dramatic change in the molecular geometry and dipole moment of the molecule by rearranging the disposition of the aromatic rings from coplanar to angular and vice-versa.<sup>7</sup> The reversible light driven isomerization of azobenzenes allows to control the relative movement of different moieties bound to an azobenzene group by converting photochemical energy into mechanical motion. Consequently, azobenzenes make

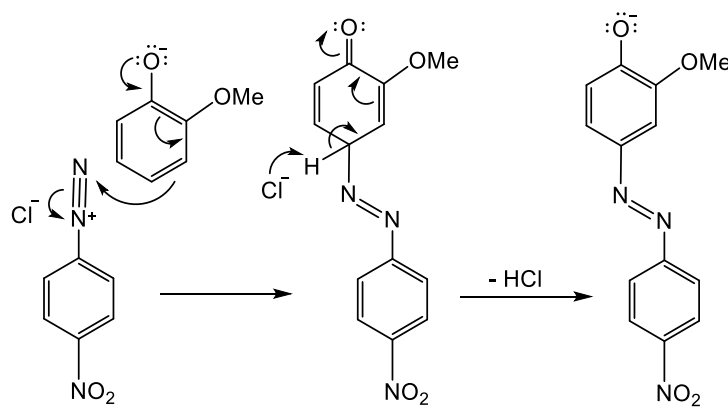


excellent candidates for molecular switches and artificial muscles.<sup>8</sup> Moreover, the photosensitive properties of azo compounds can potentially offer functional materials for optical storage, light harvesting, long-term energy storage, chemosensing, and liquid crystals.<sup>9, 10</sup> Azo compounds are also of interest for more advanced biomedical applications. For example, the photoresponse of azo compounds can be used as a diagnostic probe to visualize the physiological activity of amyloid plaques in the brains of patients with Alzheimer's disease.<sup>11</sup>

## 1.2 Methods for the Synthesis of Azobenzenes

### 1.2.1 Azo Coupling Reaction

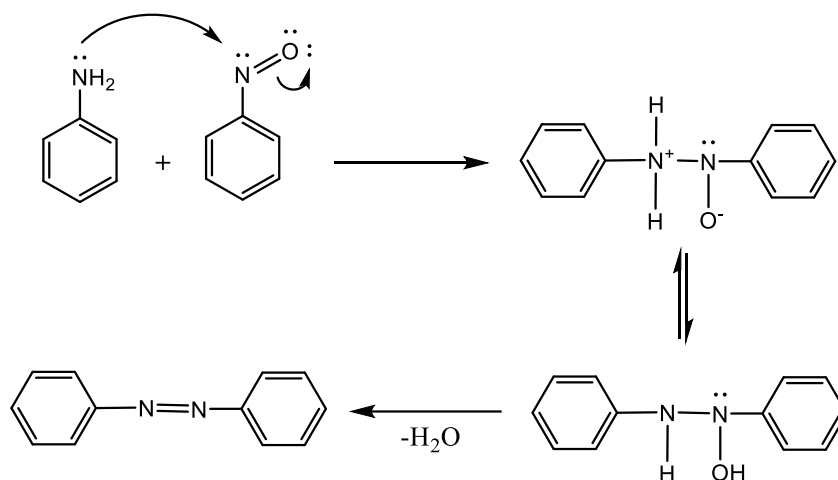
The azo coupling reaction is perhaps the most popular method for the preparation of asymmetric azo derivatives. This methodology is based on the initial formation of diazonium salts from anilines, which then undergo a nucleophilic attack by electron-rich arenes. The substitution normally takes place at the para position to the electron donor group on the aromatic nucleophile. For instance, the coupling of a diazonium salt with a deprotonated phenol gives the corresponding azo compound in excellent yields (Scheme 2).<sup>12</sup> Under basic conditions, the resulting phenolate is a sufficiently stronger electron donor group than the methoxy to selectively give the product by nucleophilic substitution at the position para to the OH group.



**Scheme 2:** Mechanistic scheme of the azo coupling reaction for synthesis of asymmetrical azo derivatives. Reagents and conditions:  $\text{K}_2\text{CO}_3$ ,  $0^\circ\text{C}$ , (92% yield).<sup>12</sup>

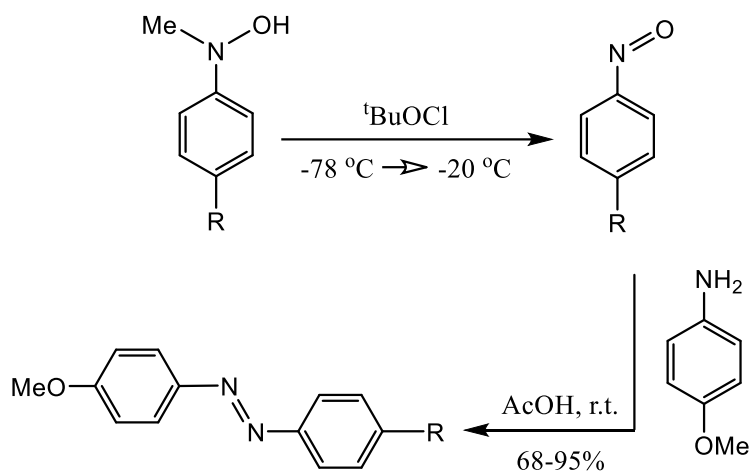
### 1.2.2 Mills Reaction

Another classical method for the synthesis of asymmetrical azobenzenes is the Mills reaction. Mechanistically, the Mills reaction involves the attack of the aniline on the nitroso nitrogen, which then leads to the azobenzene product upon dehydration of the intermediate species (Scheme 3).<sup>13</sup>



**Scheme 3:** Mechanistic scheme for coupling of primary arylamine and nitroso compounds.<sup>13</sup>

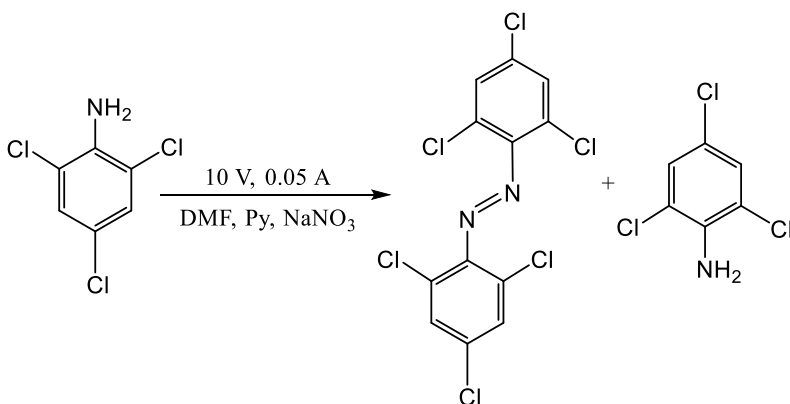
One example is the treatment of aromatic nitroso derivatives and anilines in glacial acetic acid which gives the corresponding azobenzene in good yield (Scheme 4).<sup>14</sup> Difficult to control is the formation of the nitroso reactant in the first step of the reaction. Here, the aromatic nitroso derivative was prepared by oxidation of the aromatic methylhydroxylamine precursor with tert-butyl hypochlorite. Low temperatures, a temperature gradient, and high dilution were required to prevent over-oxidation. Other oxidation agents like ferric chloride,<sup>15</sup> sodium or potassium dichromate,<sup>16</sup> hydrogen peroxide,<sup>17</sup> m-chloroperbenzoic acid,<sup>18</sup> potassium permanganate,<sup>19</sup> diethyl azodicarboxylate,<sup>20</sup> silver carbonate,<sup>21</sup> and peroxyformic acid<sup>22</sup> have all been used to generate nitroso derivatives for the Mills reaction.



**Scheme 4:** Generation of the nitroso precursor and subsequent formation of the azo product.<sup>14</sup>

### 1.2.3 Oxidation of Anilines

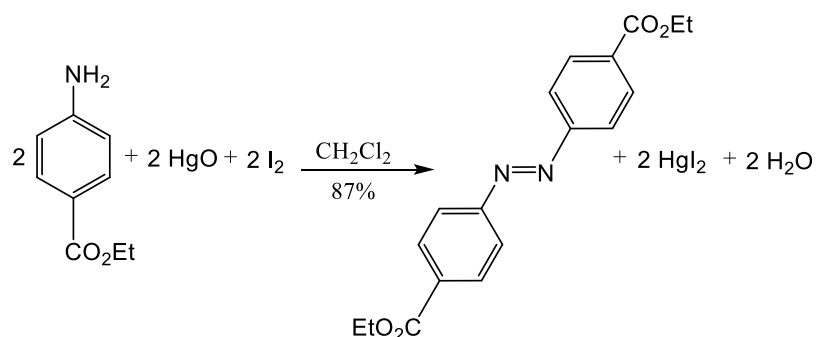
The synthesis of symmetrical azobenzene derivatives has been reported via oxidation reactions of aromatic primary amines. The electrolytic oxidation of aromatic amines using Pt electrodes in the presence of pyridine was first described in 1972 as a method to obtain azobenzenes (Scheme 5).<sup>23</sup>



**Scheme 5:** Electrolytic oxidation of aniline with Pt electrode in DMF (48% yield).<sup>23</sup>

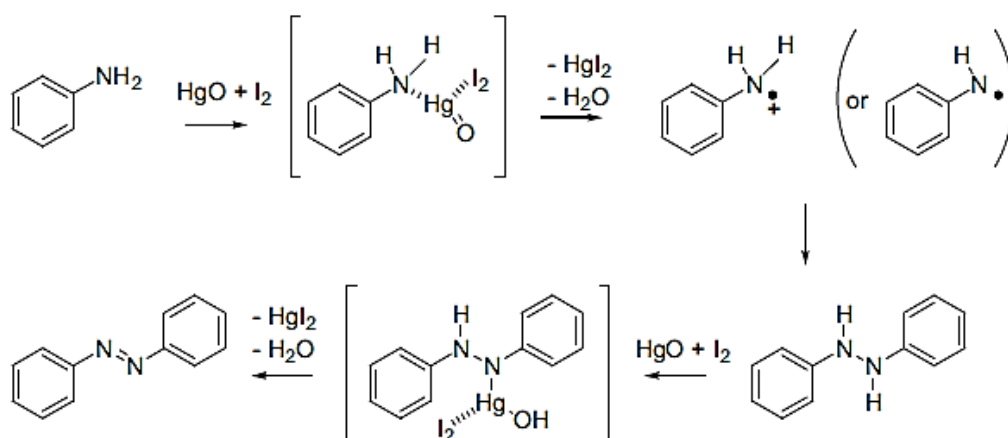
In addition to electrochemical approaches, a variety of metal oxides such as  $\text{MnO}_2$ ,<sup>24</sup>  $\text{Ag}_2\text{CO}_3$ ,<sup>25</sup>  $\text{Ag}_2\text{O}$ ,<sup>26</sup>  $\text{AgMnO}_4$ ,<sup>27</sup>  $\text{BaMnO}_4$ ,<sup>28</sup>  $\text{Pb}(\text{OAc})_4$ ,<sup>29</sup>  $\text{KO}_2$ ,<sup>30</sup>  $\text{KMnO}_4$  supported on copper (II) sulfate pentahydrate,<sup>31</sup> and nickel peroxide,<sup>32</sup> have been used either stoichiometrically or in excess

to synthesize azobenzenes from aniline derivatives. In general, the azo compounds were obtained in low to moderate yields with the methods and reagents mentioned above. However, mercury(II) oxide/iodine reagents were later reported by Orito et al. to furnish the corresponding azo product in high yields (Scheme 6).<sup>33</sup>



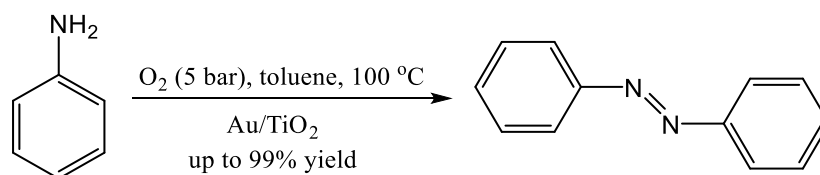
**Scheme 6:** Oxidation of anilines with 2 equivalents of HgO and I<sub>2</sub> in CH<sub>2</sub>Cl<sub>2</sub> (87% yield).<sup>33</sup>

A radical mechanism has been proposed for the oxidation of anilines by HgO and I<sub>2</sub> (Scheme 7).<sup>34</sup> The key steps are the formation of radical aniline species that couple to form a N-N bond (hydrazobenzene), which is finally converted to the azobenzene by a two electron oxidation with HgO and I<sub>2</sub>.



**Scheme 7:** Mechanistic scheme of the radical-mediated dimerization of anilines.<sup>34</sup>

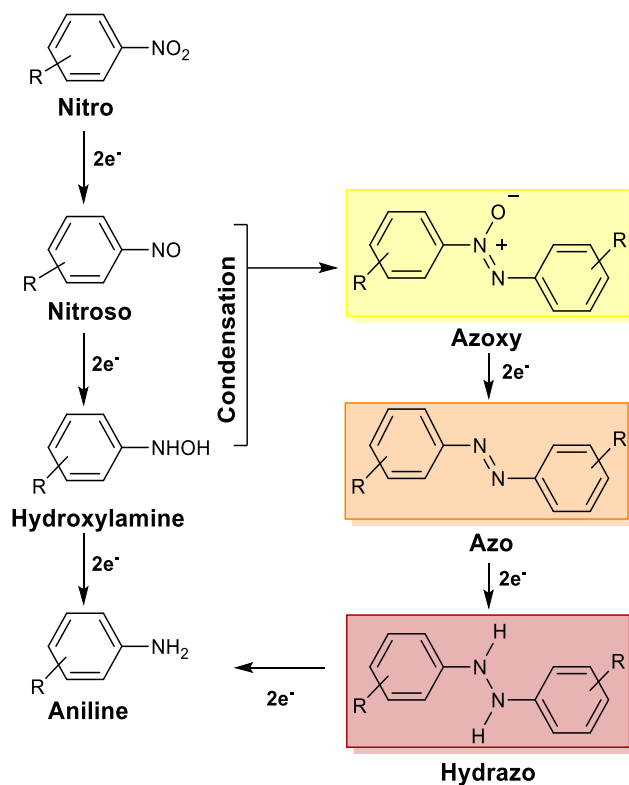
More recently, the catalytic aerobic oxidation of aniline to azobenzene was achieved with gold nanoparticles supported on titanium dioxide (Au/TiO<sub>2</sub>) and under dioxygen atmosphere (5 bar). In contrast to the environmentally unfriendly use of mercury, this approach offers a greener and higher yielding synthesis of the azobenzene (99%) under oxidative conditions (Scheme 8).<sup>35</sup>



**Scheme 8:** Catalytic oxidation of aniline with Au/TiO<sub>2</sub> under dioxygen atmosphere.<sup>35</sup>

#### 1.2.4 Reductive Coupling of Aromatic Nitro Compounds

A large number of procedures have been developed to synthesize azo compounds from the reductive coupling of nitroarenes that are typically more stable and less toxic than their aniline analogs. Symmetrical azo derivatives are directly obtainable by the reduction of aromatic nitro compounds using reducing agents such as lithium aluminum hydride,<sup>36</sup> sodium borohydride,<sup>37</sup> dicobalt octacarbonyl,<sup>38</sup> or zinc in strongly alkaline medium.<sup>39</sup> Other reductive methods involved catalytic transfer hydrogenation of nitroarenes using lead powder with triethylammonium formate,<sup>40</sup> catalytic reduction over palladium,<sup>41</sup> electrochemical reduction,<sup>42</sup> alkaline reduction with glucose,<sup>43</sup> or with aluminum/NaOH under ultrasonic conditions.<sup>44</sup> Depending on the reaction conditions, however, the reduction of nitroarenes may lead to different products, for instance, a basic medium generally favors the conversion to not only azo but also azoxy and hydrazo derivatives. Reduction to the corresponding anilines is also possible but less favourable unless acidic conditions are used.<sup>45</sup>



**Scheme 9:** Plausible reaction pathway for the reduction of aromatic nitro compounds.<sup>46</sup>

The reaction pathway shown in Scheme 9 outlines the generally accepted Haber mechanism for the reductive coupling of aromatic nitro compounds.<sup>46</sup> According to this mechanism, the nitroso and hydroxylamine intermediates undergo a dehydrative coupling reaction to form the azoxy intermediate that is further reduced to generate the azo compound. Hydrogenation of the azo compound results in the cleavage of the N-N bond to release the aniline. Alternatively, the reductive formation of aniline may also proceed stepwise without the intermediate condensation to azo derivatives. In metal-mediated reactions, these reductive pathways are driven by single electron transfers (SET) from the metal surface (e.g. Mg or Zn) to the organic substrate.<sup>47</sup>

### 1.2.5 Limitations of Current Methodologies

Despite the large number of methodologies that have been reported in the literature for the synthesis of azo compounds, there are still significant challenges to be solved. Many of these

methods present limitations including harsh conditions, expensive reagents, and lack of product selectivity, which are great disadvantages for large scale productions. In particular, the azo coupling process requires large amounts of nitrite salts to form diazonium salt precursors, and therefore generates equivalent quantities of inorganic waste. In addition, diazonium salts can be explosive, thus it is important to carefully control the temperature of the reaction. On the other hand, commonly used catalytic hydrogenation methods require high pressure equipment, and flammable hydrogen gas. Finally, other processes including Mills reaction, oxidation of anilines, and reductive coupling of nitroaromatics use excess amounts of environmentally unfriendly oxidants or reductants. In many of these cases, the azo compound is obtained in low to moderate yields along with unwanted side reactions and by-products. Consequently, there is a need for the development of practical methodologies and convenient reaction conditions that employ inexpensive and more environmentally benign reagents for the selective synthesis of azo compounds.

In recent years, ball milling has been shown to be a potent procedure for the mechanochemical synthesis of organic compounds under quasi solvent-free conditions. Hence, I wish to discuss this field as a potential alternative to the current solution-based syntheses of azobenzenes.

### **1.3 Mechanochemistry**

The inefficiencies of traditional syntheses, otherwise known as solution-based batch processes, are mainly associated with the use of large quantities of solvents. As a result, chemists search for new methods to optimize the efficiency of synthetic procedures by increasing product yield, accelerating reaction rates, lowering operating costs, and reducing the amounts of reagents and solvents. In recent years, solid-state mechanochemistry by “ball milling” has emerged as a new approach to organic synthesis with high potential not only in academia but also industry.

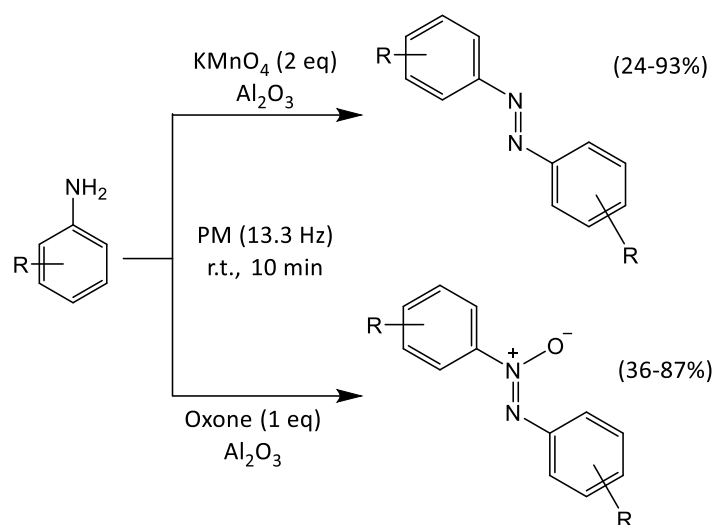
According to IUPAC, a mechanochemical reaction is defined as “a chemical reaction that is induced by the direct absorption of mechanical energy”.<sup>48</sup> Synthesis by ball milling involves the mechanochemical grinding of dry or slightly wet reagents in a contained system. The conversion of the mechanical energy into heat due to collision and friction of the grinding bodies can provide enough energy to initiate chemical reactions in the bulk material.<sup>49</sup> By contrast, the energy dispersion and mixing of chemicals in traditional solution chemistry are assured by the action of solvents and heat.

#### **1.4 Solvent-Free Redox Synthesis of Azobenzenes**

Over the last decade, numerous protocols have been reported on ball milling processes for solid-state syntheses of various organic compounds but only three publications deal with the synthesis of azobenzene derivatives.<sup>50, 51, 52</sup> Nevertheless, oxidative and reductive pathways were tested in laboratory-scale ball mills and, overall, the solvent-free synthesis of azo compounds in ball mills was found to be more efficient than in solution with regard to chemical yield and energy consumption.

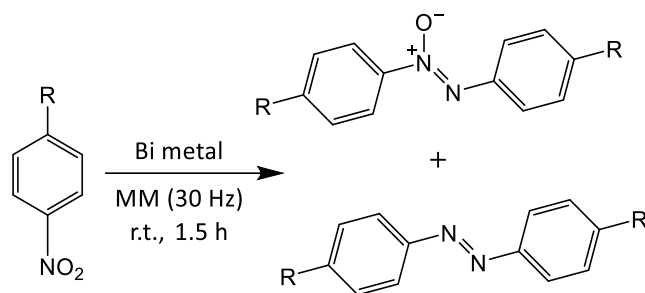
Stolle and coworkers were the first to develop a fast and solvent-free method for the direct oxidation of anilines to the corresponding azo and azoxy products using a planetary ball mill (Scheme 10).<sup>50</sup> Several oxidants and milling auxiliaries were tested along with a variety of substituted anilines. Interestingly, a judicious selection of the oxidant allowed for the selective formation of only one of the possible homocoupling products. For instance, solvent-free oxidation of the aniline using potassium permanganate exclusively furnished the azo product, whereas oxidation using Oxone afforded the azoxy compound.





**Scheme 10:** Chemoselective oxidative coupling of anilines under solvent-free conditions. Reactions were performed in a Fritsch planetary ball mill (PM) using 45 mL grinding beakers (agate or  $\text{ZrO}_2$ ) and milling balls (6–15 mm; agate or  $\text{ZrO}_2$ ).<sup>50</sup>

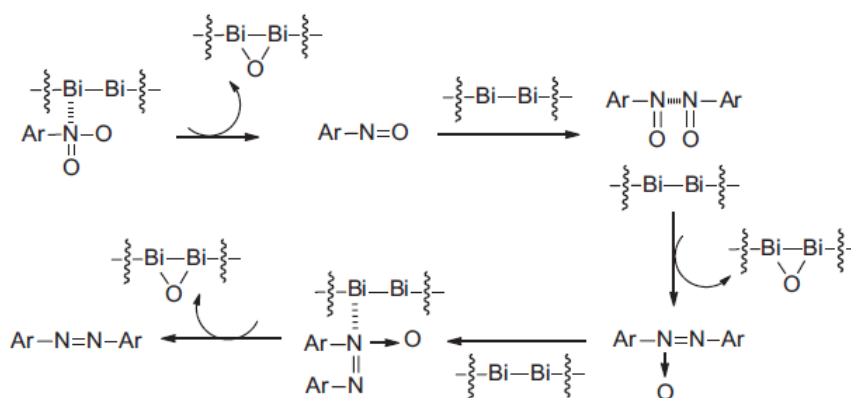
A metal-mediated solvent-free reduction of nitroarenes to azoxy and azoarenes has only been reported by Suzuki and co-workers who used bismuth shots as reducing agent under ball milling conditions (Scheme 11).<sup>51</sup>



**Scheme 11:** Solvent-free reduction of nitroarenes to azoxy and azoarenes using bismuth shots. Reactions were performed in a Retsch mixer mill (MM) using 5 mL grinding beakers (stainless steel) and milling balls (7 mm; stainless steel).<sup>51</sup>

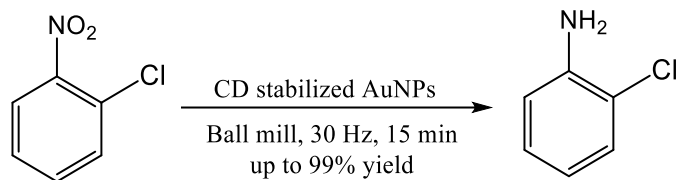
The influence of atmospheric oxygen and solvent additives on the bismuth-mediated reduction were investigated for *p*-nitroanisole. The presence of air inside the reaction vessel favored the formation of the azoxyarene (78% yield) at the expense of the azo compound (22% yield). On the

other hand, when *p*-nitroanisole and bismuth shots were subjected to ball milling under dioxygen atmosphere, the azoxy compound was obtained as the sole product in 100% yield. Interestingly, the addition of a drop of an inert organic solvent such as hexane or benzene to the nitroarene bismuth mixture prior to milling also led to the complete formation of the azoxyarene. Only under the protection of nitrogen atmosphere was the azoarene formed predominantly in 83% yield, along with the azoxy intermediate in 17% yield. Scheme 12 shows the proposed pathway for the deoxygenative dimerization of nitroareness on the activated bismuth surface.<sup>51</sup> Nitroarenes are adsorbed and deoxygenated on the bismuth surface to give nitroso intermediates, which subsequently undergo dimerization to form azoxyarenes. Based on this mechanism, the presence of oxygen or an additive can occupy the active bismuth surface and inhibit further reduction.



**Scheme 12:** Proposed pathway for the deoxygenative dimerization of nitroarenes on bismuth.<sup>51</sup>

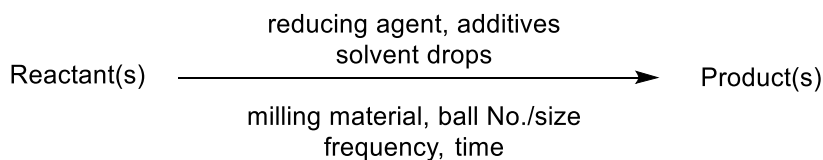
A conversion of chloro-2-nitrobenzene directly to 2-chloro-aniline by ball milling was reported by Manuel and coworkers. They described the solid-state reduction of substituted nitroarenes catalyzed by saccharide-stabilized AuNPs using a ball-mill.<sup>52</sup> The  $\beta$ -cyclodextrin additive consisting of 7 glucopyranose units, displayed the best stabilizing properties towards AuNPs, however the corresponding aniline was obtained as major product at up to 99% yield depending on the nature and location of the substituent on the nitrobenzene ring (Scheme 13).



**Scheme 13:** AuNP-catalyzed reduction of 1-chloro-2-nitrobenzene into 2-chloroaniline under ball milling conditions.<sup>52</sup> CD = Cyclodextrin.

## 1.5 Reaction Parameters for Ball Milling

Compared to solution chemistry, the parameter set for ball milling methods offers various possibilities to manipulate the outcome of a chemical reaction. However, assessing ball milling chemical processes can be rather challenging, especially since a large number of reaction parameters have been proven to influence the rates and products of mechanically-induced organic reactions.<sup>53, 54, 55</sup> Typically, the variable conditions are categorized into the following groups: i) chemical, ii) technological and iii) process related parameters (Scheme 14).



**Scheme 14:** Generic reaction scheme for the conversion of nitroarenes into azobenzenes with reaction parameters for a ball mill assisted synthesis.<sup>56</sup>

Chemical parameters consist of the type of reducing agent, the presence of additives, the reagent ratio and the addition of small amount of solvents. Like in solution chemistry, these variables directly affect the chemical transformations taking place inside the ball mill chamber. Variables like the milling material, the number and size of milling balls fall under technological parameters. These variables influence the outcome of the reaction considerably because they change the number of collisions per unit time and impact intensity during the ball milling process. The operating frequency, milling time and temperature are process parameters correlated to the stress

energy, the progression of the reaction, and chemical kinetics, respectively. Besides chemical parameters, several studies indicated that the energy input in ball mill reactions can be significantly controlled by a combination of technological and process parameters.<sup>53, 55, 57, 58, 59, 60, 61</sup>

## 1.6 Technological Parameters

### 1.6.1 Milling Material

The choice of the milling material (milling balls and milling jars) significantly influences the outcome of chemical reactions performed in ball mills. In this case, the properties of the milling material (e.g. density, Young's modulus and hardness) contribute to the energy entry and, therefore, determine the amount of stress energy transferred to the milling feed, as well as the dissipation of energy in the form of heat during the ball milling process (Eq. 1).<sup>49, 62, 63, 64</sup>

$$\text{Stress Energy} = d^3 v^2 \rho K^{-1} \quad \text{with } K = f(E_Y) \quad (1)$$

where,

$d$  (m): diameter of the milling ball(s)

$v$  (m s<sup>-1</sup>): velocity

$\rho$  (kg m<sup>-3</sup>): density of the milling ball(s)

$E_Y$  (Pa): Young's modulus

According to Eq. (2), the kinetic energy of a system is determined by the moving mass ( $m$ ) and relative velocity ( $v$ ):

$$\text{Kinetic Energy} = \frac{1}{2} mv^2 \quad (2)$$

This physical relation demonstrates the importance of the applied material density for the overall kinetic energy of a system; the higher the material density, the higher is the energy entry. Commonly known milling materials consist of tungsten carbide, steel, zirconia and agate (arranged by decreasing material density). It is not entirely applicable that the higher the material density, the higher the energy transfer and thus the product yield, as this depends on the activation energy

and reaction mechanism of the ongoing reaction itself. In some cases, the product yields increased when the milling material was changed from a light-weight agate ( $\rho = 2.7 \text{ g cm}^{-3}$ ) to a heavier zirconia ( $\rho = 5.7 \text{ g cm}^{-3}$ ).<sup>50, 65</sup> In these cases, the reactions typically have higher activation energies, and therefore require higher density milling materials in order to reach higher product yields. Moreover, higher material density is especially favorable for catalytic and metal mediated ball mill processes that require stronger mechanical crushing and abrasive effects to activate and increase the reactivity of the active chemical surfaces. In other cases, no significant effect was observed when the milling material was changed, which may suggest the reaction's activation energy is low, hence a thermodynamic equilibrium is reached quickly for any of milling materials.<sup>58, 61, 66, 67</sup> Besides energy intensity, the chemical stability of the milling material towards the ongoing chemistry must be considered. For instance, oxidation reactions involving strong inorganic oxidants can affect the condition of the milling material (e.g. corrosion of steel).

### 1.6.2 Size of Milling Balls

An important technological parameter for ball mill reactions is the size of the milling ball(s). According to Eq. (1), the stress energy transferred to the milling feed shows a cubic proportionality to the diameter of the milling ball(s) for systems operated under wet conditions (e.g. solvent-assisted ball mill reactions).<sup>64, 68, 69</sup> Furthermore, the stress energy was shown proportional to the impact energy of the colliding milling ball(s), and to the collision frequency.<sup>70</sup>

$$\text{Stress energy} \propto \text{impact energy} \cdot \text{collision frequency} \quad (3)$$

Based on this physical approximation, the direct proportionality of the impact energy to the kinetic energy, as well as to the mass/size of the moving bodies inside the milling chamber is a perceptible relation (Eq. 2). In theory, the kinetic energy generated from the mechanical action of the milling balls is converted to thermal energy through impact and frictional processes, which

then serves as chemical energy to induce a chemical reaction.<sup>48</sup> Despite the potential loss of kinetic energy through dissipation, a strong correlation between the mass/size of the milling bodies and the chemical yield was observed for several mechanically-induced organic reactions.<sup>50, 65, 71, 72 73</sup> In these cases, an increase of the milling ball diameter accelerate the rate of the chemical reaction because this generates not only larger impacts but also more thermal energy to increase the bulk temperature of the milling media.

### **1.6.3 Number of Milling Balls**

According to Eq. (3), the amount of energy generated in a milling system is proportional to the impact energy and the collision frequency of the milling ball(s). Moreover, studies have shown that the number of milling balls directly influences the collision frequency, and ultimately the outcome of a reaction. In particular, when the material density and the size of the milling ball are kept constant, a linear correlation is observed between the reaction yields and the number of milling balls.<sup>58, 59, 60, 61</sup> In another study, Rosenkranz et al. monitored and simulated the motion of milling bodies by video and discrete element analysis.<sup>74</sup> The milling balls were found to follow typical trajectories inside a milling chamber. According to these experimental investigations and modelling approximations, multiple milling balls are necessary to give the required trajectories that ensure greater mechanical impact and energy transfer.<sup>74</sup> Likewise, these observations demonstrate that the probability for collision increases with the number of balls placed inside a milling chamber.

## **1.7 Chemical Parameters**

Regardless of the type of synthetic methodology, chemical parameters are generally examined over a wide range to fully exploit the potential of a specific reaction. Among the most significant chemical parameters in ball mill synthesis is the application of wet and dry milling conditions.

Several studies have shown that small quantities of liquid deliberately added to the reaction mixture can dramatically accelerate, and even enable, mechanochemical reactions between solids. The first report of such a process involved a study of mechanochemical co-crystal formation from solid organic reactants, which demonstrated a significant improvement in the product formation rate, specifically in the presence of small amounts of solvent.<sup>75</sup> In some cases mechanochemical reactions generate small amounts of liquid products during the reaction, resulting in a solvent-assisted process. For example, experiments have shown that these reactions are accelerated when one of the reactants is a hydrate, or when liquid by-products such as water are generated in condensation reactions.<sup>76, 77</sup> Although the amount of solvent used with solvent-assisted mechanochemical synthesis is insufficient to completely dissolve the reactants, it can simply provide a pathway to facilitate the interaction between solid reactants and accelerate the reaction by locally generating solution-like conditions.<sup>78</sup>

## **1.8 Process Parameters**

### **1.8.1 Operating Frequency**

The basic principle for all types of ball mills is the generation of impact, friction and shear strains that originate from collisions between the milling balls, the containment surfaces, and the chemical content. For instance, the mechanical forces of a mixer ball mill (e.g. Retsch MM400) are initially generated by oscillation of the milling unit at variable frequencies. In this process the milling beaker is mounted on a swing arm and is oscillated horizontally across a circular arc (Figure 1). Because the oscillations generated in a mixer ball mill are restricted in one plane, the tangential displacement ( $\Delta d_{tan}$ ) of the milling beaker is small compared to its horizontal displacement ( $\Delta d_{hor}$ ), hence the milling beaker, including the milling bodies follow a straight line in the first approximation.<sup>56</sup> In this case, as the milling balls are accelerated in a similar direction as the

containment, the oscillation reaches its reversal point from position A to B, however the milling balls are kept in motion due to their inertia, resulting in collision between the milling content and the walls of the milling beaker.<sup>56</sup> Eq. (3) indicates a direct proportionality between the collision frequency and the amount of energy transferred to the feed material (e.g. substrates).<sup>70</sup> Ultimately, a higher operating frequency generates more collisions and increases the velocity of the milling bodies, and therefore increases the stress and kinetic energies of the milling system, respectively.

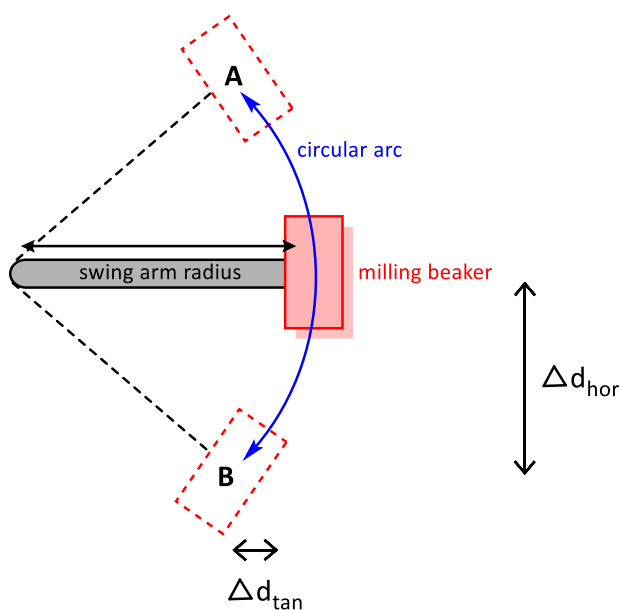


**Figure 1:** Schematic representation of the milling beaker trajectory for a mixer ball mill across a horizontal plane.

Several studies that include redox chemistry,<sup>60, 61, 79</sup> cross-coupling,<sup>58, 80</sup> condensation<sup>81, 82</sup> and organocatalytic reactions<sup>83</sup> have investigated the effect of the milling frequency in a range of 5 Hz to 30 Hz. They all reported a direct correlation between the frequency and the yield of conversion. According to literature, as the milling frequency rises, the yield of conversion increases due to increasing kinetic energy and collision between the molecules. Investigations undertaken to assess the influence of the ball-milling frequency on the AuNP-catalyzed reduction of 1-chloro-2-nitrobenzene to 2-chloroaniline, indicated the presence of N-phenylhydroxylamine



intermediate at 10 and 20 Hz, however no reaction intermediates could be detected at 30 Hz.<sup>52</sup> These observations show that the chemical kinetics of the reactions are significantly influenced by the oscillation frequency of the milling system. In certain cases, however, high energy impact induced by an increased frequency may lower the performance of a chemical process by promoting unwanted side reactions.<sup>84, 85</sup> For example, the ball milling synthesis of benzimidazoles was reported to reach a maximum point at an optimum frequency (20 Hz), beyond which any further increase in the frequency caused a decrease in the yield of the reaction.<sup>86</sup> Ultimately, the influence of the operating frequency is strongly related to the type of reaction (e.g. kinetics), the reactivity of the reagents, and the chemical stability of the products. Nevertheless, the mechanochemical reduction of 5-nitroisophthalic acid in this study was solely performed at 30 Hz.

### 1.8.2 Milling Time

In addition to the operating frequency, the reaction time is central variable determining the overall yield of solid-state reactions.<sup>58, 61, 71</sup> As for conventional reactions in solution, an increase in reaction time leads to higher product yields until full conversion has been attained unless side-products are formed. As a chemical reaction progresses with milling time, the overall number of collisions increases and more energy is distributed to the milling feed. In addition, the rate of a chemical reaction indicates that a higher number of moles can be converted with longer reaction time (Eq. 5):

$$r = \Delta n / \Delta t \quad (4)$$

where,

$r$  (mol s<sup>-1</sup>): rate of reaction

$n$  (mol): molar amount

$t$  (s): reaction time

## 1.9 Background and Scope of Thesis

### 1.9.1 Azobenzene Tetracarboxylic Acid: Organic Building Block for PCN-250

In spite of representing about two-thirds of the fossil fuels on earth, methane (the main component of natural gas) remains the least utilized fuel. Nevertheless, the wide availability and lower carbon emission of natural gas is attracting great interest as an economically valid short-term alternative to gasoline. While compressed natural gas can be suitable for large-size vehicles (e.g. trucks, buses), this solution is less than satisfactory for light-duty passenger vehicles due to the extremely low volumetric energy density of natural gas at ambient temperature and pressure. One potential solution would be to store natural gas at very high pressures (250 bar) and increase its volumetric energy density through liquefaction and compression processes, however, these options are certainly invalid for light-duty passenger vehicles. Alternatively, the widespread use of natural gas relies on the development of adsorbent materials to efficiently and safely store natural gas at ambient temperatures and moderate pressures. Among the many porous adsorbents for methane storage, the metal-organic framework (or Porous Coordination Network) PCN-250(Fe<sub>3</sub>) is particularly promising for such application, notably due to its unusually high uptake of methane (200 v/v at 35 bar and 298 K) and stability (Figure 2).<sup>87</sup> An important limitation for the commercial use of PCN-250(Fe<sub>3</sub>) in fuel tanks is the lack of a scalable and economical synthesis of its organic spacers 3,3',5,5'-azobenzene tetracarboxylic acid. The reported solution methods<sup>88, 89, 90, 91, 92, 93</sup> cannot be used for ton or even kg scale preparations of this spacer.

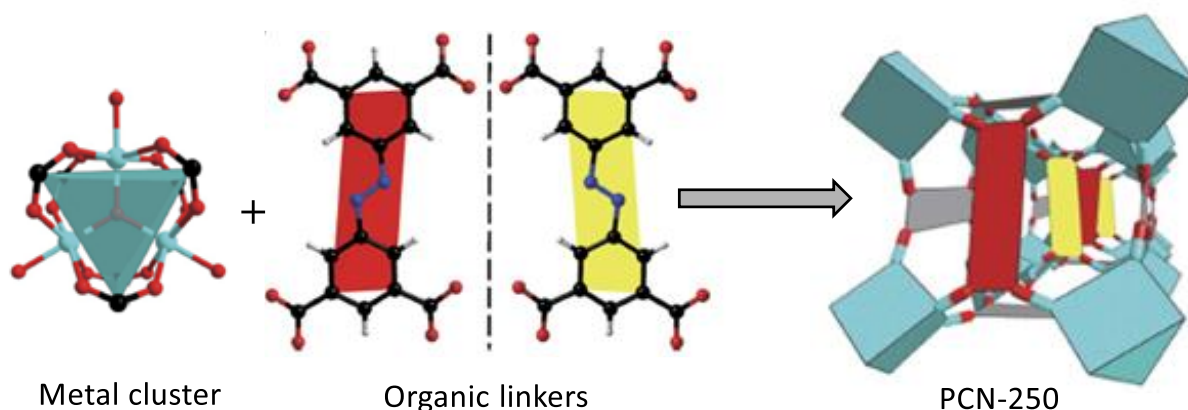


**Figure 2:** The structure of PCN-250 is composed of  $\text{Fe}_3$  metal clusters and 3,3',5,5'-azobenzene tetracarboxylic acid organic linkers. The tetra-coordinated ligands constructing the same cube in PCN-250 adopt mirror configurations and are alternatively arranged along one axis.<sup>87</sup>

### 1.9.2 Scope of Thesis

To the best of my knowledge, the synthesis of azo compounds from nitroarenes using inexpensive metal reagents such as zinc and magnesium under ball milling conditions has not been reported. Thus, in the following chapter, I wish to report a novel two-step ball milling approach using low-cost reducing agents to selectively synthesize 3,3',5,5'-azobenzene tetracarboxylic acid in excellent yields.

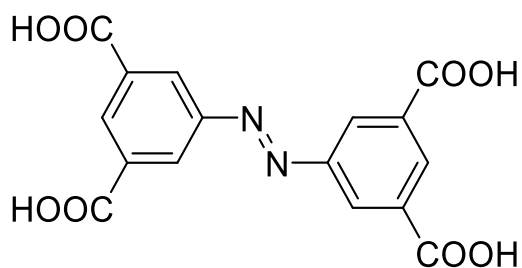
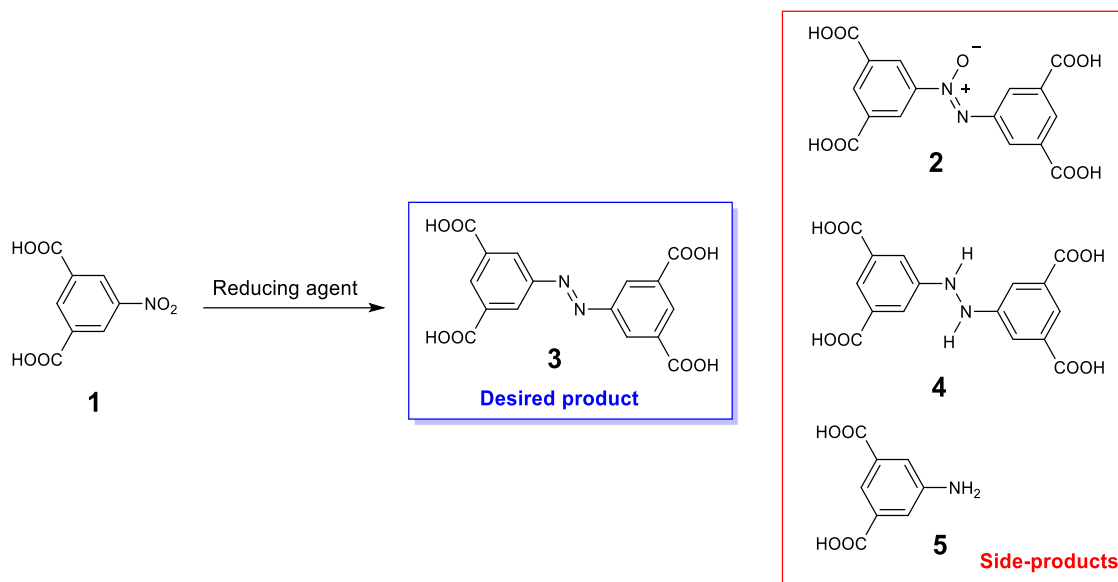


**Figure 3:** Molecular structure of 3,3',5,5'-azobenzene tetracarboxylic acid product.

# Chapter 2: Results and Discussion

## 2.1 Product Characterization

Under reducing conditions, mixtures of the following products were observed in many of the solution-based and ball mill assisted reactions (Scheme 15). The spectral and structural characterization of compounds **2**, **3**, **4**, and **5** are discussed in following sections.



**Scheme 15:** Compounds **2**, **3**, **4**, and **5** represent the azoxy, azo, hydrazo and aniline derivatives, respectively. These compounds are obtained in different yields by reduction of 5-nitroisophthalic acid (**1**) under varying conditions (e.g. type of reducing agent, amount of reducing agent, amount of solvent, reaction time, size/number of milling balls).

### 2.1.1 Compound 3 (3,3',5,5'-Azobenzene Tetracarboxylic Acid)

The structural identity of *E*-3,3',5,5'-azobenzene tetracarboxylic acid, an orange crystalline compound, was confirmed by  $^1\text{H-NMR}$ ,  $^{13}\text{C-NMR}$ , IR, and UV-Vis spectroscopy, MS, and single crystal X-ray diffraction (see experimental section for details). Its high symmetry and predominantly trans configuration generates NMR spectra with few signals.  $^1\text{H-NMR}$  in  $\text{DMSO-}d_6$  gives a multiplet for the aromatic protons between 8.60 and 8.62 ppm and a broad signal for the

carboxylic acid protons at 13.59 ppm.  $^{13}\text{C}$ -NMR generated the expected 5 carbon signals with a characteristic peak for the carbonyl carbons at 166.83 ppm. Its IR spectrum showed a distinct absorption at  $1414\text{ cm}^{-1}$  that is characteristic for the azo bridge ( $\nu_{\text{N}=\text{N}}$ ). Also present are the expected stretching modes of the carbonyl group at  $1724\text{ cm}^{-1}$  and  $1677\text{ cm}^{-1}$  ( $\nu_{\text{C}=\text{O}}$ ), the O-H group at  $3419\text{ cm}^{-1}$ , and the benzene rings at  $1614\text{ cm}^{-1}$  and  $1465\text{ cm}^{-1}$  ( $\nu_{\text{C}=\text{C}}$ ). These values agree with the reported values.<sup>88-92</sup> The molecular structure of **3** was also confirmed by high resolution MALDI mass spectra giving a  $m/z$  value of 358.0444 and a mass error of -1.96% for the  $[\text{M}^{-1}]$  peak. A value of  $m/z = 358.4$  (5.9%) has been previously reported using EI-MS.<sup>91</sup> I also investigated the thermal and chemical stability of **3** to the applied reaction and work-up conditions as they involved elevated temperatures and the use of strong bases and acids. Thermal stability was tested by variable temperature polarized optical microscopy and DSC, which revealed a high decomposition temperature of  $388\text{ }^{\circ}\text{C}$  and no melting transition. The azo compound was also found to be chemically stable in 6 M HCl (aq)/methanol solution (1:2) at elevated temperatures ( $>60^{\circ}\text{C}$ ).

The absorption spectrum of **3** recorded at the concentration of  $10^{-4}\text{ M}$  (Figure 5) shows two absorption bands in the spectral region 300-700 nm. The high-intensity band at 319 nm ( $\epsilon \sim 7700\text{ M}^{-1}\text{cm}^{-1}$ ), is assigned to the  $\pi \rightarrow \pi^*$  transition of the  $\text{N}=\text{N}$  unit and is a measure of the composition of the *trans* isomer. The low intensity band at 448 nm ( $\epsilon \sim 180\text{ M}^{-1}\text{cm}^{-1}$ ) due to the  $n \rightarrow \pi^*$  transition is much weaker as this transition is forbidden in the *trans* isomer by symmetry rules.<sup>6</sup> According to the absorption spectrum shown in Figure 6, the percentage composition of the *cis* isomer is negligible compared to that of the more stable *trans* isomer under ordinary conditions. The predominant *trans* configuration of the azo product (**3**) was also confirmed by single crystal analysis, which agrees with the values reported in the literature (see appendix for detailed single crystal data).<sup>94</sup>

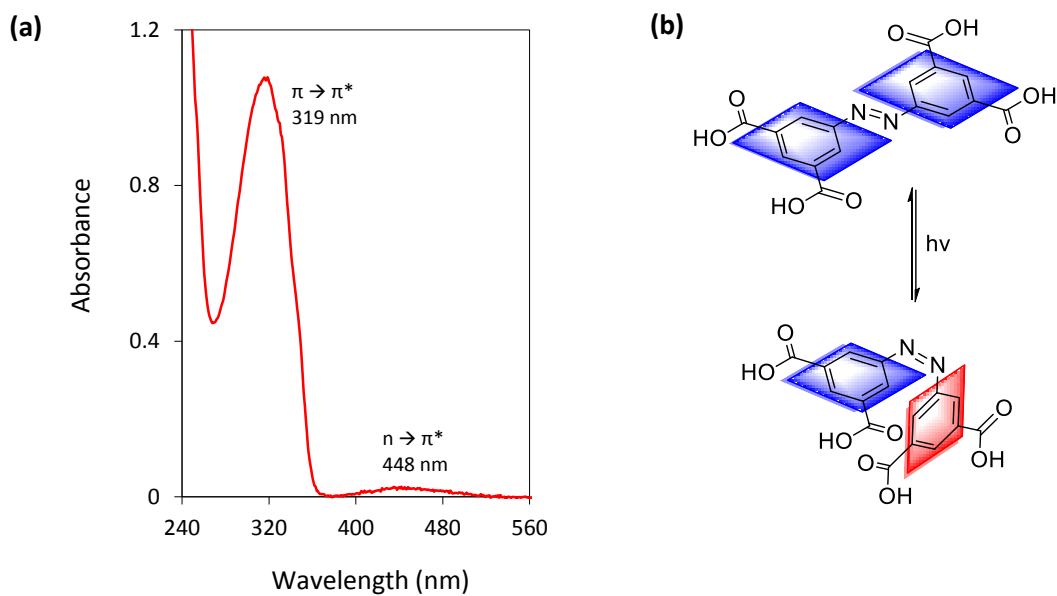


**Figure 4:** (a) UV-Vis absorption spectra of compound **3** in ethanol (0.05 mg/mL). (b) Photoisomerization process of 3,3',5,5'-azobenzene tetracarboxylic acid.

### 2.1.2 Compound **2** (3,3',5,5'-Azoxybenzene Tetracarboxylic Acid)

A typical side-product of the azo coupling reaction is 3,3',5,5'-azoxybenzene tetracarboxylic acid (**2**), which was observed as the main product when reactions were stopped prematurely. The N-oxide intermediate **2** was identified by NMR and IR spectroscopy and comparison to reported values.<sup>93</sup> Because of its lower symmetry, **2** reveals the splitting of 4 aromatic proton signals in the <sup>1</sup>H-NMR spectra (DMSO-d<sub>6</sub>): 8.50 ppm (t, 1 H), 8.68 ppm (t, 1 H), 8.79 ppm (d, 2 H) and 8.94 ppm (d, 2 H). In addition, the N-oxide intermediate (**2**) shows distinct asymmetric and symmetric stretching bands of the N=O bond at 1535 cm<sup>-1</sup> and 1350 cm<sup>-1</sup> in its IR spectrum and no isolated absorption band at 1414 cm<sup>-1</sup> for the N=N stretching mode. Different are also the UV-Vis spectra of compounds **1**, **2** and **3**, although the differences between **2** and **3** are small (Figure 4). **3** displays an absorption peak at about 319 nm ( $\epsilon \sim 7700 \text{ M}^{-1}\text{cm}^{-1}$ ), while **2** shows a lower intensity absorption peak at about 323 nm ( $\epsilon \sim 5600 \text{ M}^{-1}\text{cm}^{-1}$ ); the mentioned absorption bands correspond to the azo and azoxy chromophoric groups, respectively.

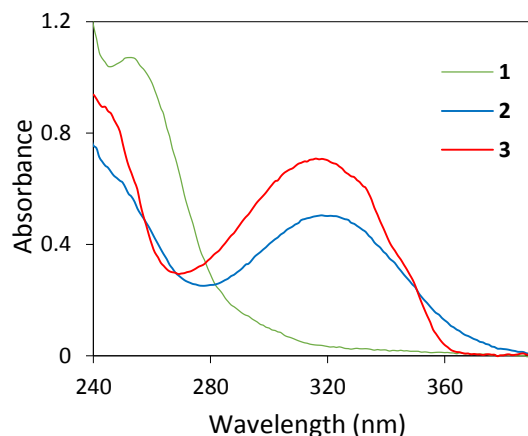


**Figure 5:** UV-Vis absorption spectra of compounds **1**, **2** and **3** in ethanol (0.033 mg/mL).

### 2.1.3 Compound **4** (3,3',5,5'-Hydrazobenzene Tetracarboxylic Acid)

Over-reduction of the azobenzene (**3**) generates 3,3',5,5'-hydrazobenzene tetracarboxylic acid (**4**) and 5-aminoisophthalic acid (**5**). The latter is commercially available and was identified by its  $^1\text{H}$ -NMR spectrum but the structure of **4** has not been previously reported. Figure 6 shows the distinctly different  $^1\text{H}$ -NMR spectra of both compounds.

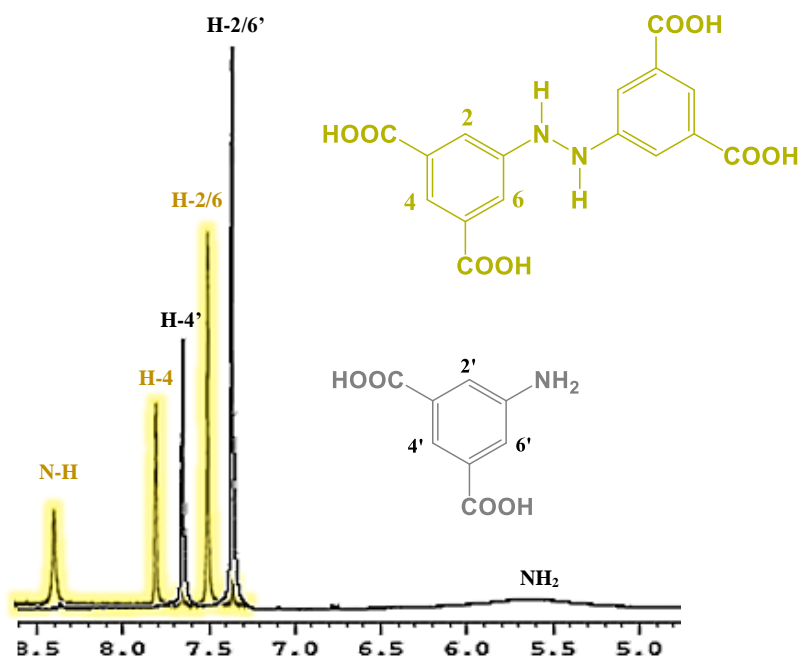


**Figure 6:** Comparison of  $^1\text{H}$ -NMR spectra for experimental **4** (yellow) and commercial 5-aminoisophthalic acid (black), recorded in  $\text{DMSO-d}_6$  (5.0-8.5 ppm range) at 300 MHz.

The assignment of the hydrazine protons by  $^1\text{H}$ -NMR was subsequently confirmed with 2D  $^{15}\text{N}$ - $^1\text{H}$  hetero-nuclear single quantum coherence spectroscopy. The HSQC experiment is a highly sensitive technique used to detect correlation of nitrogen nuclei with attached hydrogen nuclei. As expected, the  $^{15}\text{N}$ - $^1\text{H}$  HSQC spectra of **4** displayed an observable peak characteristic of the proton directly attached to the nitrogen (8.37 ppm), thus confirming the identity of the hydrazine group and the hydrazobenzene derivative overall (Figure 7).

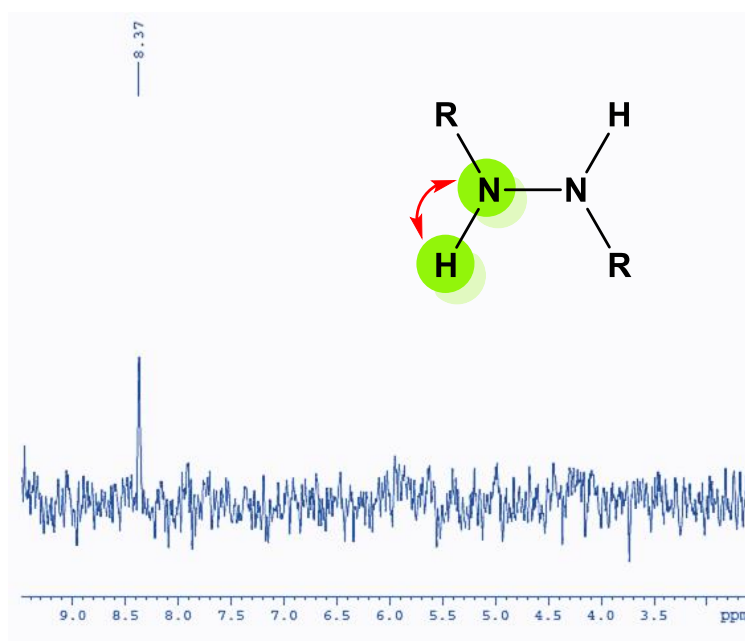


**Figure 7:**  $^{15}\text{N}$ - $^1\text{H}$  HSQC experimental spectra of **4** recorded in  $\text{DMSO-d}_6$ . The basic scheme of this experiment involves the transfer of magnetization on the proton to the  $^{15}\text{N}$  nucleus.

2D spectroscopic methods  $^1\text{H}$ - $^1\text{H}$  COSY,  $^1\text{H}$ - $^1\text{H}$  NOESY, and  $^1\text{H}$  DOSY NMR were utilized to further confirm the chemical structure of 3,3',5,5'-hydrazobenzene tetracarboxylic acid (**4**). COSY NMR, otherwise known as correlation spectroscopy allows us to easily determine which peaks in the  $^1\text{H}$ -NMR spectra are coupled to each other by exchanging magnetization. In order to detect these  $^1\text{H}$ - $^1\text{H}$  correlations via spin coupling interactions, nuclei must be closely connected by chemical bonds. Specifically, the cross peaks observed off-diagonal in the COSY NMR spectrum

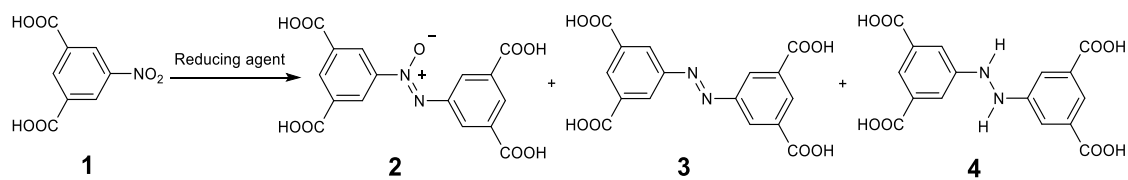


of **4** indicated that the protons in the ortho (H-2/6) and para (H-4) positions are indeed correlated through scalar coupling (Figure 28). On the other hand, NOESY is another type of 2D  $^1\text{H}$ - $^1\text{H}$  NMR that uses the nuclear Overhauser effect to detect correlation peaks due to proton nuclei that are spatially near to each other, even if they are not coupled through bonds. This effect is described as a through-space correlation rather than a scalar coupling interaction. In the NOESY spectrum of **4** (Figure 29), we see a significant cross peak indicating a spatial interaction between the hydrazine proton (N-H) and the protons in the ortho position (H-2/6). All these spectroscopic findings agree with the chemical structure of the hydrazobenzene derivative, especially since the hydrazine and ortho protons are theoretically close enough in space to observe through-space transfer of nuclear spin polarization. Finally, 2D DOSY NMR experiments were conducted to further differentiate 3,3',5,5'-hydrazobenzene tetracarboxylic acid from 5-aminoisophthalic acid. Diffusion ordered spectroscopy is mainly used to determine the diffusion coefficients of solute molecules based on their hydrodynamic volume size. According to the NMR diffusion experiments, **4** has a calculated diffusion coefficient of  $7.39 \times 10^{-10} \text{ m}^2\text{s}^{-1}$  (Figure 27), whereas **5** was found to have a diffusion coefficient of  $1.21 \times 10^{-9} \text{ m}^2\text{s}^{-1}$  (Figure 33). The difference in the values of diffusion coefficient of these two compounds is quite apparent. These results are well correlated with the fact that the hydrazobenzene derivative is nearly twice as larger than the aniline derivative, therefore as expected, the aniline was experimentally shown to diffuse 1.64 times faster than **4**. MS measurements for compound **4** were not conclusive since no m/z peaks were observable in the range of 360-361 using ASAP mass spectra in (+) resolution mode. Surprisingly, a significant m/z peak was observed at 182.0455, possibly suggesting the decomposition of the hydrazo (**4**) into the aniline form (**5**).

## 2.2 Solution-Based Synthesis of 3,3',5,5'-Azobenzene Tetracarboxylic Acid

I started the development of a scalable and economical synthesis of 3,3',5,5'-azobenzene tetracarboxylic acid from 5-nitroisophthalic acid by studying suitable reported reactions that were exclusively run in solution as batch reactions.<sup>88-92</sup> All reported procedures use either zinc or D-glucose as reducing agents and alcohols and/or water as solvents. Reactions investigated here were run under aqueous basic conditions at temperatures between 60-65 °C. The methods differed in their concentrations of base, reaction time, and work-up steps. The solution-based syntheses discussed herein were optimized by changing the amount of reducing agent, the amount of base, and reaction time. Table 1 lists the reaction and work-up conditions for the highest yielding test runs, along with the obtained yields of isolated 3,3',5,5'-azobenzene tetracarboxylic acid.

**Table 1** Highest yielding conditions for batch reduction of 5-nitroisophthalic acid<sup>a</sup>



Entry	Reducing agent (equiv.)	[Base]	Solvent (ratio)	Temperature (°C)	Time (h)	CY <sup>b</sup> (%)	Yield <sup>c</sup> (%)		
							2	3	4
1	Zn (4.0)	2 M NaOH	MeOH: H <sub>2</sub> O (3:1)	Reflux	24	68	-	48	20
2	C <sub>6</sub> H <sub>12</sub> O <sub>6</sub> (4.0)	1M NaOH	H <sub>2</sub> O	60	24	65	5	35	25

<sup>a</sup> Reaction conditions: **1** (1.0 equiv.) was reduced in solution under basic conditions. The organic filtrate was acidified with 3 M HCl (aq) to a pH = 3 to obtain a precipitate from aqueous solution. Recrystallization from DMF was carried out to purify product **3**. For details, see Experimental Section. <sup>b</sup> Combined yield as the sum of isolated yields of products **2**, **3** and **4**. <sup>c</sup> Compound ratios were determined by <sup>1</sup>H NMR.

Treatment of 5-nitroisophthalic acid with only 2 equivalents of Zn in 0.3 M NaOH solution of ethanol/water (3:1) mixture was reported as a suitable preparation of compound **3** with a yield of 65%.<sup>88, 89</sup> Under these reaction conditions, however, I found that the azoxy intermediate (**2**) was obtained as the major product, along with a negligible amount of compound **3**. I then successfully isolated compound **2** as yellow crystals in 60% yield by recrystallization from DMF. Our best outcome achieved for zinc mediated reduction was based on the procedure reported by Bigelow.<sup>90</sup> The reaction was run with 4 equivalents of Zn in a 2 M NaOH solution of a mixture of methanol and distilled water (3:1). A higher base concentration was used to facilitate the interaction amongst the reagents in solution by assuring full deprotonation of all four carboxylic acid sites of the starting material and intermediate species. This mixture was heated to reflux for 24 hours and the product was crystallized out by a slow addition of acid. In this case, when the starting material was treated with an excess amount of zinc metal, no azoxy intermediate was detected, and NMR analysis revealed a product mixture of the expected azo compound (48% yield) and the over-reduced hydrazo derivative (20% yield). Recrystallization of the product mixture from DMF gave compound **3** as pure orange crystals in 45% yield.

According to a procedure reported by Miller and coworkers, the reduction of 5-nitroisophthalic acid with 6 equivalents of glucose stirring in strongly alkaline water solution (3 M NaOH) for 4 hours at room temperature gives compound **3** in 70% yield.<sup>92</sup> Our test reactions revealed the formation of appreciable amounts of the azoxy intermediate and hydrazo by-product, but no trace of the azo compound was detected. Next, our highest yield for glucose-mediated reduction was achieved with a combination of conditions and work-up steps reported by Westphal<sup>91</sup> and Miller.<sup>92</sup> The optimized reaction conditions were as follows: compound **1** and 4 equivalents of glucose were stirred in a 1 M NaOH solution at 60 °C for 24 h. In particular, the base concentration in our test

reaction was increased to 6 equivalents of base with respect to the procedure reported by Westphal, which used 4 equivalents of base instead.<sup>91</sup> The product was precipitated by careful addition of 3 M HCl<sub>(aq)</sub>, and recrystallized from DMF to obtain pure **3** in 30% yield (Table 1, entry 2). Based on these results, an increase of the reaction time and temperature in the presence of 4 equivalents of glucose increased the formation of the azo compound. A general problem with the use of glucose is that it is difficult to remove from the product mixture, which causes over-reduction of **3** to the aniline form if heated in aqueous solution to temperatures exceeding 60°C. This typically resulted in the formation of a black sticky solid.

In principle, the reduction of nitroarenes to the corresponding azobenzene requires six metal electrons, otherwise the oxidation of three equivalents of zinc metal (Scheme 9). In this study, however, reduction using less than three equivalents of zinc stops at the azoxy intermediate (**2**), while three or more equivalents of zinc generate a mixture of azo (**3**) and over-reduced hydrazoarenes (**4**). Despite the lower reducing strength of glucose ( $E^{\circ}_{\text{ox}} = 0.60 \text{ V}$ ) being half as strong as zinc ( $E^{\circ}_{\text{ox}} = 1.25 \text{ V}$ ), over-reduced by-products were also formed in glucose-mediated reactions. To explain this phenomenon, one needs to examine the electrochemical properties of azoxy, azo, and hydrazo derivatives relative to one another. Chuang et al. investigated the voltammetric reduction of azobenzene and azoxybenzene, and the oxidation of hydrazobenzene in aqueous 50% ethanol solutions over the pH range of 1.6 to 12.5 (Figure 8).<sup>95</sup> These experiments are comparable to the synthetic conditions (e.g. in alcoholic solution with pH >12) and relative voltammetric behavior of compounds **2**, **3** and **4**.

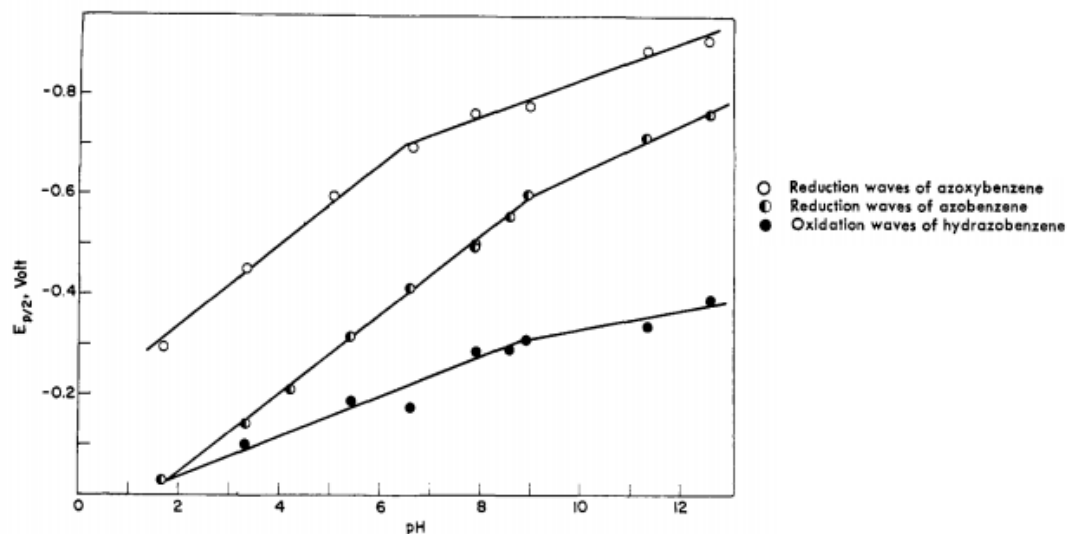


**Figure 8:** Variation with pH of half-peak potentials of azobenzene, azoxybenzene, and hydrazobenzene at P.G.E in 50% aqueous-ethanol buffered solutions.<sup>95</sup>

At the pyrolytic graphite electrode (P.G.E), azoxybenzene undergoes a two-electron reduction to azobenzene, while azobenzene undergoes a two-electron reduction to hydrazobenzene. The half-peak potential of these compounds shown in Figure 8 varies linearly over the pH range, however a change in slope is observed at about a pH of 6.5 for azoxybenzene, and pH 9 for the other two compounds. According to these values, azoxybenzene has a half-peak reduction potential of -0.91 V at pH 12.5, whereas azobenzene a half-peak reduction potential of -0.76 V. Due to its lower reduction potential, it is easier to electrochemically reduce azobenzene to the hydrazo form than it is to reduce azoxybenzene to the azo product. Consequently, reducing agent in solution chemistry will reduce the formed azo product faster than the azoxy intermediate. Although four carboxylic acid groups could decrease the reduction potential of compound **2** by increasing the electron affinity of the N-oxide bond due to their moderately electron withdrawing nature, the formation of compound **4** is nearly impossible to avoid in the presence of a reducing agent that is sufficiently strong to simultaneously overcome the reduction potentials of compounds **2** and **3**.

### **2.3 Ball Mill Synthesis of 3,3',5,5'-Azobenzene Tetracarboxylic Acid**

Optimization of the batch reaction did not lead to yields higher than 45%, which was an encouragement to search for other synthetic methodologies without having to significantly change the involved chemicals. Attempts to run these reactions by microwave or flow chemistry were not fruitful. The heterogeneous mixture with Zn as reducing agent was expectedly difficult to transfer to a flow setup or a microwave reactor, and test reactions with glucose gave complex dark mixtures that were difficult to separate. Mechanochemistry by ball milling was then chosen to be a better alternative, especially for the heterogeneous mixture with zinc. Also, the very small amounts of solvent used for ball milling make it environmentally more benign and potentially more economical.

All experiments were conducted using a laboratory-scale ball milling unit (Retsch mixer mill MM400) equipped with a pair of 15 mL stainless steel jars and stainless steel milling balls. The milling jars were oscillated in a horizontal position at an operating frequency of 30 Hz. The general reaction procedure is as follows: A mixture of 5-nitroisophthalic acid and sodium hydroxide powder was placed in a stainless steel jar with one or two stainless steel ball(s). Two to three drops of solvent (3:1 methanol/water) were added before closing the screw-top jar to allow the formation of a paste during milling. The reaction vessel was shaken on the ball mill apparatus at a frequency of 30 Hz for 10 minutes. The milling was stopped and zinc dust was added to the resulting pink paste with a drop of solvent (3:1 methanol/water). The reaction mixture was ball milled at a frequency of 30 Hz for 2 to 4 hours. The resulting gray to olive green paste consisted of a mixture of precipitated zinc oxide and organic compounds. The solid mixture was poured in 10 mL of water to give an orange or yellow supernatant and then filtered. The filtrate was acidified with 2 M HCl (aq) to a pH of 3, and the resulting orange precipitate was filtered and air dried to give

mixtures of the azoxy (**2**), azo (**3**) and hydrazo (**4**) compounds that were quantified by  $^1\text{H}$  NMR. Unreacted starting material (**1**) found in all of the crude reaction mixtures and occasional small amounts of aniline derivative (**5**) were not quantified because they remained in the aqueous acidic solution.

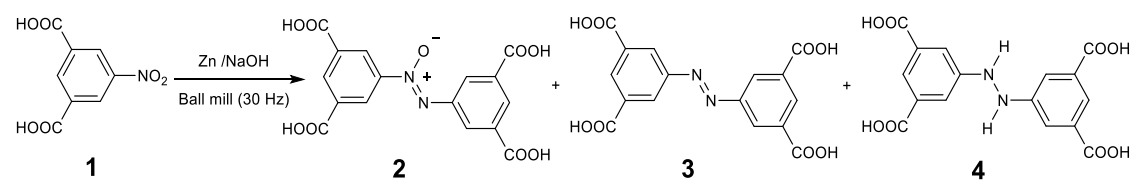
The following part describes and discusses the optimization of the reaction conditions for ball milling. It is subdivided by the optimization of technological parameters (size and number of milling balls), process parameters (milling time) and chemical parameters (type and relative amount of reducing agent). A potential influence of atmospheric oxygen on the product composition was inevitable as the milling reactor was not airtight.

## 2.4 Optimization of Technological Parameters

### 2.4.1 Optimization of Size and Number of Milling Balls

The size of the milling ball(s) is an important technological parameter and, hence, was investigated thoroughly. Milling balls that measure 5 mm, 7 mm, and 8 mm in diameter were tested in single ball mode reactions (Table 2). To confirm the consistency of the ball size effect on the experimental outcome, the reactions were repeated with different amounts of zinc.

**Table 2** Zinc-mediated mechanochemical reduction under single ball milling mode <sup>a</sup>



Entry	Zinc (equiv.)	No. of balls (diameter)	Milling time (h)	CY <sup>b</sup> (%)	Yield <sup>c</sup> (%)		
					2	3	4
1	4.0	1 x (5 mm)	3	50	20	20	10
2	5.0	1 x (5 mm)	3	58	9	17	32
3	3.0	1 x (7 mm)	3	54	19	20	15
4	4.0	1 x (7 mm)	3	60	10	16	34
5	3.0	1 x (8 mm)	3	60	16	27	17
6	4.0	1 x (8 mm)	3	64	4	9	51

<sup>a</sup>Reaction conditions: **1** (1.66 mmol, 1.0 equiv.), NaOH powder (10 mmol, 6.0 equiv.), 3:1 methanol/water solvent (0.35 mL) under ball-milling at 30 Hz. For details, see Experimental Section. <sup>b</sup>Combined yield as the sum of isolated yields of products **2**, **3** and **4**. <sup>c</sup>Compound ratios were determined by <sup>1</sup>H NMR.

Contrarily, while the diameter of the milling ball was kept constant, I investigated the effect of the number of milling balls on the outcome of this reaction. The milling procedures in Table 2 were repeated with two milling balls of the respective diameters (Table 3). These reactions were also repeated with different amounts of zinc to confirm the consistency of the experimental trend.



**Table 3** Zinc-mediated mechanochemical reduction under two-balls milling mode

Entry	Zinc (equiv.)	No. of balls (diameter)	Milling time (h)	CY (%)	Yield (%)		
					2	3	4
1	3.0	2 x (5 mm)	3	60	12	14	34
2	4.0	2 x (5 mm)	3	65	7	15	43
3	3.0	2 x (7 mm)	3	64	-	22	42
4	4.0	2 x (7 mm)	3	69	-	18	51
5	3.0	2 x (8 mm)	3	71	-	12	59
6	4.0	2 x (8 mm)	3	75	-	7	68

Figure 9 highlights the change in the combined yield with respect to the size and number of milling balls for reactions of the following conditions: 4 equivalents of Zn, 6 equivalents of sodium hydroxide and 0.35 mL of solvent are ball milled at 30 Hz for a duration of 3h. The results reveal a linear correlation between the chemical yield and the diameter of the milling ball; a single 5 mm milling ball affords a combined yield of 50%, a single 7 mm milling ball gives 60% combined yield, while a single 8 mm milling ball increases the combined yield to 64% (Table 2, entries 1, 4, 6). These observations indicate that the larger milling ball is more effective in the mechanically induced reduction of 5-nitroisophthalic acid. A similar correlation between the mass/size of the milling bodies and the chemical yield was previously observed for several other mechanically-induced organic reactions.<sup>50, 65, 71-73</sup> In particular, reactions involving cross-<sup>50</sup> and homo-coupling<sup>58</sup> processes have higher activation energies, and therefore require a greater amount of stress energy to initiate conversion. Based on Eq. (1), larger milling balls generate stronger impacts and increase the stress energy and bulk temperature of the milling media allowing to overcome higher activation energies and accelerate the rate of chemical reactions.<sup>64, 68, 69</sup> As expected, the increase in chemical conversion observed with larger milling balls clearly agrees with the observations of previous ball mill studies.

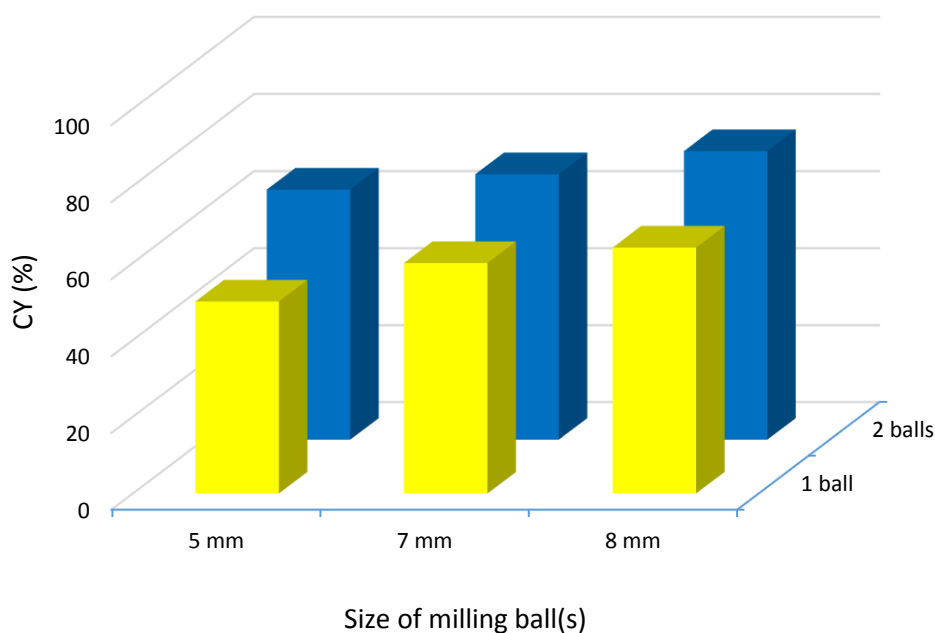


**Figure 9:** Correlation of the combined yield with the number of milling balls for each ball diameter (5 mm, 7 mm, and 8 mm). Reaction conditions: 4.0 equiv. of Zn, 6.0 equiv. of NaOH and 0.35 mL of solvent ball milled for 3h at 30 Hz.

Under the same mill operating conditions, the data also reveals a direct correlation between the yield and the number of milling balls (Figure 9). For each reaction of a particular ball size, the doubling of the number of balls had led to a 10-15% increase in the overall product yield. Additionally, the results indicate that the combination of the largest ball size with the higher number of milling balls (8mm x 2 balls) is most effective for reductive conversion, affording the highest combined yield of 75% (Table 3, entry 6). According to Rosenkranz et al., the probability for collision increases proportionally with the number of milling balls.<sup>74</sup> As a result, changing the number of balls is one possibility to influence the system's kinetic energy. The relationship between the product yield and number of milling balls was previously reported for several reactions including the Suzuki-Miyaura cross coupling reaction of aryl halides with phenylboronic

acid, and the oxidative homo-coupling of p-toluidin.<sup>50, 59-61</sup> Likewise, the influence of the number of milling balls on the outcome of the ball mill reduction of 5-nitroisophthalic acid is consistent with the physical relations and studies mentioned above.

## 2.5 Optimization of Process Parameters

### 2.5.1 Optimization of Milling Time

The reaction progress of the mechanochemical reduction of 5-nitroisophthalic acid was evaluated based on reaction time while the oscillation frequency was kept constant at 30 Hz. The reaction mixtures reported below were subjected to the same workup procedure.

**Table 4** Mechanochemical reduction of 5-nitroisophthalic acid with respect to milling time

Entry	Zinc (equiv.)	No. of balls (diameter)	Milling time (h)	CY (%)	Yield (%)		
					2	3	4
1	4.0	1 x (5 mm)	2	50	20	20	10
2	4.0	1 x (5 mm)	3	54	14	18	22
3	4.0	1 x (5 mm)	4	62	10	36	16
4	4.0	2 x (5 mm)	2	60	15	17	28
5	4.0	2 x (5 mm)	3	65	7	15	43
6	4.0	2 x (5 mm)	4	75	-	54	21
7	3.0	2 x (7 mm)	2	57	29	21	7
8	3.0	2 x (7 mm)	3	64	-	22	42
9	2.5	2 x (8 mm)	2	62	41	19	2
10	2.5	2 x (8 mm)	3	65	33	29	3
11	3.0	2 x (8 mm)	2	67	12	20	35
12	3.0	2 x (8 mm)	3	71	-	12	59

Reactions of entries 1-12 in Table 4 were carried out to evaluate the influence of milling time under different milling conditions (e.g. ball size, number of milling balls, and amount of reducing agent). For all tested conditions, quantifiable amounts of compound **3** (17- 21% yield) were generated only after 2 hours of milling time, however the reaction also proceeded to generate

compound **4**. Figure 10 highlights the trend observed in the product composition of the following reactions with respect to time. In the presence of 3 equivalents of zinc, the N-oxide intermediate product (**2**) was completely consumed after 3 hours when using a pair of 7 mm balls (Table 4, entry 8) or 8 mm balls (Table 4, entry 12). With all of compound **2** consumed, one assumes that the time it takes for one equivalent of starting material (**1**) to completely undergo reductive coupling under these specific conditions is approximately 3 hours. Moreover, the results revealed a consistent increase in the formation of compound **4** as the time was increased to 3 hours. For instance, the amount of hydrazo by-product (**4**) increased from 7% to 42% when the milling time was increased from 2 to 3 hours using a pair of 7 mm balls (Table 4, entries 7 and 8). Similarly, compound **4** increased from 35% to 59% yield upon 3 hours of milling time using a pair of 8 mm balls (Table 4, entries 11 and 12).

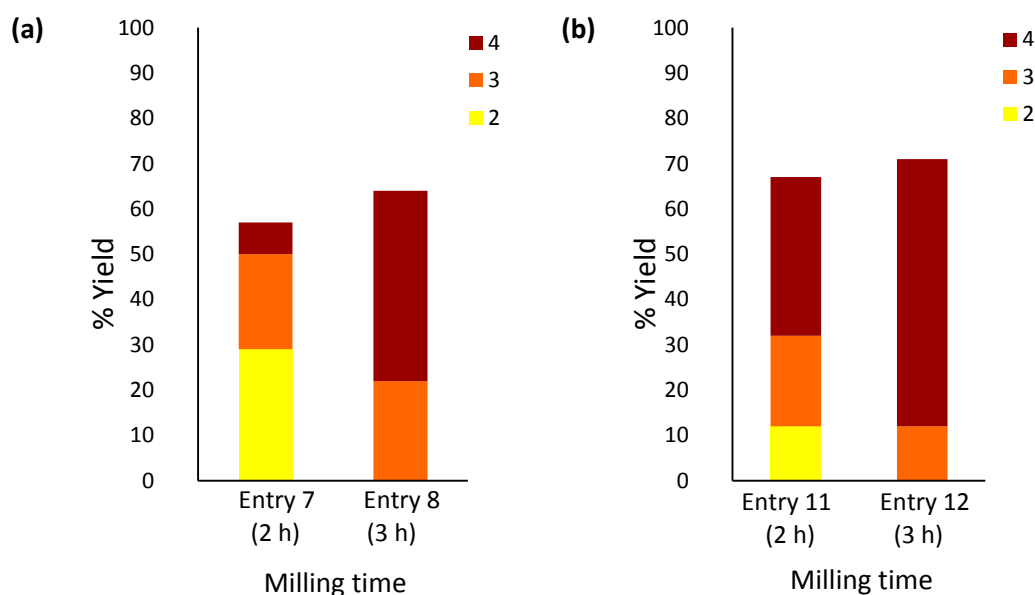


**Figure 10:** Influence of milling time (h) on the product composition (%). These results correspond to specific experimental entries operated at 30 Hz. Milling conditions: (a) 3.0 equiv. of Zn, 2 x 7 mm balls (b) 3.0 equiv. of Zn, 2 x 8 mm balls. Yields of compounds **2**, **3** and **4**.

Whether one or two milling balls were used in the following set of reactions, significant shifts in product distributions towards compound **4** were also observed after 3 hours. For example, milling compound **1** with 4.0 equivalents of Zn and one 5 mm ball for a period of 2 hours gave a combined product yield of 50% that is composed of 20% **2**, 20% **3**, and 10% **4** (Table 4, entry 1). After 3 hours of ball milling, the combined yield increased to 54% and the product distribution changed to 14% **2**, 18% **3**, and 22% **4** (Table 4, entry 2). In another set of reactions, milling compound **1** with 4.0 equivalents of Zn and two 5 mm balls for 2 hours gave a combined yield of 60% that is composed of 15% **2**, 17% **3**, and 28% **4**, whereas after 3 hours, the product distribution expectedly changed to 7% **2**, 15% **3**, and 43% **4**, giving a combined yield of 65% (Table 4, entry 5). After 4 hours of ball milling, the combined yield of the latter had increased to 75%, however the percentage of compound **3** had increased to 54%, whereas the amount of compound **4** had unexpectedly decreased by one half to 21% (Table 4, entry 6). Such fluctuations in product distributions of the reaction mixtures at different milling times were observed in both of the one and two milling balls reactions as highlighted in Figure 11. In this case, the reduction of compound **1** to compound **4** seemed to be most effective within 3 hours of milling time most likely because of a potential influence of atmospheric oxygen on the reaction mixture that is prolonged with longer milling time and could oxidize compound **4** and convert it to compound **3**. Clearly, longer reaction times in non-airtight milling containers could counteract the effect of the reducing agent and reverse the reaction pathway.

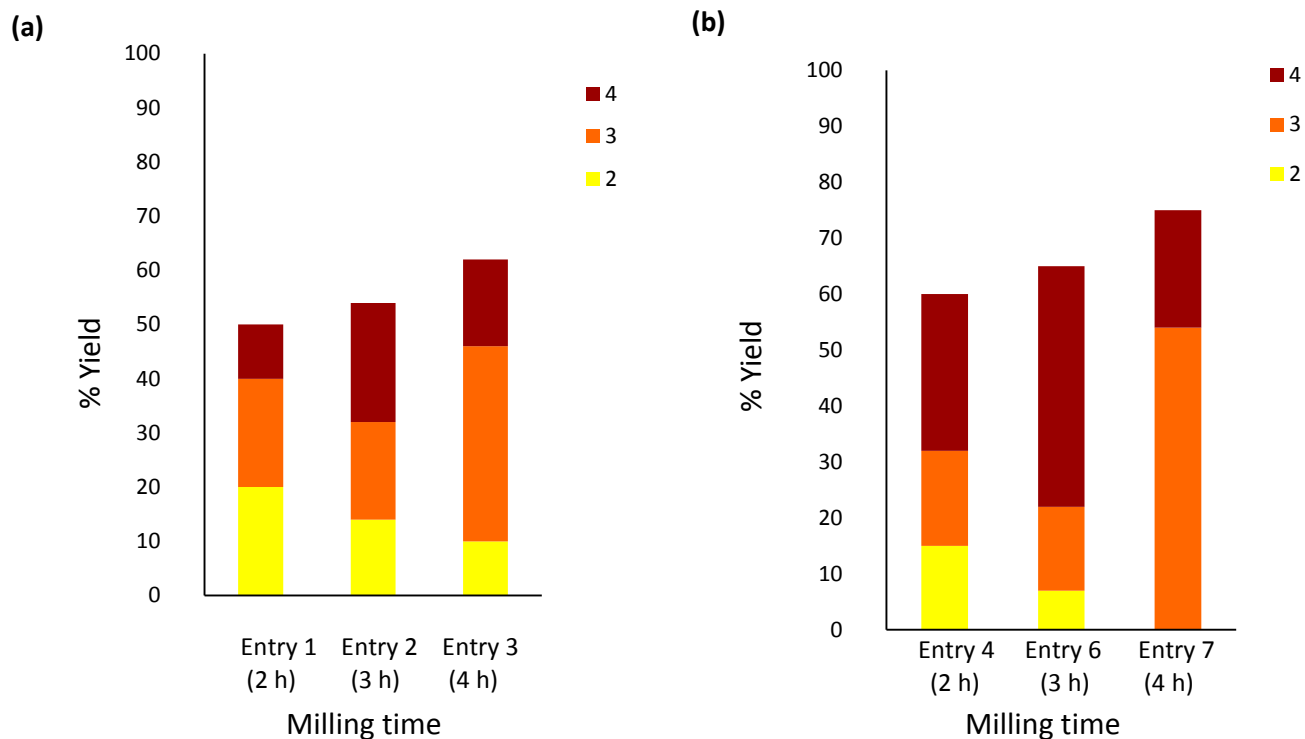


**Figure 11:** Influence of milling time (h) on the product composition (%). These results correspond to specific experimental entries operated at 30 Hz. Milling conditions: (a) 4.0 equiv. of Zn, 1 x 5 mm ball (b) 4.0 equiv. of Zn, 2 x 5 mm balls. Yields of compounds **2**, **3** and **4**.

The obvious question here is what happens after 5 to 6 hours of milling time? With limited amounts of reducing agent and the infiltration of atmospheric oxygen into the reaction vessel, the reaction reaches a chemical equilibrium in which the reduction of the azo (**3**) proceeds at the same rate as the oxidation of the hydrazo (**4**). As a result, the product ratio of compounds **3** and **4** have no further tendency to change with time.

## 2.6 Optimization of Chemical Parameters

### 2.6.1 Optimization of the Amount of Zinc Reducing Agent

The influence of the quantity of reducing agent on the mechanochemical reduction of 5-nitroisophthalic acid is summarized in Table 5.

**Table 5** Mechanochemical reduction of 5-nitroisophthalic acid with various amounts of zinc dust

Entry	Zinc (equiv.)	No. of balls (diameter)	Milling time (h)	CY (%)	Yield (%)		
					2	3	4
1	4.0	1 x (5 mm)	3	54	14	18	22
2	5.0	1 x (5 mm)	3	58	9	17	32
3	3.0	2 x (5 mm)	3	60	12	14	34
4	4.0	2 x (5 mm)	3	65	7	15	43
5	3.0	1 x (7 mm)	3	54	19	20	15
6	4.0	1 x (7 mm)	3	60	10	16	34
7	2.5	2 x (7 mm)	3	64	41	23	-
8	3.0	2 x (7 mm)	3	64	-	22	42
9	4.0	2 x (7 mm)	3	69	-	18	51
10	3.0	1 x (8 mm)	3	60	16	27	17
11	4.0	1 x (8 mm)	3	64	4	9	51
12	2.5	2 x (8 mm)	3	65	33	29	3
13	3.0	2 x (8 mm)	3	71	-	12	59
14	4.0	2 x (8 mm)	3	75	-	7	68

Based on the reaction equation (Scheme 9), a minimum of 3 equivalents of zinc are required for the complete conversion of **1** to **3**, while 2 equivalents of zinc are sufficient for the formation of compound **2** and 4 equivalents are required for the generation of compound **4**. Below the required theoretical amount of zinc (e.g. 2.5 equivalents), 41% azoxy was obtained as major intermediate product, along with 23% azo when treated with 7 mm balls, while 33% azoxy, 29% azo, and a negligible amount of hydrazo by-product (3% yield) were obtained using 8 mm balls (Table 5, entries 7 and 12). For reactions using 3 equivalents of zinc instead, mixtures of azoxy,

azo, and hydrazo products were consistently obtained after 3 hours of mechanochemical treatment regardless of the applied size and number of milling balls (Table 5, entries 3, 8, 10, and 13). For all tested conditions, an increase of the relative amount of zinc by 1 equivalent expectedly increased the amounts of formed products, but only by 8% or less. More significant were the large shifts in product distributions towards **4**. For example, 3 equivalents of zinc and a 7 mm ball yielded 19% **2**, 20% **3**, and 15% **4**, giving a combined yield of 54%, whereas 4 equivalents of zinc and a 7 mm ball yielded 10% **2**, 16% **3**, and 34% **4**, giving a combined yield of 60% (Table 5, entries 5 and 6). In particular, over-reduction in the presence of 4 equivalents of zinc was most significant for reactions using a single 8 mm ball. This can be seen in the following example: ball milling **1** with 4 equivalents of zinc for 3 hours using a single 8 mm ball had tripled the yield of **4** to 51 % while drastically decreasing the yield of **2** and **3** relative to the treatment with 3 equivalents of zinc (Table 5, entry 11). In contrast, ball milling **1** with 4 equivalents of zinc for 3 hours using two 8 mm balls had slightly shifted the yields of **4** and **3** with respect to the treatment using 3 equivalents of zinc (Table 5, entry 14).

The random movement of the ball mill content may be responsible for the formation of product mixtures of azo, hydrazo, and N-oxide derivatives. In this case, parts of the mixture which undergo more impact are more likely to be over-reduced. Moreover, the unequal distribution of the solid reagents causes a portion of the metal content to react with the starting material and form the azoxy intermediate (**2**), while another portion simultaneously reacts with the initially formed azo product only to give the over-reduced hydrazo compound (**4**). Although the formation of mixtures could not be avoided, the composition of these mixtures could be shifted in favour of a particular product by modifying the amount of reducing agent. These shifts were surprisingly most pronounced for reactions using one 8 mm ball in comparison to two 8 mm balls, most likely because of a



dependence of the momentum of the colliding bodies on the filling degree of the milling jar. In general, the milling bodies require space for movement and efficient energy transfer.<sup>56</sup> When two of the largest balls (8 mm) are added to the milling reactor, the ball-to-powder ratio increases and the milling space becomes more restricted. As a result, the milling balls cannot accelerate nor gain enough momentum to make their way through the vessel. While the filling level did not exceed 40% of the milling volume for all experiments, doubling the number of 8 mm balls hampers the amount of energy that could be transferred to the system, and thus counteracts the effect of the amount of zinc on the chemical conversion.

### 2.6.2 Influence of Wet and Dry Milling Conditions

Table 6 below reports on experiments that investigate the influences of dry and wet milling methods on the mechanochemical reduction of 5-nitroisophthalic acid. In this context, ball milling under dry conditions (e.g. strictly in the absence of liquid that can act as a solvent) is pertinent to the term “solvent-free” mechanochemical synthesis. Contrarily, reactions that require minimal solvent are more properly labeled as “solvent-assisted” mechanochemical synthesis.

**Table 6** Mechanochemical reduction of 5-nitroisophthalic acid under dry and wet conditions<sup>a</sup>

Entry	Reducing agent (equiv.)	Base (equiv.)	Solvent (mL)	No. of balls (diameter)	Time (h)	CY <sup>b</sup> (%)	Yield <sup>c</sup> (%)		
							<b>2</b>	<b>3</b>	<b>4</b>
1 <sup>e</sup>	Zn dust (3.0)	NaOH (6.0)	-	2 x (5 mm)	3	32	21	11	-
2	Zn dust (3.0)	NaOH (6.0)	MeOH (0.35)	2 x (5 mm)	3	60	8	14	38

<sup>a</sup> Reaction conditions: **1** (1.66 mmol, 1.0 equiv.), ball-milling at 30 Hz. Anhydrous methanol (0.35 mL) and thin magnesium turnings, as such, were used. <sup>b</sup> Combined yield as the sum of isolated yields of products **2**, **3** and **4**. <sup>c</sup> Compound ratios were determined by <sup>1</sup>H NMR. <sup>e</sup> Ball-mill reaction was carried out without solvent (dry ball-milling).

In the absence of 2-3 drops of solvent, the reaction of 5-nitroisophthalic acid with 3 equivalents of zinc gave low conversion (32% combined yield); most of the starting material was recovered unreacted (Table 6, entry 1). To our surprise, dry milling the solid reagents resulted in more compacted and heterogeneous agglomeration of the zinc mixture rather than a single-colored solid paste. These observations demonstrate the crucial role of the availability of the metal surface in the reductive coupling of nitroarenes. On the other hand, liquid-assisted milling under the same conditions revealed that the addition of a drop of organic solvent such as methanol to the nitroarene-zinc mixture prior to milling afforded a twice as high yield (Table 6, entry 2). As in previously reported studies,<sup>77, 78</sup> the presence of small amounts of solvent was shown to have advantageous effects on the performance of this particular reaction. In this case, these observations suggest that methanol plays an important mechanistic role in the zinc-mediated reduction of aromatic nitro compounds. Due to its protic nature, methanol is likely capable per se of functioning as a proton source to allow reductive hydrogenation under basic conditions.

### 2.6.3 Optimization of Type of Reducing Agent

After achieving appreciable amounts of azo derivatives from the zinc-mediated reduction of 5-nitroisophthalic acid, it was our interest to find other low cost reducing agents with stronger reducing power (Table 7) that could potentially generate **3** fast and in high yields, and without the formation of any **4**. Zechmeister and Rom reported the reduction of aromatic nitro compounds to azoxy compounds using Mg metal and methanol as solvent (30-90% yield).<sup>68</sup> Depending upon the amount of Mg, they also obtained azo products, while a large excess of Mg would produce hydrazobenzene derivatives. On the other hand, Pasha et al. reported the preparation of azoarenes in high yields (>90%) by reduction of nitroarenes using aluminum metal also in the presence of sodium hydroxide in methanol but under the influence of ultrasound.<sup>44</sup> These reported methods

share very similar conditions with the current methodology, thus I decided to investigate the utility of Al and Mg as two inexpensive and readily available oxide protected reducing agents in the ball mill assisted reduction of compound **1**, as well as D-glucose as it was also tested in solution. These reducing agents were evaluated by tuning various parameters including milling time, quantities, and milling balls (Table 8).

**Table 7** Standard reduction potentials of selected reducing agents vs. SHE under basic conditions.

$C_6H_{12}O_7 + 2 H^+ + 2 e^- \rightleftharpoons C_6H_{12}O_6 + H_2O$	-0.60 V	
$Fe(OH)_2(s) + 2 e^- \rightleftharpoons Fe(s) + 2 OH^-$	-0.89 V	
$Zn(OH)_2(s) + 2 e^- \rightleftharpoons Zn(s) + 2 OH^-$	-1.25 V	
$Al(OH)_3(s) + 3 e^- \rightleftharpoons Al(s) + 3 OH^-$	-2.31 V	
$Mg(OH)_2(s) + 2 e^- \rightleftharpoons Mg(s) + 2 OH^-$	-2.69 V	

**Table 8** Mechanochemical reduction of 5-nitrosophthalic acid with different reducing agents

Entry	Reducing agent (equiv.)	Base (equiv.)	Solvent (mL)	No. of balls (diameter)	Time (h)	CY (%)	Yield (%)			
							2	3	4	5
1	Mg (4.0)	NaOH (6.0)	MeOH (0.35)	2 x (5 mm)	1	0	-	-	-	-
2	Mg (4.0)	-	MeOH (0.35)	2 x (5 mm)	1	33	33	-	-	-
3	Mg (8.0)	-	MeOH (0.35)	2 x (5 mm)	3	36	34	2	-	-
4	Mg (8.0)	-	MeOH (0.35)	2 x (7 mm)	3	37	33	4	-	-
5	Mg (12.0)	-	MeOH (0.35)	2 x (8 mm)	4	49	41	8	-	-
6	Mg (12.0)	-	MeOH (0.35)	2 x (8 mm)	6	50	35	15	-	-
7	Al (4.0)	NaOH (6.0)	MeOH (0.35)	2 x (8 mm)	3	60	21	12	27	-
8	D-glucose (4.0)	NaOH (7.0)	H <sub>2</sub> O (0.5)	1 x (7 mm)	4	42	42	-	-	-
9	D-glucose (8.0)	NaOH (7.0)	H <sub>2</sub> O (0.5)	1 x (7 mm)	4	43	39	2	2	-
10	D-glucose (4.0)	NaOH (7.0)	H <sub>2</sub> O (0.5)	1 x (8 mm)	4	47	33	2	5	7
11	D-glucose (6.0)	NaOH (14.0)	H <sub>2</sub> O (0.5)	2 x (5 mm)	4	52	40	7	1	4
12	D-glucose (6.0)	NaOH (14.0)	H <sub>2</sub> O (0.5)	2 x (7 mm)	4	58	35	9	10	4

First, the solvent-assisted ball mill reactions were conducted using anhydrous methanol and thin magnesium turnings. Intriguingly, our control experiment using 4 equivalents of magnesium in the presence of a base did not yield any product, therefore no reduction had occurred (Table 8, entry 1). However, when the reaction was repeated without a base, compound **1** readily underwent reductive coupling to form the azoxy intermediate (**2**) in 33% yield (Table 8, entry 2). The resulting magnesium mixture had a pH of 11 in water, which suggests that the dark-gray rather than silver-white magnesium turnings were covered with a thin oxide layer. Activated and polished magnesium turnings were also tested for the same purpose, but no advantageous effect was observable for this reaction. Nevertheless, the reaction of compound **1** with magnesium as reducing agent was quite slow and incomplete. Attempted reductions of the nitro compound using larger amounts of magnesium (8 equiv.), longer milling time (3-6 h), as well as larger milling balls (8 mm), revealed insignificant changes in the product yield (Table 7, entries 3-6). While full conversion to the azoxy product was not observed, 41% yield of **2** was obtained in the presence of 12 equivalents of Mg and two 8 mm balls after 4 hours of milling time (Table 8, entry 5).

In comparison to magnesium, aluminum displayed stronger reducing capabilities for this particular reaction. Ball milling compound **1** with 4 equivalents of Al using two 8 mm balls led to the formation of a mixture consisting of 21% azoxy (**2**), 12% azo (**3**), and 27% hydrazo (**4**) (Table 8, entry 7). However, under the same milling conditions, zinc was more reducing than aluminum: the respective yields were 7 % azo (**3**), and 68 % hydrazo (**4**) as major product (Table 3, entry 6).

Finally, D-glucose was evaluated as a metal-free reducing agent for the mechanochemical reduction of **1** in the presence of sodium hydroxide and drops of water. Based on the optimized reaction conditions of our glucose-mediated reduction in solution, the ball milling experiment using glucose as reducing agent did not yield the desired azo product. Only the intermediate

product (**2**) was generated in 42% yield (Table 8, entry 8). However, doubling the amount of glucose generated small amounts of azo (**3**) and hydrazo (**4**) compounds in the resulting product mixture (Table 8, entry 9). An increase in the size of the milling ball from 7 mm to 8 mm even generated the over-reduced aniline derivative (**5**) in 7% of the overall yield (Table 8, entry 10). This was no surprise as glucose/NaOH systems have been previously reported for the reduction of nitro compounds to their corresponding amines.<sup>69</sup> Although the reduction was slightly improved with significantly greater amounts of base and a larger number and size of milling balls, the major product was always **2** under all of the examined reaction conditions (Table 8, entries 11, 12).

Magnesium metal has often appeared in literature as an excellent electron transfer reagent due to its ability to reduce a variety of functional groups such as nitro, oxime, and ketones.<sup>67</sup> However, despite its higher reduction potential magnesium cannot efficiently reduce the azoxy intermediate to the azo compound under ball milling conditions. This is probably because most of the magnesium is passivated with an oxide layer, which deactivates the metal surface. This also explains why no reduction had occurred with the addition of sodium hydroxide; the magnesium requires acidic conditions to help dissolve the protective oxide layer and expose the reactive metal surface. Even when activated magnesium turnings were used instead, this did not make any difference in the outcome of this reaction, presumably because magnesium is easily passivated in these abrasive conditions while under the influence of atmospheric oxygen. In this case, a huge excess of magnesium turnings may provide enough magnesium metal of zero oxidation state to reach higher conversion yields, however, after many experiments with increased quantities of magnesium, I finally abandoned this reducing agent as a mean of passing from the azoxy to the azo compound. On the other hand, glucose could not be easily removed from the product mixture;

even after multiple washings with water, small amounts of glucose still remained. For these purposes, it is more advantageous to use zinc as reducing agent in the synthesis of compound **3**.

## 2.7 Optimization of Workup of Mechanochemical Synthesis of 3,3',5,5'-Azobenzene Tetracarboxylic Acid

It is clear from the studies described above that all the variations of the reaction conditions for the ball milling can be used to accelerate the reaction and to alter the product ratios but no method allows for a selective synthesis of just the azobenzene derivative **3**. In principle, however, **3** is energetically lower than **2** and **4**, which should provide pathways for converting **2** and **4** into **3** and improve the overall yield. Fortuitously, I found that the workup applied to the crude solid mixture crucially affects the generated amount of the desired product (**3**). Consequently, I developed an additional step in the general workup procedure, in which the crude zinc mixture obtained after ball milling was simply immersed in alkaline solution while exposed to air (see experimental section for details).

**Table 9** Optimization of reaction parameters under basic conditions for mechanochemical synthesis of azobenzene <sup>a</sup>

Entry	Metal (equiv.)	No. of balls (diameter)	Milling time (h)	Exposure time in solution <sup>b</sup> (h)	CY <sup>c</sup> (%)	Yield <sup>d</sup> (%)		
						<b>2</b>	<b>3</b>	<b>4</b>
1	Zn dust (3.0)	2 x (5 mm)	3	48, NaOH (aq, 1 M)	90	-	90	-
2	Zn dust (3.0)	2 x (8 mm)	3	48, NaOH (aq, 1 M)	82	-	73	9
3 <sup>e</sup>	Mg turnings (12.0)	2 x (8 mm)	6	48, NaOH (aq, 1 M)	68	14	47	7

<sup>a</sup> Reaction conditions: **1a** (1.66 mmol, 1.0 equiv.), NaOH powder (10 mmol, 6.0 equiv.), 3:1 methanol/water solvent (0.35 mL) under ball-milling at 30 Hz. <sup>b</sup> Resulting solid mixture was transferred to NaOH (aq, 1 M) for 24-48 h under air. Ball-milling conditions and product extraction are optimized. <sup>c</sup> Combined yield as the sum of isolated yields of products **2**, **3** and **4**. <sup>d</sup> Compound ratios were determined by <sup>1</sup>H NMR. <sup>e</sup> Anhydrous methanol (0.35 mL) and thin magnesium turnings with oxide layer, were used. Ball-mill reaction was carried out without NaOH powder.

When compound **1** was milled with 3 equivalents of zinc and 5 mm balls for 3 hours, the mixture showed a 14% yield for **3**, along with an 12% yield for **2**, and 34% yield for **4** after the acidic workup (Table 3, entry 1). Some unreacted starting material **1** was also present but its amount was not quantified because it remains in solution during the workup. The yield for product **3** could be improved to 90% when the crude mixture generated by the reaction above (3.0 equiv. of Zn, 2 x 5 mm balls, 3 h) was kept in 1.0 M sodium hydroxide solution for 48 hours instead of proceeding directly to the acidic workup (Table 9, entry 1). Having established the optimal reaction conditions for the formation of azobenzene, I then hypothesized that, if the reaction mixture produced from different milling conditions was transferred to the same basic solution, the chemical equilibrium might be directed toward the selective formation of **3**. To verify this, another mill run of 3 hours long was performed using a combination of 3 equivalents of zinc and 8 mm balls. The corresponding product mixture of this particular reaction consisted of 12% **3**, and 59% **4** after the acidic workup (Table 3, entry 5). However, when the zinc mixture was kept in alkaline aqueous solution under atmospheric conditions instead of directly subjecting it to the acidic treatment, a chemical transformation was observed as indicated by the color change of the solution: the supernatant which was initially lemon yellow becomes bright orange, owing to the formation of the azobenzene derivative. Without the aid of expensive chromatographic purification, the crystalline product (**3**) simply precipitates out upon acidification in the final stage of the workup in 73% yield (Table 9, entry 2).

For the majority of the tested ball mill conditions, azobenzene **3** was readily reduced to hydrazobenzene **4**, yet a simple treatment had reversed the chemical equilibrium in favour of the azo product. At this point, one questions what are the possible pathways that are responsible for these conversions? My first assumption is that the only way a reaction mixture containing

compounds **1**, **2**, **3**, **4**, and **5**, can undergo an auxiliary and reversible oxidation-reduction process is if both reducing and oxidizing reagents are trapped inside the alkaline solution (Figure 12).

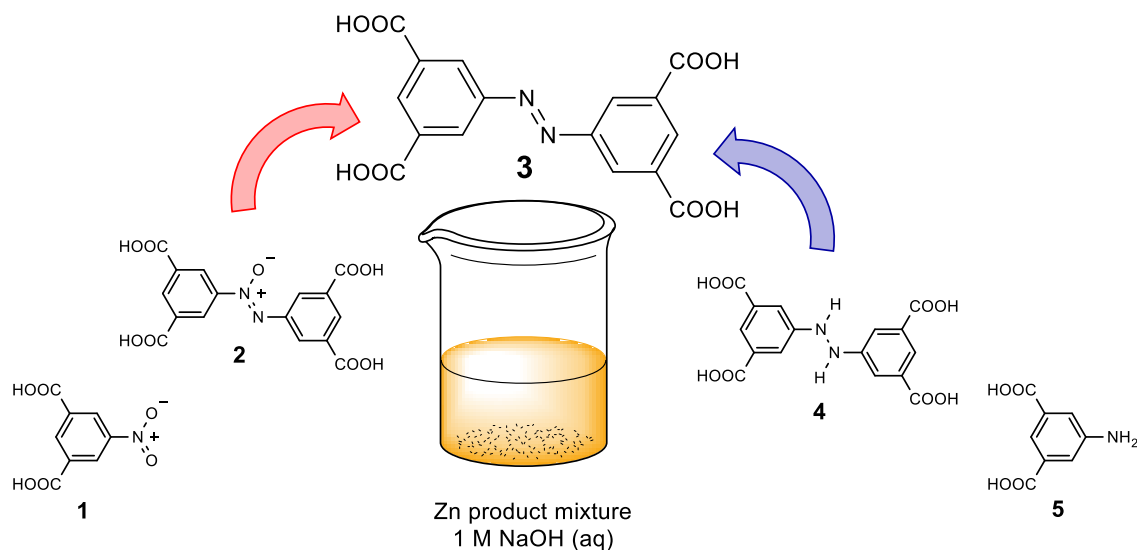


**Figure 12:** The workup procedure carried out in alkaline solution readily initiates a reversible oxidation-reduction process to form the azo product.

One of the most obvious chemical transformations is the oxidation of compound **4**. In general, hydrazo compounds are quite reactive and may be readily oxidized to the corresponding azo compounds by a variety of oxidizing agents including air. In fact, the oxidation of hydrazo compounds using atmospheric oxygen to achieve azo conversion has been proved to be a convenient method in other studies.<sup>96, 97, 98</sup> Hence, the presence of atmospheric oxygen is likely responsible for the oxidation of compound **4** into **3**. To further support this hypothesis, an attempt to oxidize the over-reduced species to the azo form was made by drawing dry air through an ethanolic solution of **4**. As shown in Figure 13, chemical changes associated with the conversion of **4** to **3** were monitored by UV-Vis spectroscopy. Initially, **4** displayed two major peaks. As the oxidation continued, the absorption at about 275 nm disappeared, while the absorption at about 330 nm, which was associated with the hydrazine group, shifted to a shorter wavelength that is



characteristic of the azo group (319 nm). These results not only prove the role of atmospheric oxygen as a mild oxidizing agent in the equilibrium process, but also show that compound **4** is less stable than compound **3** due to its tendency toward aerial oxidation.

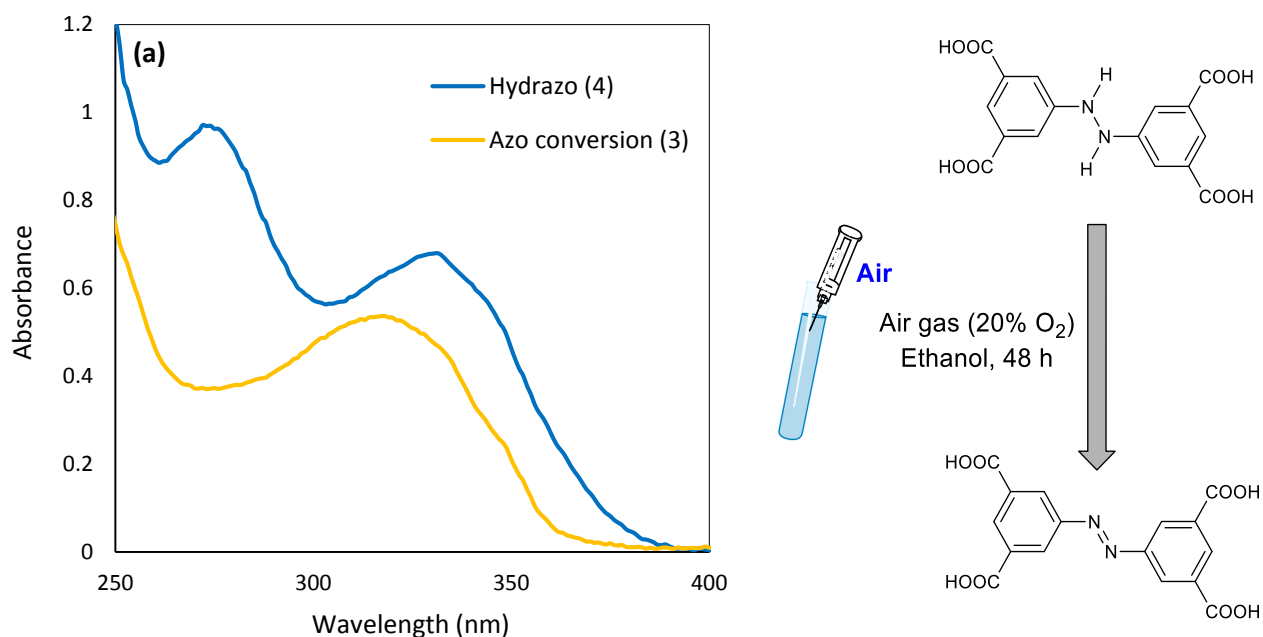
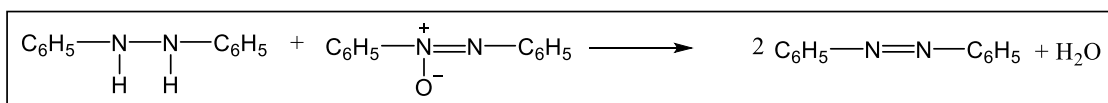
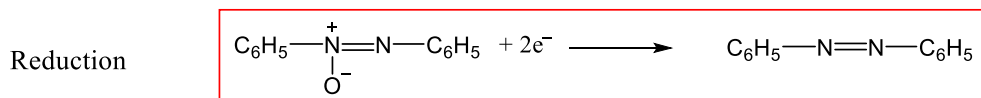
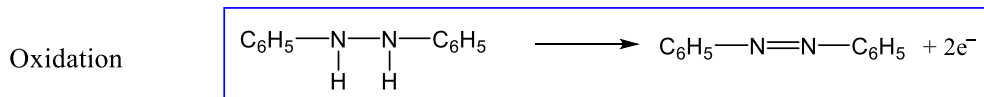


**Figure 13:** (a) Changes in the UV-Vis absorption spectra reflected the conversion of **4** (blue) to **3** (yellow). (b) Oxidation of **4** in ethanol was carried out by purging solution with air (20% O<sub>2</sub>). This process can be accelerated by stirring one equivalent of silver oxide in dry ethanol.

A significant transformation besides the aerial oxidation of the hydrazo compound (**4**) is the conversion of residual azoxy intermediate (**2**) to the azo product (**3**) in the same two-days old solution. Under these conditions, consideration was given to the hydrazo compound (**4**) as a possible reductant for the azoxy intermediate (**2**). Based on voltammetric data,<sup>95</sup> the reduction of azoxybenzene by hydrazobenzene has a significant driving force ( $\Delta G^\circ = -100.34$  kJ/mol) that allows these species to undergo a two-electron transfer from the hydrazo to the azoxy group (Scheme 16). The relationship between the change in Gibbs free energy (driving force) and the electric potential of a reaction is described in Eq. (5).



$$E^\circ = 0.52 \text{ V}$$

**Scheme 16:** Azoxybenzene reacts with hydrazobenzene by redox chemistry to form two equivalents of azobenzene and a water molecule. In this proposed mechanism, azoxybenzene is the oxidant while hydrazobenzene is the reductant. The overall reaction has an electric potential of 0.52V.<sup>95</sup> The relationship between  $\Delta G^\circ$  and  $E^\circ$  is used to determine if the chemical reaction would be spontaneous.

$$\Delta G^\circ = -nFE^\circ \quad (5)$$

$$\Delta G^\circ = - (2) (96,485 \text{ C/mol } e^-) (0.52 \text{ V})$$

$$\Delta G^\circ = -100.34 \text{ kJ/mol}$$

where,

$\Delta G^\circ$  (J): Gibbs free energy change

$F$  (C/mol  $e^-$ ): Faraday's constant = 96,485 C/mol  $e^-$

$n$  (moles  $e^-$ ): number of electrons transferred

$E^\circ$  (V): cell potential

In order to confirm the validity of this chemical pathway, a mixture solely consisting of compounds **2** and **4** must be dissolved in a basic solution for a period of 48 hours; if a high product yield is achieved for compound **3**, the intermediate and side-products are capable of reacting without the use of additional reagents, and only then one could highlight the synthetic versatility of these compounds. However, because these reactions remain unconfirmed, over-reduction by

ball milling is thought to be more advantageous due to the easy re-oxidation of hydrazo compounds, and by this means only can the complete conversion of the azoxy intermediate (**2**) be insured. Although all of the nitro starting material (**1**) is presumably used up when the conversion of the azoxy intermediate (**2**) reaches its maximum, the aniline derivative can be continuously formed at this stage of the ball mill reaction. This effect can be problematic as demonstrated in entry 2 of Table 9; the zinc mixture which contained no more starting material gave a 17% lower yield of compound **3** in comparison to entry 1 of Table 9 which by contrast contained both starting material and azoxy intermediate. The lower product yield suggests that aniline by-product (**5**) was formed in the ball milling process and was not converted to the azo product during the 48-hours workup. The question thus arises as to the action of the nitro compound (**1**) on the conversion of the aniline derivative (**5**), which ultimately contributes to the overall yield of the azo product (**3**). Despite numerous investigations have been made on the reduction of aromatic nitro compounds, there is no experimental evidence in the literature reporting about a direct reaction between nitrobenzene and aniline derivatives. In this case, it is very likely that the intermediate species involved in this chemical pathway is the nitroso compound formed through a two-electron transfer of the nitro group, which then undergoes condensation with the aniline (**5**) to afford the azo product; this reaction is known as Mills reaction (Scheme 3). The assumption that such pathway is responsible for the conversion of compound **5** is evidenced by the presence of nitro starting material in the alkaline solution which allowed for a greater production of compound **3**. Overall, much more experimental evidence will be required before a complete theory of the process can be formed. Most importantly, the mechanistic role of each compound on the conversion of other by-products are well worthy of being tested more closely in the future; based on these studies, one could target the ideal product ratio of compounds **1**, **2**, **3**, **4** and **5** in order to achieve optimal yields.

## 2.8 Is Ball Milling a Better Method for the Synthesis of Azo Compounds?

Over the last decade, the literature has reported many examples of organic synthesis performed in ball mills. However, compared to other green methods (e.g. microwave, ultrasound, and flow syntheses), ball mill synthesis is underrepresented in the field of sustainable organic chemistry. Moreover, studies comparing the effectiveness of this technique over the corresponding solution-based reactions are seldom. The present study is illustrative of how mechanochemistry can be a better method for the synthesis of azo compounds. Our experimental results indicated that the mechanically-assisted synthesis of 3,3',5,5'-azobenzene tetracarboxylic acid offers numerous advantages over the liquid-phase counterpart in terms of product yield, selectivity, reaction time, material usage and energy efficiency, making this technology an interesting and sustainable tool for a wide range of applications.

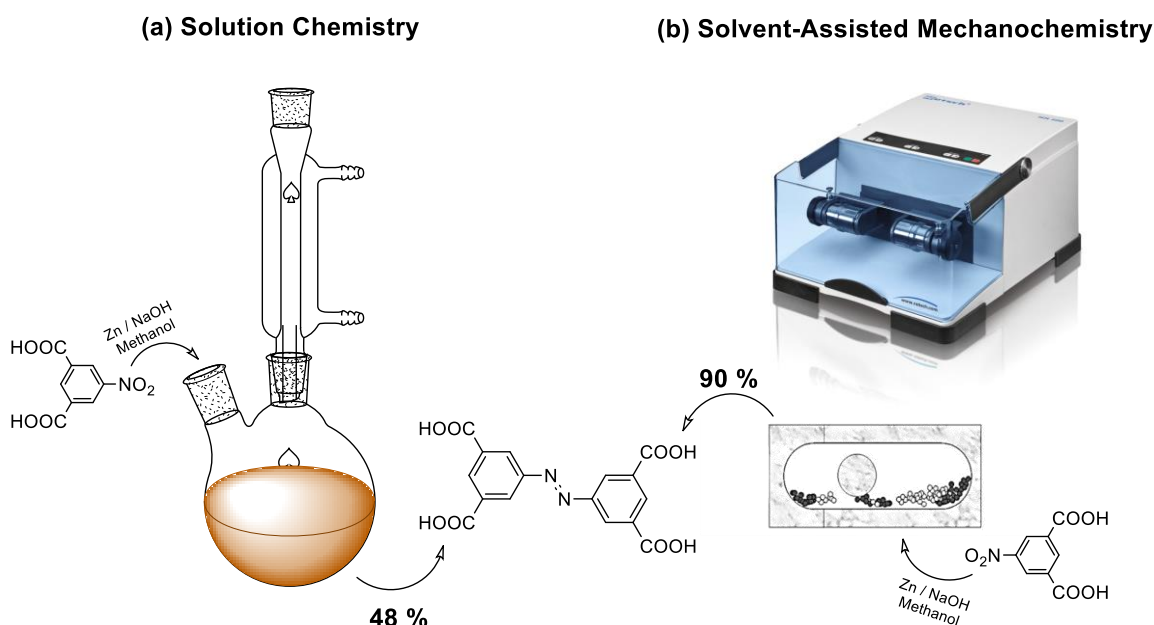


**Figure 14:** Schematic representation and comparison of the synthetic methodologies. Reaction conditions: (a) **1**, Zn (4 equiv.), and NaOH (6 equiv.) stirring in methanol under reflux for 24h (48% yield). (b) **1**, Zn (3 equiv.), and NaOH (6 equiv.) ball milled with two 5 mm balls for 3h at 30 Hz. Solid mixture was kept in 1 M NaOH<sub>(aq)</sub> for 48 h (90% yield).

### 2.8.1 Advantages of Ball Mill Chemistry

- i. The omission of solvents in the ball mill reaction step is certainly one of the main advantages of this synthetic method. Moreover, 4 equivalents of zinc were used in our optimized traditional synthesis, whereas 3 equivalents were used instead in our optimized ball mill assisted methodology. A significant decrease in the amount of solvent and reductant reduces harmful chemical waste, allows safer handling of reagents, and most importantly, it is more economic.
- ii. The ball mill technique is easy to implement, and involves a simpler work-up procedure in which a powder is easily extractable with small amounts of aqueous or organic solvents for analysis and isolation.
- iii. The efficient mixing in ball mills and increased activity through process intensification that is driven by the intensive collisions of the milling bodies ensure an efficient energy transfer to the reaction mixture. As a result, the ball mill assisted reaction exhibited a higher product yield (90%), better selectivity of **3**, and a shorter reaction time.
- iv. The mechanochemical treatment of the nitro aromatic compound under ball milling conditions is significantly more reactive than the classical synthesis of the azo compound under batch conditions. Various reason for this have been proposed, the main one being a dependence of the chemical potential of a solid surface on the surface curvature such that the potential of particles increases with decreasing particle size (the Gibbs–Thomson effect).<sup>80</sup> Precisely, the grinding and milling action on solid reactants into the powder form can increase their chemical potential and provide a further driving force for the reaction.
- v. Finally, the most attractive feature of the mechanochemical methodology is that up-scaling of the reactions is possible, and is therefore suitable for industrial applications.

### 2.8.2 Disadvantages of Ball Mill Chemistry

- i. Despite the advantages of ball milling, one of the main disadvantages is the lack of control over the temperature and pressure. These important parameters are difficult to regulate if operating in a laboratory scale ball mill unit. As a result, chemical reactions that require high temperature are not suitable for this method.
- ii. In spite of the various possibilities to manipulate the outcome of a chemical reaction, harmonization of the reaction variables can be quite challenging, especially since a large number of parameters contribute to the overall performance of ball mill reactions. Consequently, the applicability of mechanochemical synthesis for a particular reaction may require extensive examination and countless test runs.
- iii. Deterioration of the milling material over time due to abrasive effects can be problematic from an economic and synthetic point of view, therefore the density and chemical resistance of the milling material, as well as the hardness and nature of the milling feed must be taken into account. For example, oxidation reactions with inorganic oxidants can corrode milling materials such as steel.<sup>56</sup> On the other hand, abrasion of particles from the surface of the milling material can interact with the milling feed and contaminate the product. In this case, zirconia is the material of choice for organic synthesis. Although they are very expensive, they are chemically inert towards most reagents and the material abrasion is comparably low.

## 2.9 Summary and Conclusions

The objective of this thesis was the development of a green, low cost, and scalable synthesis of 3,3',5,5'-azobenzene tetracarboxylic acid. Having addressed the important limitations of previous methodologies, it was our interest to find an environmentally compatible methodology that could be easily replicated in large scale industrial setups. The investigation of ball milling as a synthetic alternative was based on relatively “green” procedures that synthesize 3,3',5,5'-azobenzene tetracarboxylic acid from the reductive coupling of 5-nitroisophthalic acid using either zinc or D-glucose as reducing agent in alkaline solutions. Interestingly, mixtures of three different azobenzene derivatives were exclusively generated with solvent-assisted ball mill chemistry. Consequently, the ball mill reactions were tested under variable parameters in order to optimize the chemical yields. Finally, a highly efficient two-step approach was developed for the selective formation of 3,3',5,5'-azobenzene tetracarboxylic acid. The target product was achieved in 90% yield under the optimized milling conditions and workup protocol highlighted below:

- i. Ball mill 5-nitroisophthalic acid and 3 equivalents of zinc at 30 Hz for three hours using a pair of 5 mm stainless steel balls.
- ii. Immerse crude zinc mixture in 1.0 M sodium hydroxide solution for 48 hours.

An essential feature of this novel approach is that the switchable products, including the azoxy, azo and hydrazo compounds can be selectively obtained in good yields by simply varying the ball milling conditions accordingly. Moreover, the ball mill assisted method offered several advantages such as high conversion, shorter reaction time, clean synthesis and simple work-up procedure, which make this methodology a convenient and sustainable alternative for traditional syntheses of azobenzenes. Advantageously, this method does not require any toxic or expensive reagents, or the use of high-pressure equipment. Most importantly, the cheapness and general availability of

the reagents (e.g. Zn and NaOH), as well as the reduction of the amount of solvent ensure cost efficiency and easy up-scaling for an economical production of PCN-250(Fe<sub>3</sub>).

Overall, ball mills have proven to be powerful tools for conducting organic reactions in the solid state, yet by optimizing the step-economy in synthesis planning, I expect this method to be easily applied for industrial synthesis of more complex molecules

## 2.10 Future Work

My contribution to this project was twofold; first an experimental comparison of traditional and alternative methodologies has been performed, and second a novel two-step protocol for the synthesis of 3,3',5,5'-azobenzene tetracarboxylic acid have been designed. Although the main focus of my thesis was the optimization of the synthesis itself, many different adaptations, tests, and experiments have been left for the future due to lack of time. In particular, the preliminary understanding of these experiments do not seem to be satisfactory, and further study is still required in order to understand the behavior of the azo-based derivatives. Hence, future work concerns deeper analysis of particular mechanisms, new proposals to try different methods, and simply curiosity. These are following aspects that could be tested to achieve stronger mechanistic hypotheses and to better understand these reactions:

1. Interestingly, mixtures of compounds **1**, **2**, **3**, **4** and **5** obtained from ball mill reactions were found to be advantageous in the formation of the azo product during the alkaline workup conditions. In particular, I proposed a series of possible chemical reactions between the various species based on the voltammetric behaviour of simple analogs (e.g. reduction potentials of azobenzene, azoxybenzene, and hydrazobenze). However, it could be more consistent to elucidate the reduction and oxidation mechanisms based on the exact reduction potentials of compounds **1**, **2**, **3**, **4** and **5** (cyclic voltammetric studies are required



for this purpose). These values would help distinguish the role of each compound whether it is likely to behave as an oxidant or as a reductant in the same solution.

2. The difference in chemical yields between entries 1 and 2 of Table 9 indicated the necessity of also investigating of a system containing only commercial 5-nitroisophthalic acid (**1**) and 5-aminoisophthalic acid (**5**) in alkaline conditions with and without zinc powder. The outcome not only determines whether the nitro compound is involved in the conversion of the aniline (**5**), but also if unreacted zinc metal can reduce the nitro compound and source the formation of the nitroso intermediate required for Mills reaction. Same process would apply to a system containing azoxy intermediate (**2**) and hydrazo by-product (**4**) to evaluate whether a redox reaction can occur among these species through a two-electron transfer mechanism. These investigations would also allow us to determine the approximate product ratio of the azoxy, azo, and hydrazo compounds required for optimal yields after applying the workup procedure.
3. On the basis of  $^1\text{H}$  NMR, it would be interesting to monitor in situ the change in the product composition of a crude ball mill sample dissolved in basic deuterium oxide (such chemical environment replicates the alkaline workup conditions). These studies could help us understand the kinetics of these transformations toward the formation of the azo product.
4. Finally, it appears desirable to reinvestigate the ball mill reactions under inert conditions and with different milling materials like zirconia to see whether the exclusion of air during the ball mill process and different surfaces could influence the production of the azo product.

# Chapter 3: Experimental

## 3.1 General Information

Unless otherwise stated, all commercial reagents and solvents were obtained from Sigma-Aldrich and used without further purification. Analytical thin-layer chromatography (TLC) was performed on aluminum-backed silica gel 60 plates (Silicycle) and visualized under UV light to monitor reactions. Purifications were performed by recrystallization using commercial grade solvents.  $^1\text{H}$  NMR was recorded on a Bruker Avance 300 spectrometer operating at 300 MHz. Chemical shifts were quoted in parts per million (ppm) referenced to the appropriate deuterated solvent peak, DMSO- $d_6$  ( $\delta$  2.50 ppm) or MeOD- $d_4$  ( $\delta$  4.87 ppm). The following abbreviations were used to describe peak splitting patterns: br = broad, s = singlet, d = doublet, t = triplet, q = quartet, m = multiplet. Coupling constants,  $J$ , are reported in hertz (Hz).  $^{13}\text{C}$  NMR was recorded on a Bruker Avance 300 spectrometer operating at 75.47 MHz and was fully decoupled by broad-band proton decoupling. Chemical shifts were reported in ppm referenced to the center line of a septet at 39.7 ppm of DMSO- $d_6$ . Gradient phase-sensitive 2D  $^1\text{H}$ - $^1\text{H}$  NOESY, 2D  $^1\text{H}$ - $^1\text{H}$  COSY and gradient phase-sensitive 1D  $^{15}\text{N}$ - $^1\text{H}$  HSQC experiments were performed on a Bruker Avance 300 spectrometer operating at 300 MHz. NMR data acquisition and processing were performed with the Topspin 2.1 software.  $^1\text{H}$  DOSY experiments were performed on a Bruker Avance III spectrometer operating at 500 MHz. The acquisition time was 1.6 s (AQ) s and the relaxation delay was 3 s (D1). Diffusion time was 0.1 s (D20) and rectangular gradient pulse duration was 1 ms (P30). Gradient recovery delays of 200  $\mu\text{s}$  followed the application of each gradient pulse. Data was accumulated by linearly varying the diffusion encoding gradients over a range from 5 to 95 % for 64 gradient increment values. DOSY data was processed with the Topspin 3.5.6 software. Infrared spectra were recorded on Bruker Alpha FT-IR Spectrometer. Frequencies are given in

reciprocal centimeters ( $\text{cm}^{-1}$ ), and only selected absorbance peaks are reported. High-resolution mass spectra were obtained by matrix assisted laser desorption ionization (MALDI) and atmospheric solids analysis probe ionization (ASAP) operated in negative mode and positive mode, respectively. UV-VIS absorption spectra of solutions in methanol (spectroscopic grade) were recorded on a Varian Cary 50 spectrophotometer and corrected for solvent absorption. Melting points were measured with an SRS OptiMelt MPA100 system equipped with a high-resolution digital camera. Batch syntheses of the azo compound were performed based on procedures reported in the literature after small modifications to optimize yields.<sup>88-93</sup> Previously reported products including **2** and **3** were identified by comparison of physical properties and spectral data with literature (e.g.  $^1\text{H-NMR}$ ,  $^{13}\text{C-NMR}$ , IR, and MS). Ball mill reactions were conducted using a laboratory-scale ball milling unit (Retsch mixer mill MM400) equipped with a pair of 15 mL stainless steel jars containing stainless steel balls (5 mm, 7 mm or 8 mm in diameter). The mill jars were oscillated in a horizontal position at a frequency of 30 Hz (the frequency of the rocking back-and-forth motion of the mill jars). The number of impacts mainly depends on the ball mill frequency, the ball size and the number of balls. Product mixtures were analyzed by TLC on silica and  $^1\text{H-NMR}$  after initial precipitation and at the end of the work-up procedure since the work-up conditions were found to critically affect the distribution of products. Product yields were optimized by varying the milling time, size and number of the balls, amounts of materials, and work-up procedures.

## 3.2 General Procedures

### 3.2.1 Batch Synthesis of 3,3',5,5'-Azobenzene Tetracarboxylic Acid (3) with Zinc as Reducing Agent

This procedure is based on two literature procedures after the optimization of the amount of base and reducing agent.<sup>89,90</sup> Solutions of 5-nitroisophthalic acid (2.1 g, 10 mmol) in methanol (20 mL), and NaOH (2.4 g, 60 mmol) in deionized water (6 mL) were added to a 50 mL two-necked RB flask equipped with a condenser. Zinc dust (Aldrich 209988, 2.6 g, 40 mmol) was added to the vigorously stirred solution and the resulting mixture was refluxed for 24 hours. The progress of the reaction was monitored by following the consumption of 5-nitroisophthalic acid by TLC and the reaction was stopped as soon as no starting material was detected. Filtration of the hot mixture removed precipitated zinc salts, the filter residue was washed with warm methanol to recover all products, and the filtrate was acidified to a pH of 3 by the addition of 3 M HCl (aq). Methanol was distilled off the mixture, more deionized water was added (20 mL), and the mixture was cooled in a fridge to precipitate all azo fully products. The resulting orange precipitate was filtered and washed with cold water. Recrystallization from DMF gave the product as orange crystals in 45% yield.

### 3.2.2 Batch Synthesis of 3,3',5,5'-Azoxybenzene Tetracarboxylic Acid (2) with Zinc as Reducing Agent

The N-oxide derivative was prepared according to a reported procedure.<sup>93</sup> A mixture of 5-nitroisophthalic acid (2.10 g, 10 mmol), Zn (1.30 g, 20 mmol), and NaOH (0.80 g, 20 mmol) in a mixed solvent of ethanol (60 mL) and water (20 mL) was refluxed for 24 h. The reaction mixture was poured into 50 mL of NaOH (aq, 1 M), and filtered to remove insoluble zinc residue. The filtrate was acidified to pH of 3 with 3 M HCl (aq), recrystallized overnight at low temperature and

filtrated to obtain a yellow amorphous solid in 60% yield. Yellow precipitate collected by filtration was dried under high vacuum at 60 °C.

### **3.2.3 Batch Synthesis of 3,3',5,5'-Azobenzene Tetracarboxylic Acid (3) with Glucose as Reducing Agent**

This was prepared according to a modified combination of reported conditions and work-up steps.<sup>91</sup> Solution of 5-nitroisophthalic acid (1.00 g, 4.73mmol) and NaOH (1.14 g, 28.5 mmol) in deionized water (20 mL) was heated to 60 °C. Glucose (Sigma G8270, 3.58 g, 19.9 mmol) was dissolved in deionized water (6 mL) and was added dropwise to the vigorously stirred solution. The resulting solution was stirred at 60 °C for 24 h. The suspension was dissolved in 50 mL of NaOH (aq. 1 M) and filtered to remove any insoluble solids. The filtrate was acidified with 3 M HCl (aq) to a pH = 3 to obtain a precipitate. The resulting orange solid was recovered by filtration and washed with cold water. Recrystallization from DMF gave the product as orange crystals in 30% yield.

### **3.2.4 General Procedure for the Reduction of 5-nitroisophthalic acid using Zinc under Milling Conditions**

The product mixture synthesized under this procedure was collected for direct analysis to study the initial outcome of the experiment. A mixture of 5-nitroisophthalic acid (0.35 g, 1.66 mmol) and NaOH powder (0.40 g, 10 mmol) was introduced into a stainless steel jar (15 mL volume) with the chosen weight and number of stainless steel balls. A small amount of methanol/water (3:1) mixed solvent (0.35 mL) was added before closing the screw-top jar to allow the formation of a paste during milling. The reaction vessel was shaken on a ball mill apparatus at a frequency of 30 Hz for 10 minutes. The milling was stopped and zinc dust (0.22-0.54 g, 3.36-8.26 mmol) was added to the resulting pink pasty solid with a drop of mixed solvent. The contents were ball

milled at a frequency of 30 Hz for different times (2 hours to 4 hours) to give a gray to olive green pasty solid. The jar was considerably warmed by mechanical friction. The reaction mixture was poured into 10 mL of water and allowed to stand for 2 minutes to give a clear orange or yellow supernatant (the coloration is attributed to the formation of orange azoxy or yellow hydrazo by-products). The supernatant liquid was collected by filtration and the resulting filtrate was acidified in an ice water bath to a pH of 3 with 2 M HCl (aq). The orange precipitate was filtered off and dried under air to give a mixture of azoxy, azo and hydrazo compounds in 50-75 % combined yields as determined by  $^1\text{H}$  NMR.

### **3.2.5 General Procedure for the Reduction of 5-nitroisophthalic acid using Glucose under Milling Conditions**

A mixture of 5-nitroisophthalic acid (0.35 g, 1.66 mmol) and NaOH powder (0.46-0.93 g, 11.6-23.3 mmol) was introduced into a stainless steel jar (15 mL volume) with the chosen weight and number of stainless steel balls. A small amount of water (0.5 mL) was added before closing the screw-top jar to allow the formation of a paste during milling. The reaction vessel was shaken on a ball mill apparatus at a frequency of 30 Hz for 10 minutes. The milling was stopped and glucose (1.20-2.40 g, 6.7-13.3 mmol) was added to the resulting yellow pasty solid with a drop of solvent. The contents were ball milled at a frequency of 30 Hz for 4 hours to give a brown-orange viscous mixture. The jar was considerably warmed by mechanical friction. The reaction mixture was dissolved in 10 mL of water to give a dark brown-orange solution, and acidified with 2 M HCl (aq) to a pH = 3 to obtain a precipitate. The resulting orange solid was recovered by filtration to give a mixture of azoxy, azo, hydrazo and aniline derivatives in 42-58% combined yields as determined by  $^1\text{H}$  NMR.

### **3.2.6 General Procedure for the Reduction of 5-nitroisophthalic acid using Magnesium under Milling Conditions**

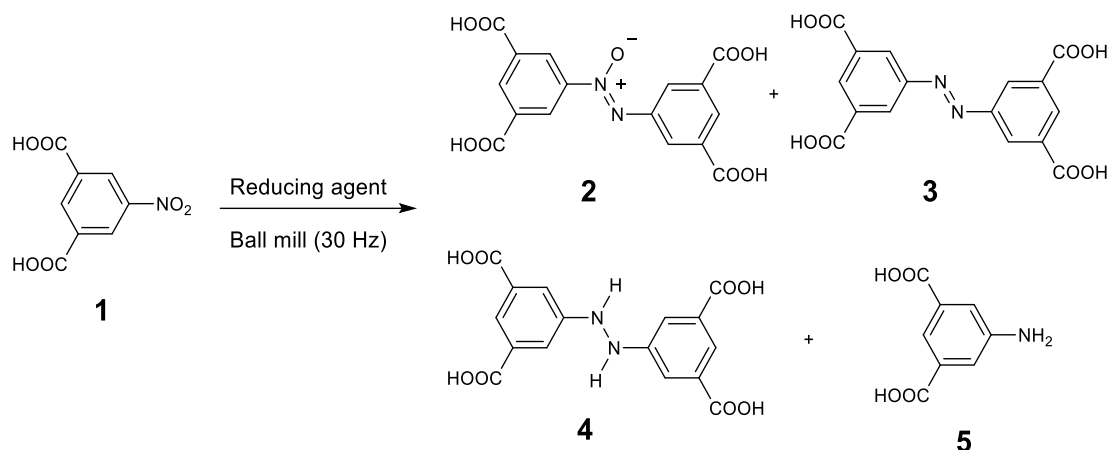
5-nitroisophthalic acid (0.35, 1.66 mmol) and magnesium turnings (Sigma-Aldrich 200905, 0.16 g, 6.64 mmol) were introduced into a stainless steel jar (15 mL volume) with the chosen weight and number of stainless steel balls. The thin dark gray rather than silver-white magnesium turnings suggests the presence of an oxide layer. A small amount of anhydrous methanol (0.35 mL) was added before closing the screw-top jar to allow the formation of a paste during milling. The contents were ball milled at a frequency of 30 Hz for different times (1 hours to 6 hours). The jar was considerably warmed by mechanical friction. The resulting rocky paste was cooled and dried by allowing it to stand for a few minutes under air to give a dark grey powder. The reaction mixture was poured into 10 mL of water, and kept in a cold water bath. The mixing of the magnesium mixture with water generated an excessively-fizzing and exothermic suspension. The yellow-green supernatant was filtered and the resulting yellow filtrate was acidified with 2 M HCl (aq) to a pH = 3 to obtain a precipitate. The orange/beige solid was recovered by filtration to give a mixture of azoxy, azo and hydrazo compounds in 30-50 % combined yields as determined by <sup>1</sup>H NMR.

### **3.2.7 Final Optimized Synthesis of 3,3',5,5'-Azobenzene Tetracarboxylic Acid using Zinc under Milling Conditions**

A mixture of 5-nitroisophthalic acid (0.35, 1.66 mmol) and NaOH powder (0.40 g, 10 mmol) was introduced into a stainless steel jar (15 mL volume) with the two 5 mm stainless steel balls. A small amount of methanol/water (3:1) (0.35 mL) was added before closing the screw-top jar to allow the formation of a paste during milling. The reaction vessel was ball milled at a frequency of 30 Hz for 10 minutes. The milling was stopped and zinc dust (0.33 g, 5.05 mmol) was added to the resulting pink pasty solid with a drop of methanol/water (3:1). The contents were ball milled

at a frequency of 30 Hz for 3 hours to give a green-olive pasty solid. The jar was considerably warmed by mechanical friction. The resulting paste of product was cooled and dried by allowing it to stand for a few minutes under air. The reaction mixture was transferred to a 50 mL beaker and was kept in 20 mL of NaOH (aq, 1 M) for 24 hours while exposed to air. After full conversion to the desired product, as monitored by TLC, the bright orange supernatant was filtered to remove zinc residue, and the filtrate was acidified in an ice water bath to a pH of 3 with 2 M HCl (aq). Orange precipitate was collected by filtration and dried under air to give the pure azo derivative in 86-90 % yield.

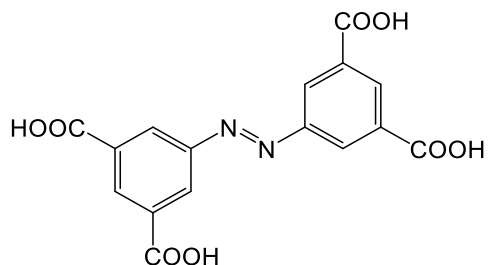
### 3.3 Product Characterization and Spectral Data



**Scheme 17:** The reductive coupling of 5-nitroisophthalic acid under ball milling conditions generates a mixture of products.



### 3,3',5,5'-Azobenzene tetracarboxylic acid (**3**)



Orange crystalline solid; no mp; decomposition at 388 °C;  $^1\text{H}$  NMR (300 MHz, 25 °C, DMSO- $d_6$ , ppm):  $\delta$  = 13.62 (s, br, 4H), 8.62-8.60 (m, 6H);  $^{13}\text{C}$  NMR (75.47 MHz, 25 °C, DMSO- $d_6$ , ppm)  $\delta$  = 166.52, 152.37, 133.47, 133.18, 127.64; FTIR (solid,  $\text{cm}^{-1}$ ): 3419 (m,  $\nu\text{OH}$ ), 1724 (s,  $\nu\text{C=O}$ ), 1677 (s,  $\nu\text{C=O}$ ), 1614 (m,  $\nu\text{C=C}$  of benzenoid rings), 1465 (m,  $\nu\text{C=C}$  of benzenoid rings), 1419 (m,  $\nu\text{N=N}$ ), 890 (w,  $\delta\text{CH}$ ), 763 (m,  $\delta\text{CH}$ ), 669 (m,  $\delta\text{CH}$ ); MALDI-TOF-MS:  $m/z$  calcd for  $\text{C}_{16}\text{H}_{10}\text{N}_2\text{O}_8$  [ $\text{M}^-$ ] 358.0437, found 358.0444; UV-Vis: ( $\lambda_{\text{max}}$  in EtOH) 319 nm. The analytical data agree with the values in the literature.<sup>89, 91</sup>

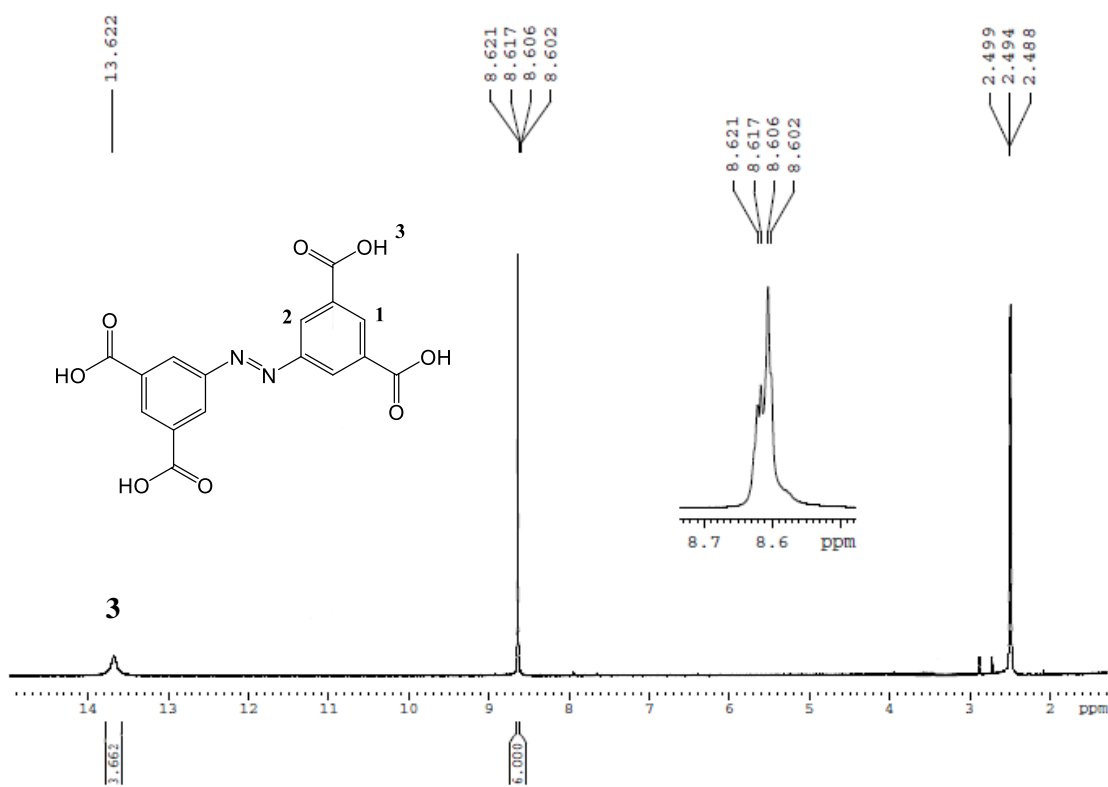


**Figure 15:**  $^1\text{H}$  NMR of **3** recrystallized from DMF (DMSO- $d_6$ , 300 MHz).

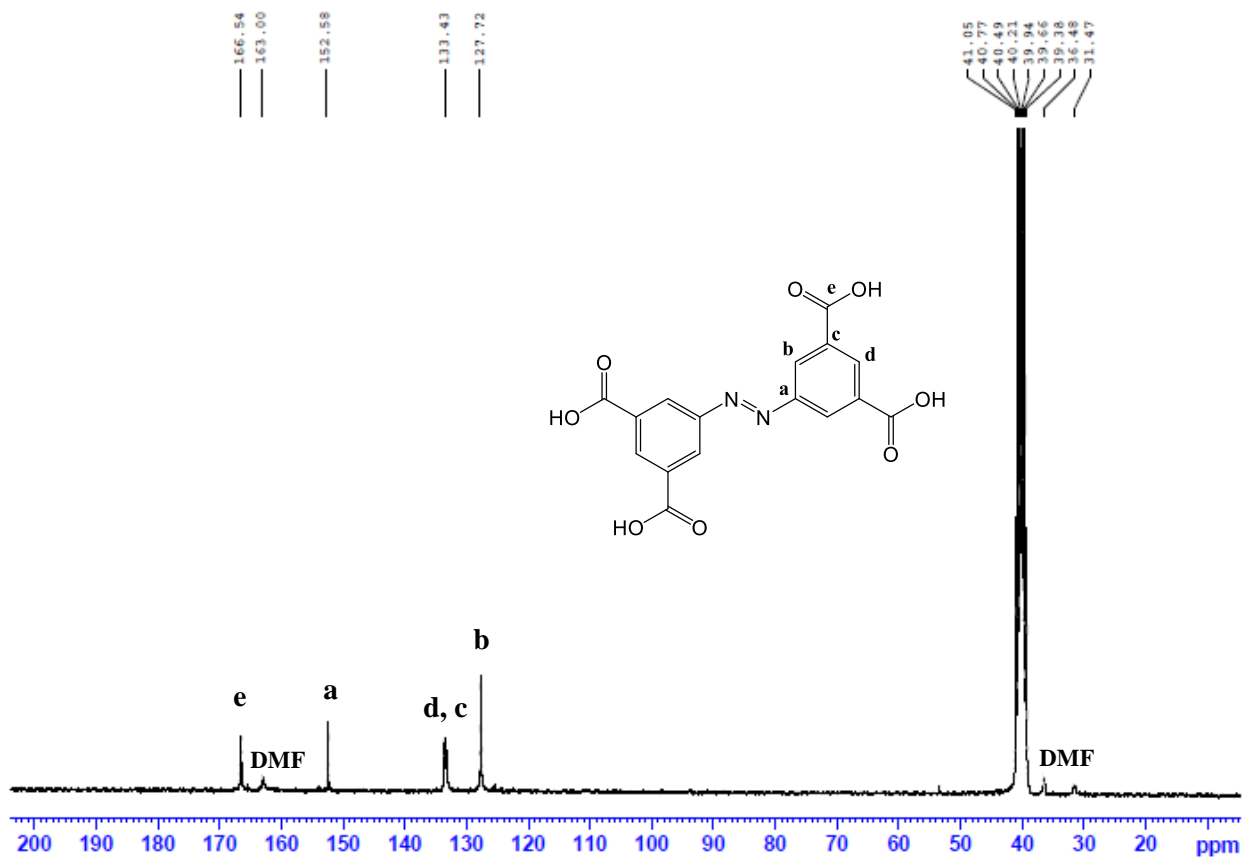


**Figure 16:**  $^{13}\text{C}$  NMR **3** recrystallized from DMF (DMSO- $d_6$ , 75.47 MHz).

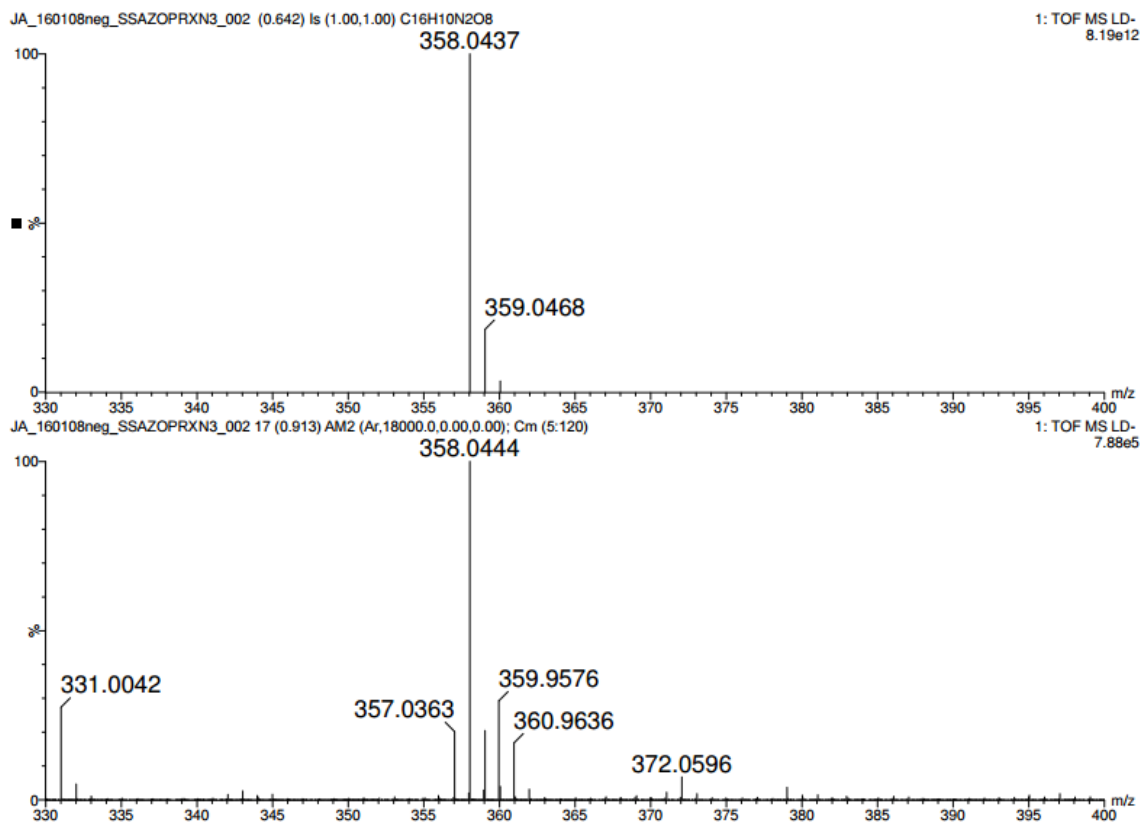


**Figure 17:** Negative mode MALDI-MS of **3** with lockmass (NaI: 2,5 DHB), laser energy 450.

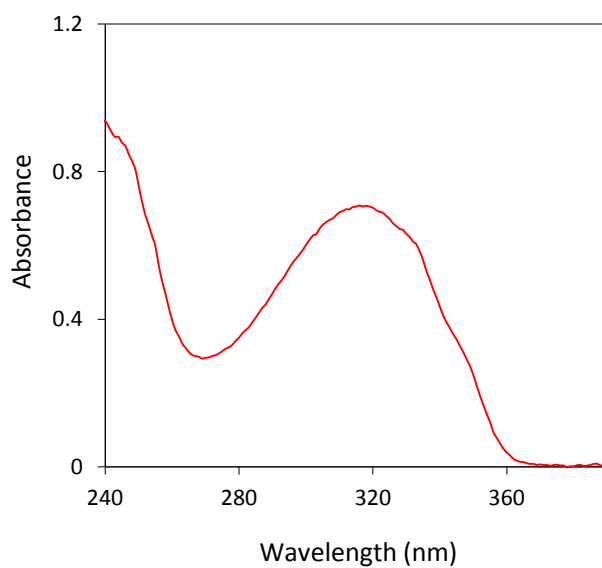


**Figure 18:** UV-Vis absorption spectra of compound **3** in ethanol (0.033 mg/mL).

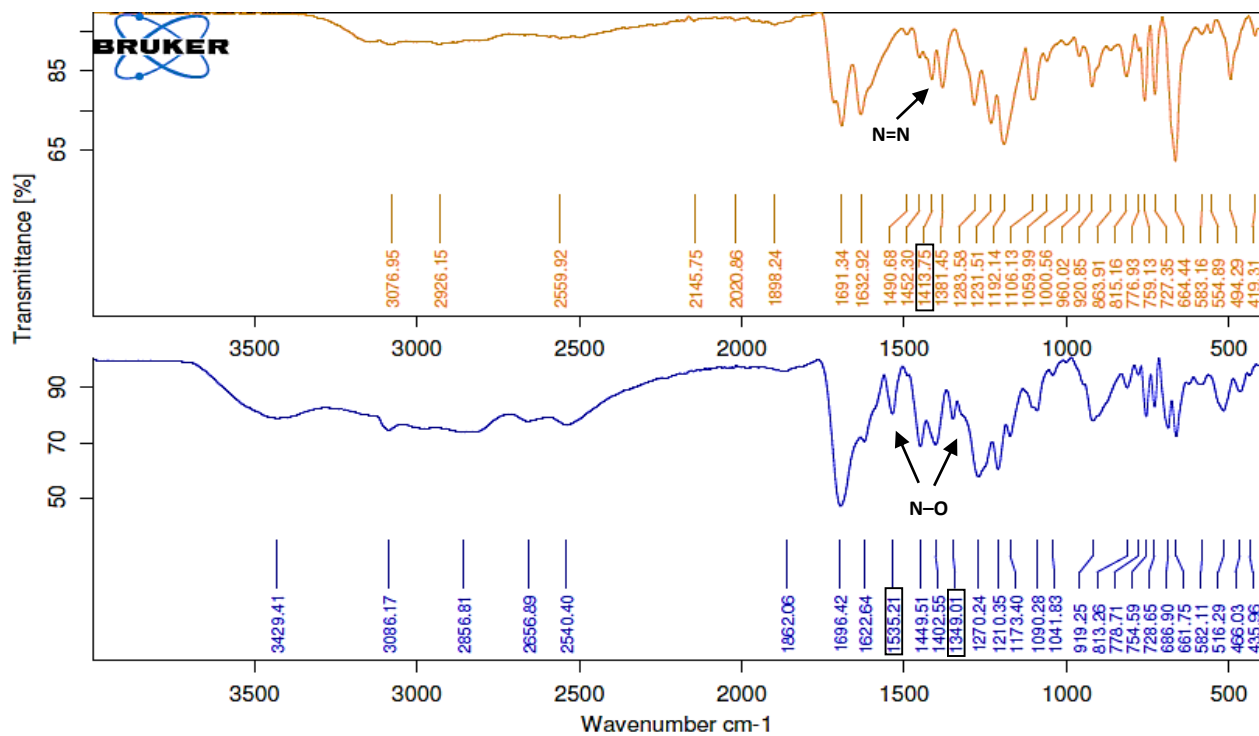


Figure 19: IR spectra of **3** azo product (top) and **2** N-oxide intermediate (bottom).

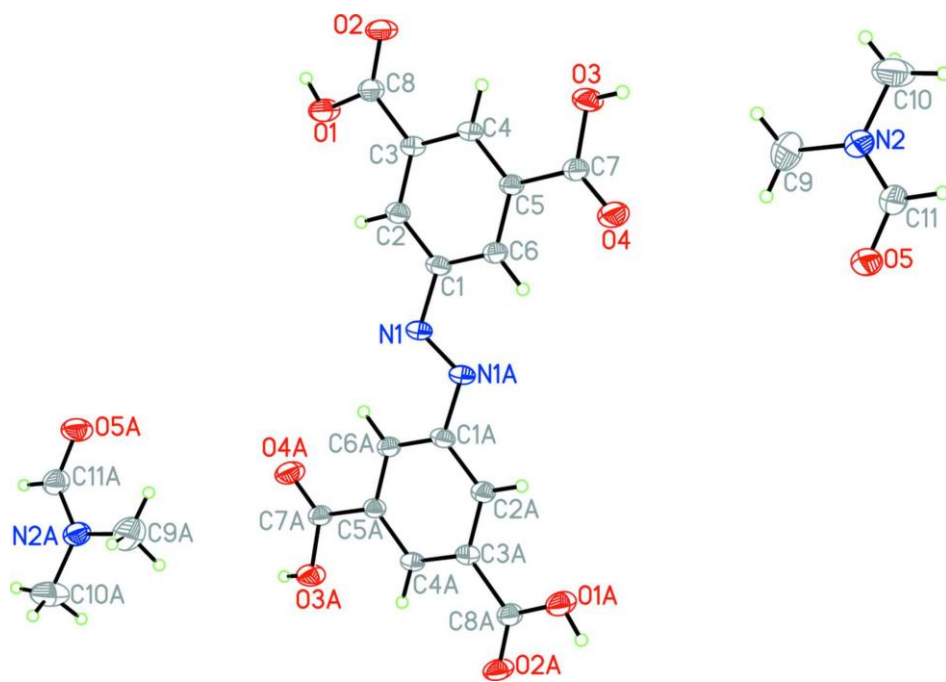
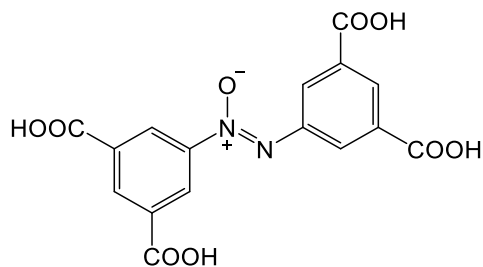
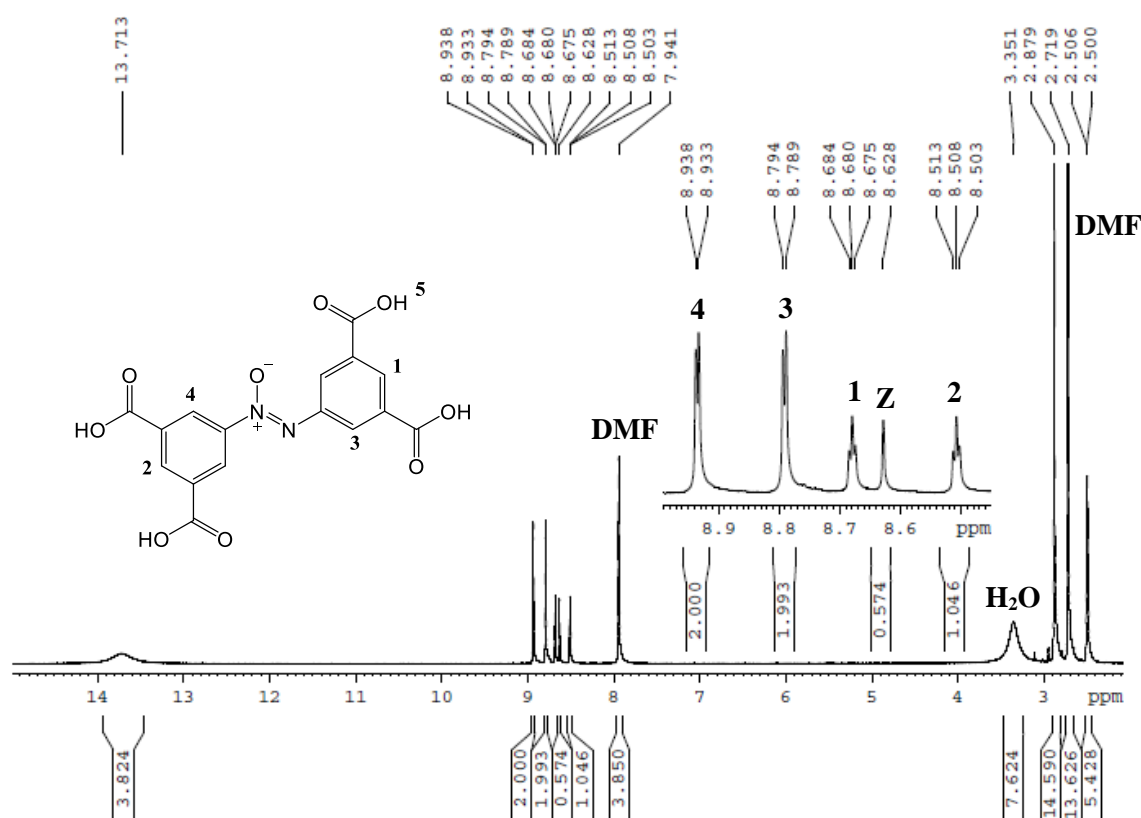


Figure 20: Single crystal structure of **3** in trans configuration.<sup>94</sup>

### 3,3',5,5'-Azoxybenzene tetracarboxylic acid (2)



Yellow solid;  $^1\text{H}$  NMR (300 MHz, 25 °C, DMSO- $d_6$ , ppm):  $\delta$  = 13.71 (s, br, 4 H), 8.93 (d,  $^4J$  = 1.5 Hz, 2 H), 8.79 (d,  $^4J$  = 1.5 Hz, 2 H), 8.68 (t,  $^4J$  = 1.5 Hz, 1 H), 8.50 (t,  $^4J$  = 1.5 Hz, 1 H).  $^{13}\text{C}$  NMR (75.47 MHz, 25 °C, DMSO- $d_6$ , ppm)  $\delta$  = 165.91, 165.29, 147.81, 143.46, 132.99, 132.76, 132.13, 130.63, 129.43, 126.47. UV-Vis: ( $\lambda_{\text{max}}$  in EtOH) 323 nm. The analytical data agree with the values in the literature.<sup>93</sup>



**Figure 21:**  $^1\text{H}$  NMR of **2** recrystallized from DMF (DMSO- $d_6$ , 300 MHz). Peak 'Z' is attributed to the small amount of compound **3** inside the sample.

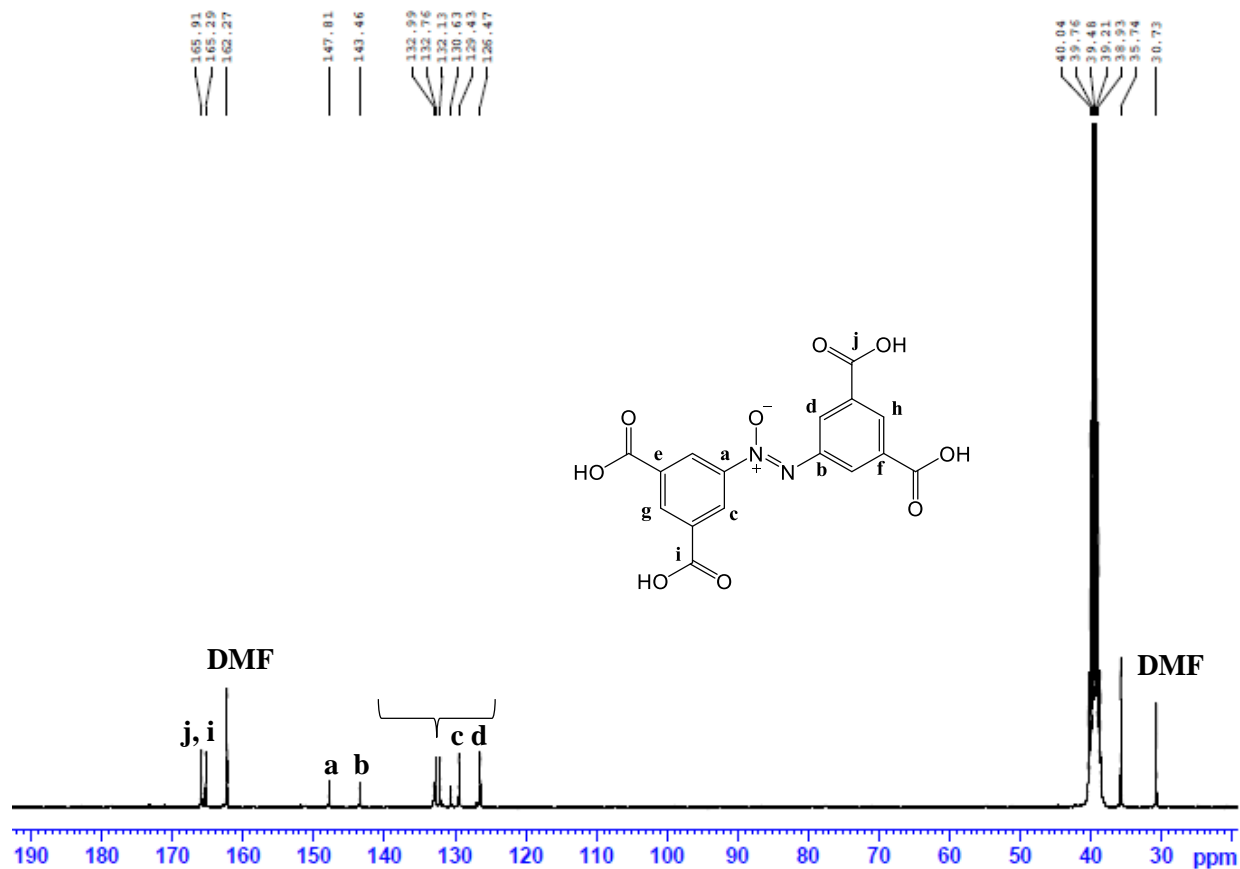


**Figure 22:**  $^{13}\text{C}$  NMR **2** recrystallized from DMF (DMSO- $d_6$ , 75.47 MHz).

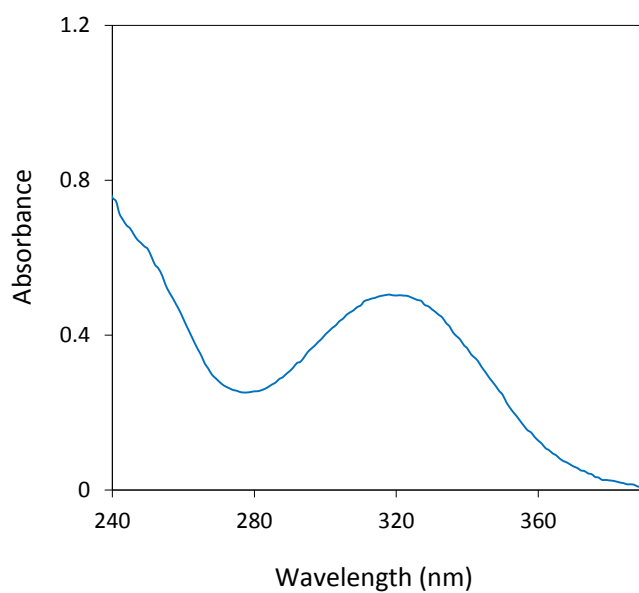
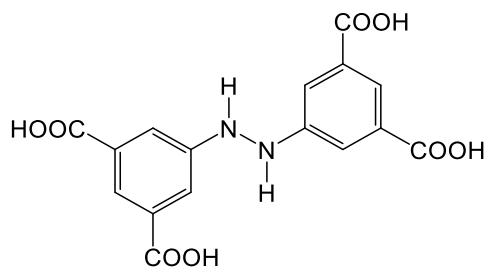


**Figure 23:** UV-Vis absorption spectra of compound **2** in ethanol (0.033 mg/mL).

### 3,3',5,5'-Hydrazobenzene tetracarboxylic acid (4)



Orange solid; mp = 280 °C;  $^1\text{H}$  NMR (300 MHz, 25 °C, DMSO- $d_6$ , ppm):  $\delta$  = 13.18 (s, br, 4H), 8.38 (s, br, 2H), 7.82 (t, 2H), 7.54 (d, 4H);  $^{13}\text{C}$  NMR (75.47 MHz, 25 °C, DMSO- $d_6$ , ppm)  $\delta$  = 166.83, 149.95, 132.47, 119.82, 115.92. UV-Vis: ( $\lambda_{\text{max}}$  in EtOH) 330 nm, 275 nm.

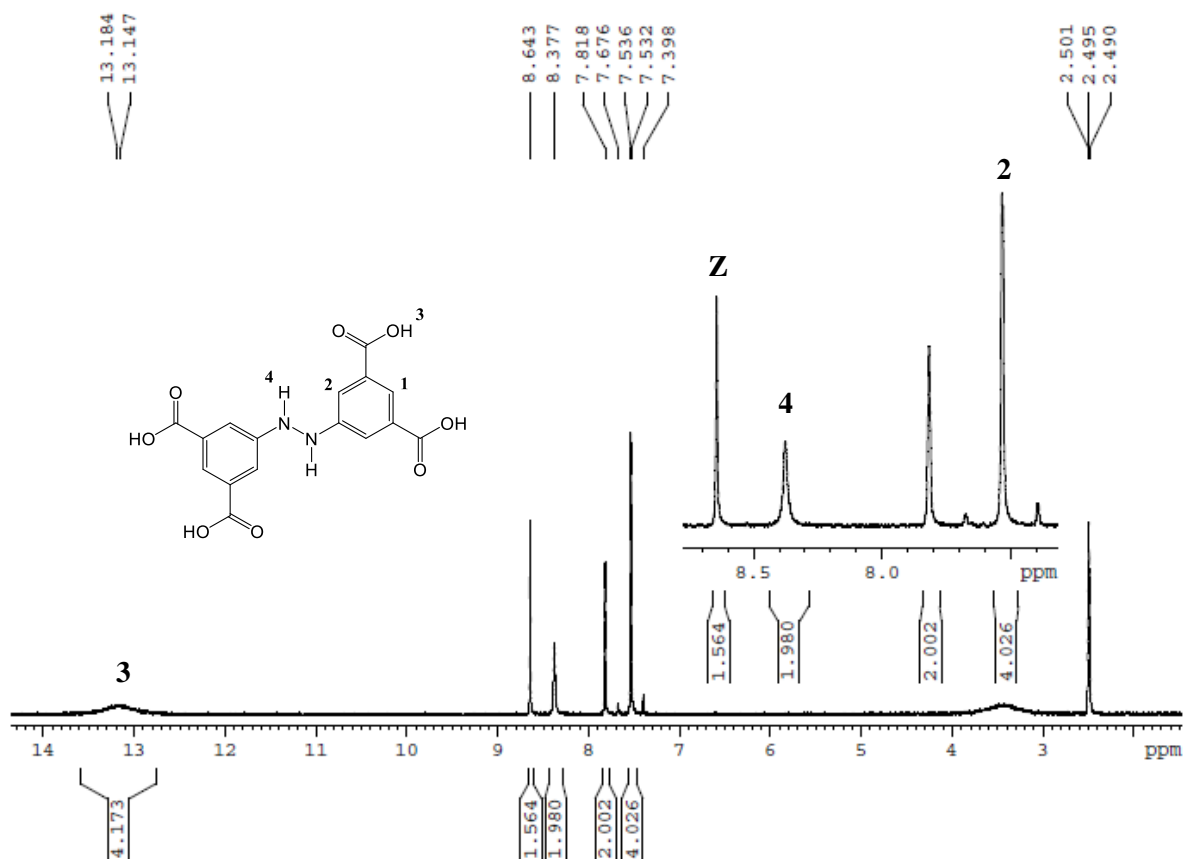


**Figure 24:**  $^1\text{H}$  NMR of 4 and 3 mixture (DMSO- $d_6$ , 300 MHz). Peak 'Z' is attributed to the presence of compound 3 due to incomplete over-reduction.

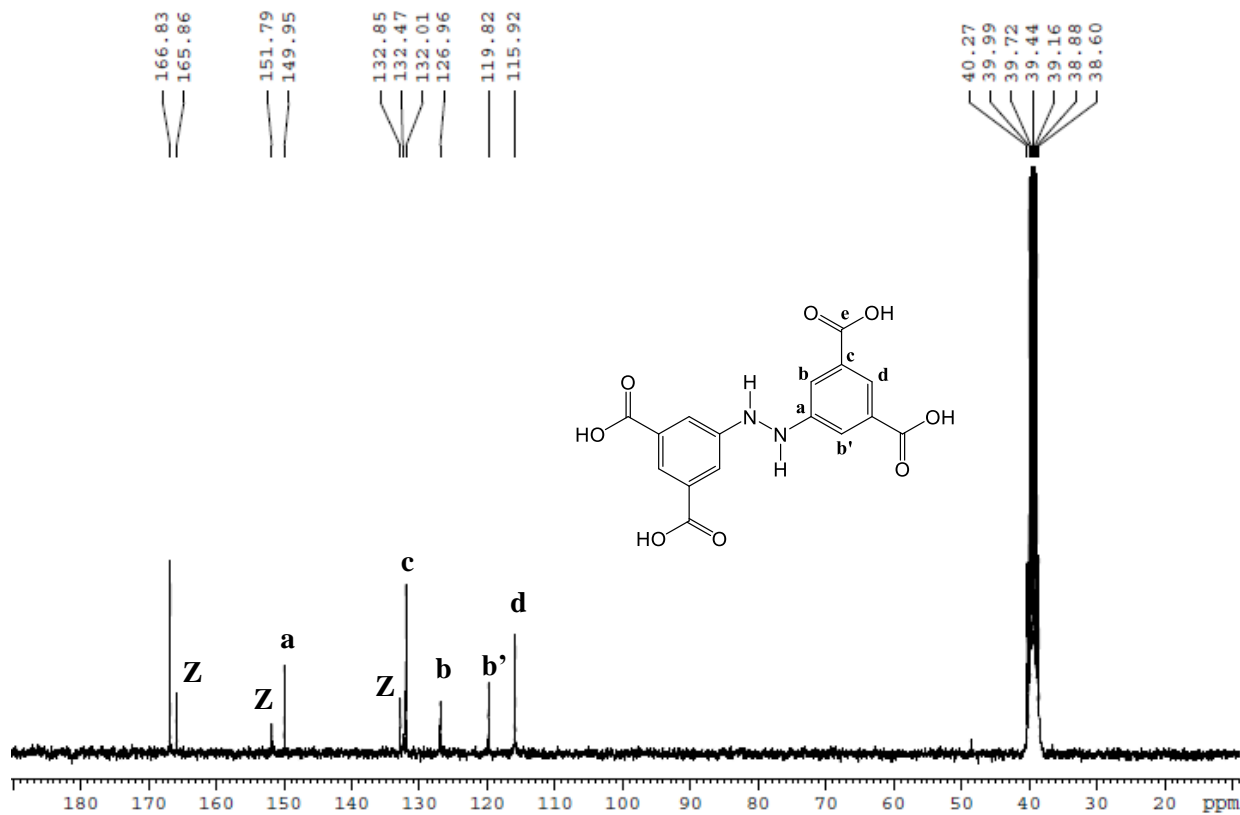


**Figure 25:**  $^{13}\text{C}$  NMR of **4** and **3** mixture (DMSO- $d_6$ , 75.47 MHz). Peak ‘Z’ is attributed to the presence of compound **3** due to incomplete over-reduction.

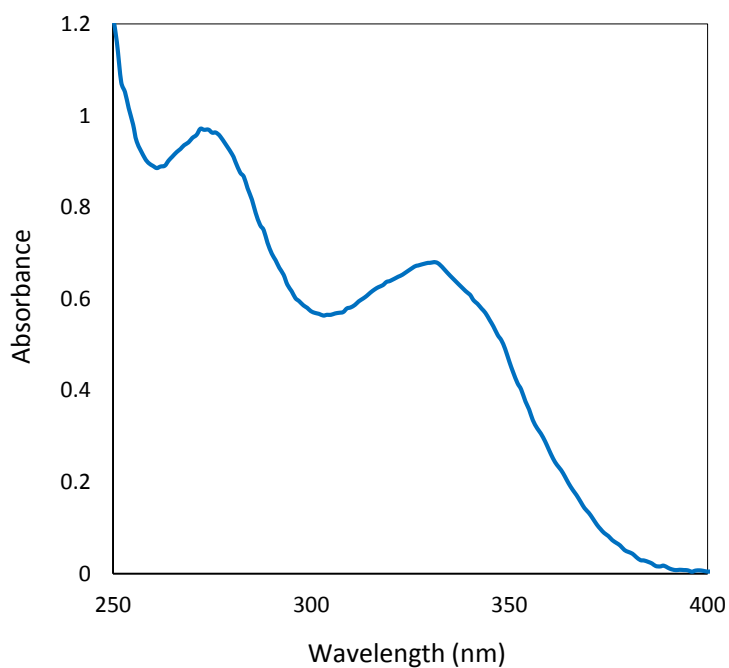


**Figure 26:** UV-Vis absorption spectra of compound **4** in ethanol (0.033 mg/mL).



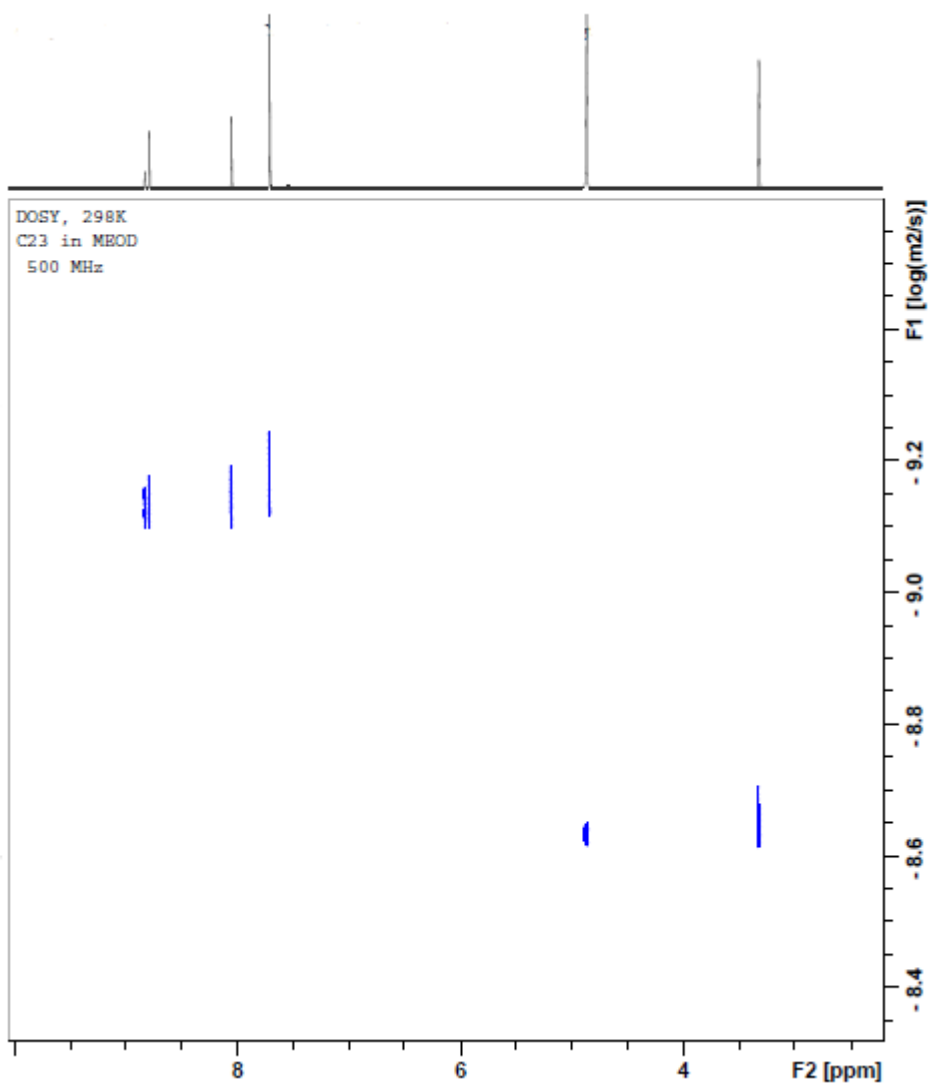


**Figure 27:** <sup>1</sup>H DOSY NMR of **4** and **3** mixture (MeOD-d<sub>4</sub>, 500 MHz).

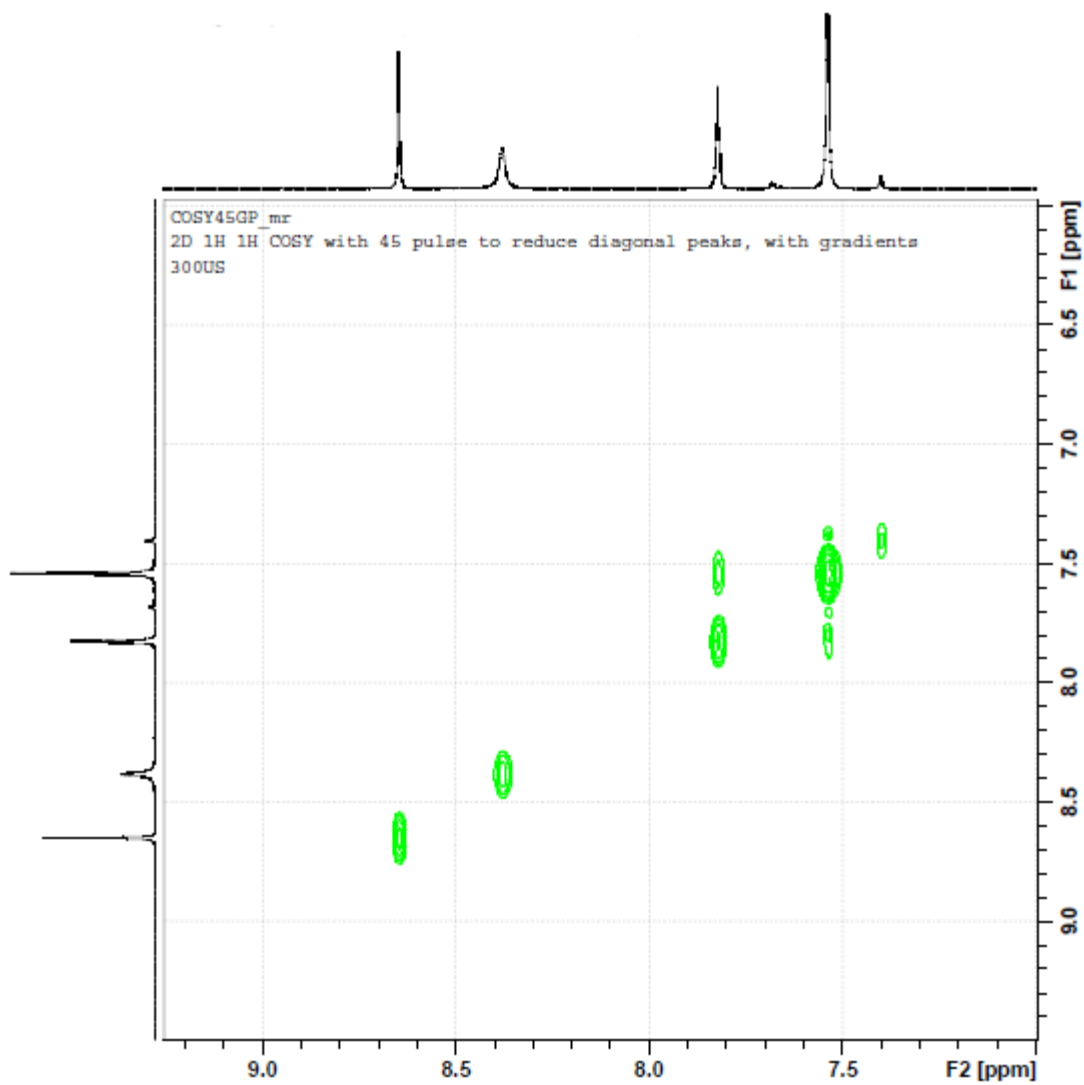


**Figure 28:** 2D  $^1\text{H}$ - $^1\text{H}$  COSY NMR of **4** and **3** mixture (DMSO- $d_6$ , 300 MHz).

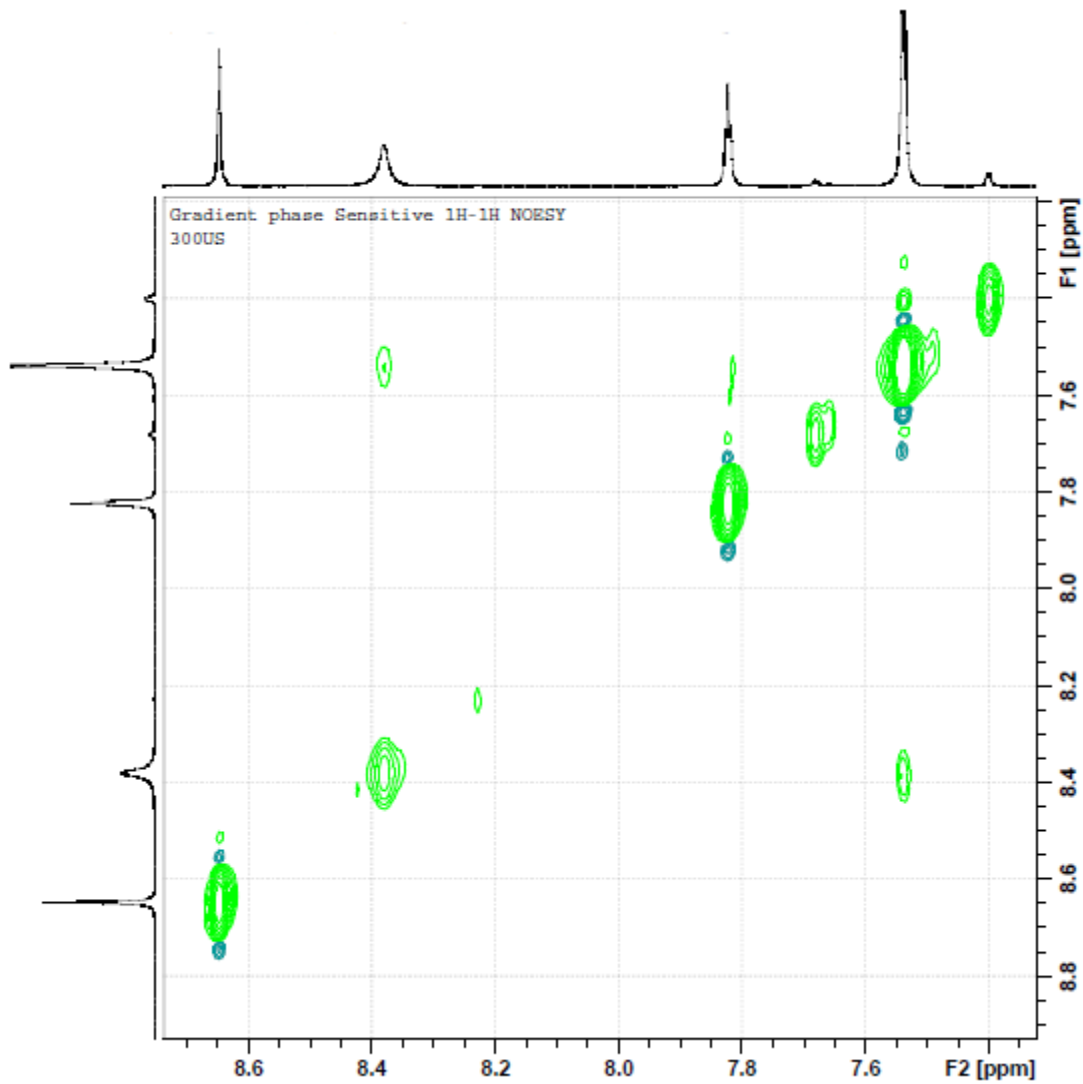


**Figure 29:**  $^1\text{H}$ - $^1\text{H}$  NOESY NMR of **4** and **3** mixture (DMSO- $d_6$ , 300 MHz).

N15 HSQC GPPH  
1D HSQC N15-H1, gradients, phase sensitive  
300US

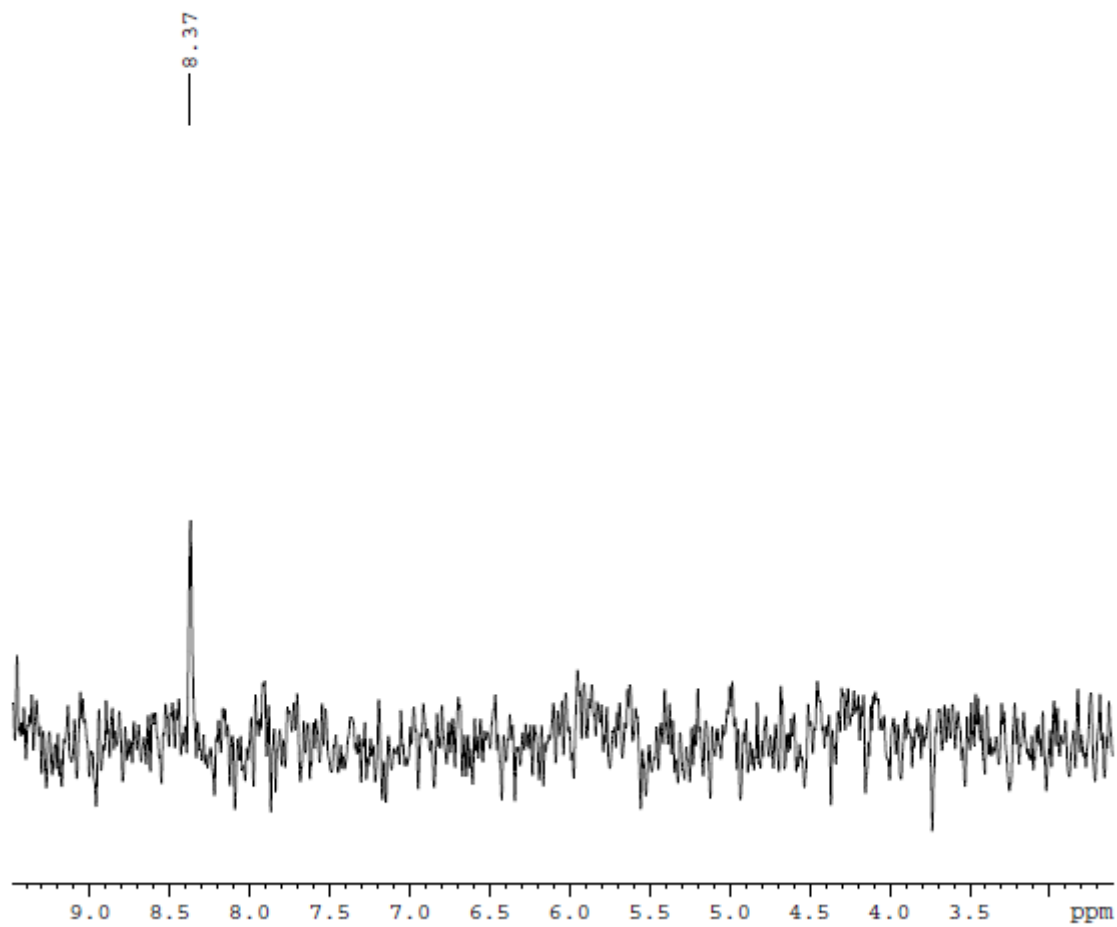
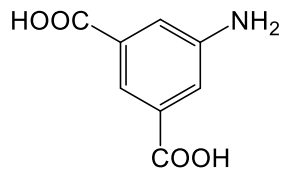


**Figure 30:** 1D  $^{15}\text{N}$ - $^1\text{H}$  HSQC NMR of **4** (DMSO- $d_6$ , 300 MHz).

### 5-Aminoisophthalic acid (5)



Obtained from Sigma-Aldrich, 186279 Aldrich. White to light brown powder; mp = 305 °C;  $^1\text{H}$  NMR (300 MHz, 25 °C, DMSO- $d_6$ , ppm):  $\delta$  = 7.65 (t, 1H), 7.37 (d, 2H), 5.65 (s, br, 2H);  $^{13}\text{C}$  NMR (75.47 MHz, 25 °C, DMSO- $d_6$ , ppm)  $\delta$  = 167.23, 149.16, 131.73, 118.08, 117.41.

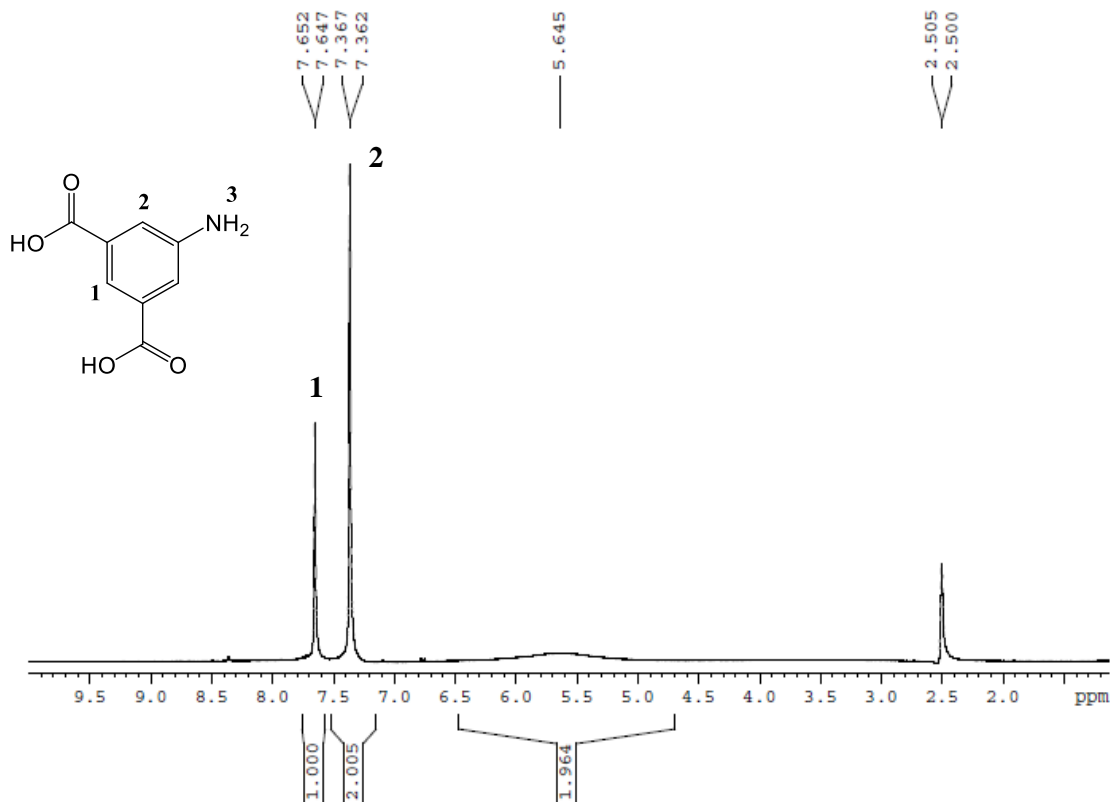


**Figure 31:**  $^1\text{H}$  NMR of commercial 5-aminoisophthalic acid (DMSO- $d_6$ , 300 MHz).

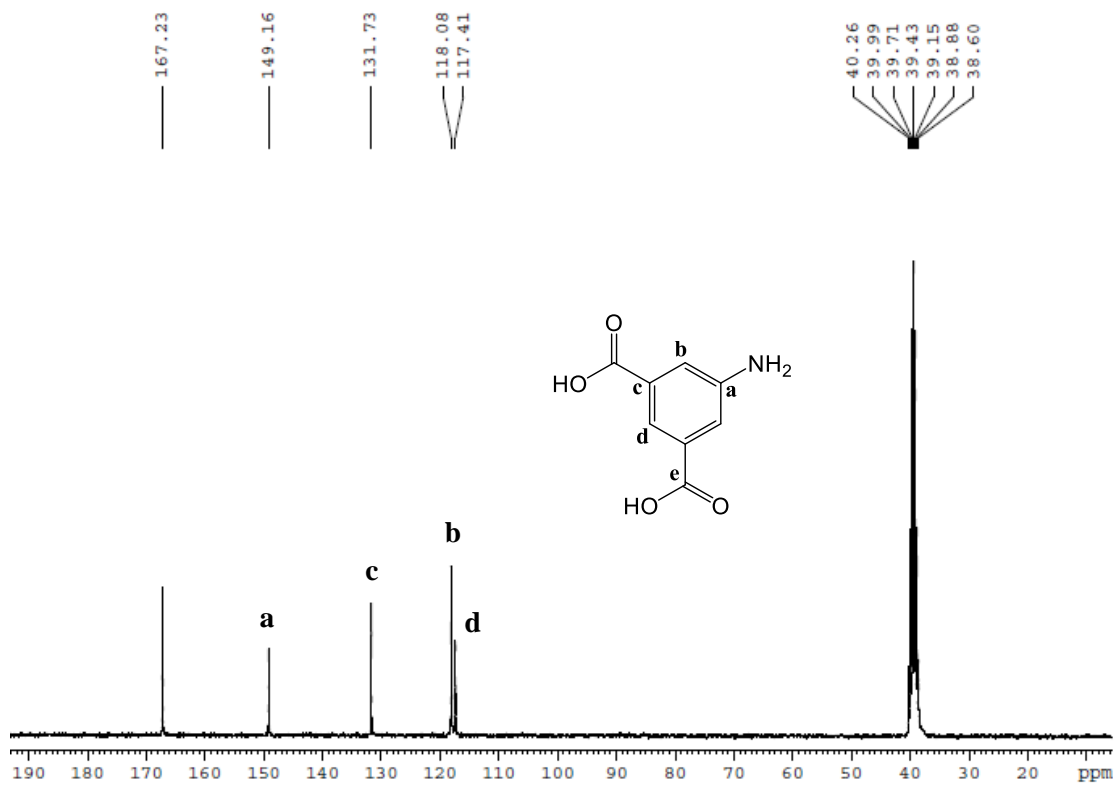


**Figure 32:**  $^{13}\text{C}$  NMR of commercial 5-aminoisophthalic acid ( $\text{DMSO-d}_6$ , 75.47 MHz).

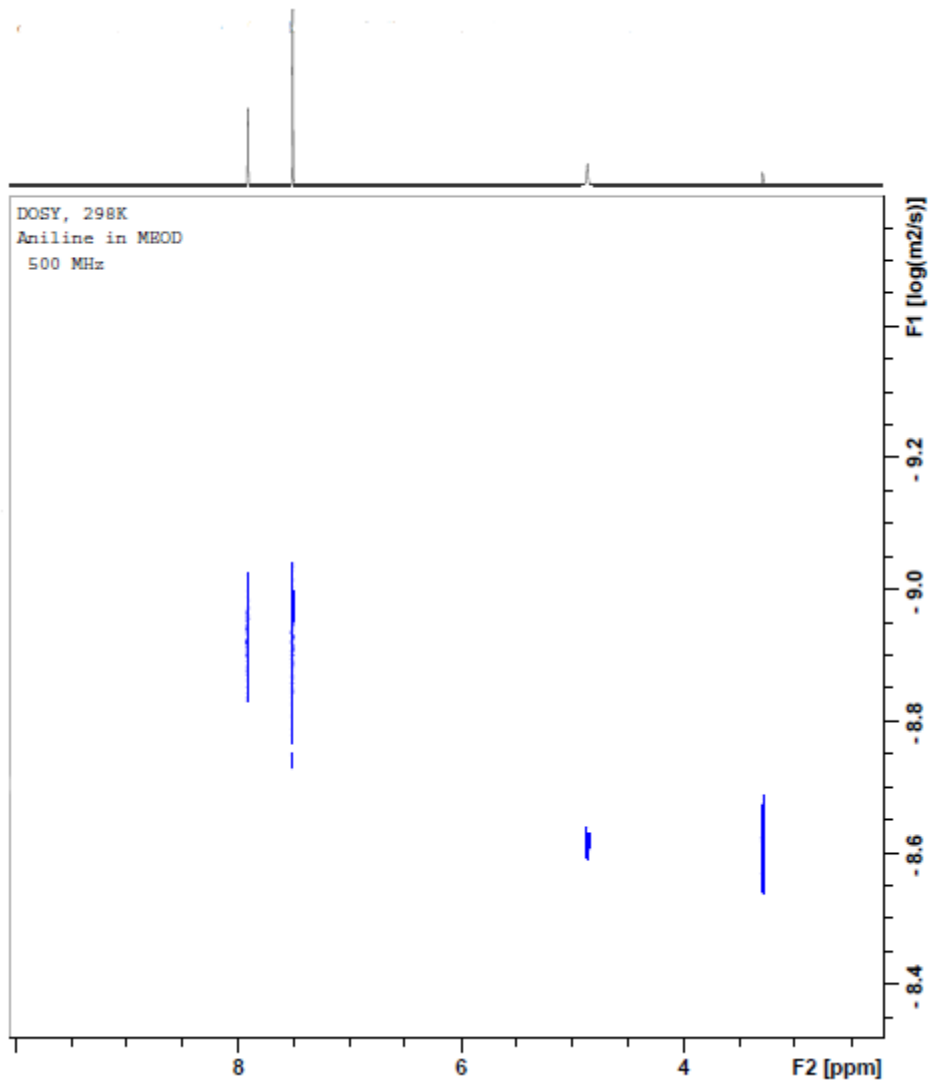
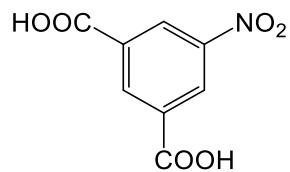


**Figure 33:** <sup>1</sup>H DOSY NMR of 5-aminoisophthalic acid (MeOD-d<sub>4</sub>, 500 MHz).

### 5-Nitroisophthalic acid (1)



Obtained from Sigma-Aldrich, N18005 Aldrich. White to faint yellow powder; mp = 260°C;  $^1\text{H}$  NMR (300 MHz, 25 °C, DMSO- $d_6$ , ppm):  $\delta$  = 8.75 (t, 1H), 8.73 (d, 2H).

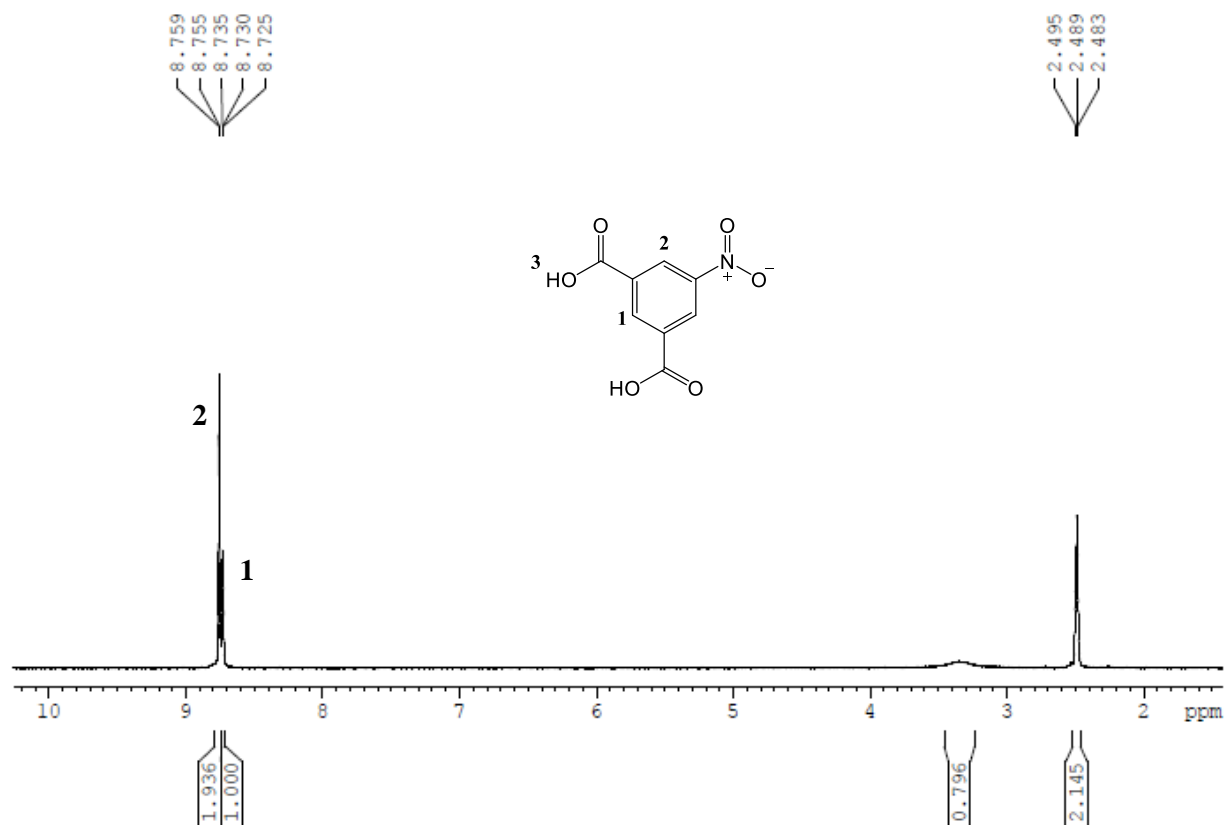


**Figure 34:**  $^1\text{H}$  NMR of commercial 5-nitroisophthalic acid (DMSO- $d_6$ , 300 MHz)



## REFERENCES

---

- <sup>1</sup> Hunger, Klaus. *Chemistry, properties, application* **2003**.
- <sup>2</sup> Zollinger, H. *Wiley* (New York) **1987**, 85.
- <sup>3</sup> Velasco, M. I. *Dyes and Pigments* **2011**, 90 (3), 259-264.
- <sup>4</sup> Freeman H.S.; Peters A.T. *Elsevier Science B.V* **2000**.
- <sup>5</sup> Gregory, P. *High-Technology Applications of Organic Colorants* **1991**, 175-205.
- <sup>6</sup> Merino, E.; María, R. *Beilstein journal of organic chemistry* **2012**, 8 (1) 1071-1090.
- <sup>7</sup> (a) Rau, H. *Photochromism, Molecules and Systems* (Amsterdam) **2003**, 1, 165–192. (b) Maruyama, K.; Kubo, Y.; Horspool, W. M.; Song, P. S. *CRC Handbook of Organic Photochemistry and Photobiology* **1995**, 222-228. (c) Henzl, J.; Mehlhorn, M.; Gawronski, H.; Rieder, K.-H.; Morgenstern, K. *Angew. Chem., Int. Ed.* **2006**, 45, 603–606. (d) Choi, B.-Y.; Kahng, S.-J.; Kim, S.; Kim, H.; Kim, H. W.; Song, Y. J.; Ihm, J.; Kuk, Y. *Phys. Rev. Lett.* **2006**, 96, 156106.
- <sup>8</sup> (a) Norikane, Y.; Tamaoki, N. *Org. Lett.* **2004**, 6, 2595-2598. (b) Iwamoto, M.; Majima, Y.; Naruse, H.; Noguchi, T.; Fuwa, H. *Nature* **1991**, 353, 645-647. (c) Zhang, C.; Du, M. H.; Cheng, H. P.; Zhang, X. G.; Roitberg, A. E.; Krause, J. L. *Phys. Rev. Lett.* **2004**, 92, 158301-158301.
- <sup>9</sup> Wang, S.; Wang, X.; Li, L.; Advincula, R. C. *J. Org. Chem.* **2004**, 69, 9073-9084.
- <sup>10</sup> Ikeda, T.; Tsutsumi, O. *Science* **1995**, 268, 1873.
- <sup>11</sup> Zhen, W.; Han, H.; Anguiano, M.; Lemere, C.; Cho, C. G.; Lansbury, P. T.; *J. Med. Chem.* **1999**, 42, 2805.
- <sup>12</sup> Haghbeen, K.; Tan, E. W. *J. Org. Chem.* **1998**, 63, 4503.
- <sup>13</sup> Ueno, K.; Akiyoshi, S. *J. Am. Chem. Soc.* **1954**, 76, 3670.
- <sup>14</sup> Davey, H. H.; Lee, R. D.; Marks, T. J. *J. Org. Chem.* **1999**, 64, 4976.
- <sup>15</sup> Entwistle, I. D.; Gilkerson, T.; Johnstone, R. A. W.; Telford, R. P. *Tetrahedron* **1978**, 34, 213.
- <sup>16</sup> Haworth, R. D.; Lapworth, A. *J. Chem. Soc.* **1921**, 119, 768.
- <sup>17</sup> Ibne-Rasa, K. M.; Lauro, C. G.; Edwards, J. O. *J. Am. Chem. Soc.* **1963**, 85, 1165.
- <sup>18</sup> Bleasdale, C.; Ellis, M. K.; Farmer, P. B.; Golding, B. T.; Handley, K. F.; Jones, P.; McFarlane, W. *Radiopharm.* **1993**, 33, 739.
- <sup>19</sup> Gowenlock B. G.; Richter-Addo, G. B. *Chem. Rev.* **2004**, 104, 3315.
- <sup>20</sup> Brill, E. *Experientia* **1969**, 25, 680.

- 
- <sup>21</sup> Maassen, J. A.; De Boer, J. *Recl. Trav. Chim. (Pays-Bas)* **1971**, *90*, 373.
- <sup>22</sup> Berry, D. J.; Collins, I.; Roberts, S. M.; Suschitzky, H.; Wakefield, B. J. *J. Chem. Soc.* **1969**, 1285.
- <sup>23</sup> Wawzonek, S. McIntyre, T. W. *J. Electrochem. Soc.* **1972**, *119*, 1350.
- <sup>24</sup> Hombrecher H. K.; Ludtke, K. *Tetrahedron* **1993**, *49*, 9489.
- <sup>25</sup> Fetizon, M.; Golfier, M.; Milcent, R.; Papadakis, I. *Tetrahedron* **1975**, *31*, 165.
- <sup>26</sup> Ortiz, B., Villanueva, P.; Walls, F. *J. Org. Chem.* **1972**, *37*, 2748.
- <sup>27</sup> Firouzabadi, H.; Vessal, B.; Naderi, M. *Tetrahedron Lett.* **1982**, *23*, 1847.
- <sup>28</sup> Firouzabadi H.; Mostafavipoor, Z. *Bull. Chem. Soc.* **1983**, *56*, 914.
- <sup>29</sup> Baer, E.; Tosoni, A. L. *J. Am. Chem. Soc.* **1956**, *78*, 2857.
- <sup>30</sup> Crank, G.; Makin, M. I. H.; *Aust. J. Chem.* **1984**, *37*, 845.
- <sup>31</sup> Noureldin, N. A.; Bellegarde, J. W. *Synthesis* **1999**, 939.
- <sup>32</sup> Nakagawa, K.; Tsuji, T. *Chem. Pharm. Bull.* **1963**, *11*, 296.
- <sup>33</sup> Orito, K.; Hatakeyama, T.; Takeo, M.; Uchiito, S.; Tokuda, M.; Suginome, H. *Tetrahedron* **1998**, *54*, 8403.
- <sup>34</sup> Farhadi, S.; Zaringhadam, P.; Sahamieh, R. Z. *Acta Chim. Slov.* **2007**, *54*, 647.
- <sup>35</sup> Grirrane, A; Corma, A; Garcia, H. *Science* **2008**, *322*, 1661-1664.
- <sup>36</sup> Nystrom R. F.; Brown, W. G. *J. Am. Chem. Soc.* **1948**, *70*, 3738.
- <sup>37</sup> Hutchins, R. O.; Lamson, D. W.; Rua, L.; Milewski, C.; Maryanoff, B. *J. Org. Chem.* **1971**, *36*, 803-806.
- <sup>38</sup> Alper, H.; Paik, H. N. *J. Organomet. Chem.* **1979**, *172*, 463-466.
- <sup>39</sup> Olah, G.; Pavlath, A.; Kuhn, I. *Acta Chim. Acad. Sci. Hung.* **1955**, *7*, 71-84.
- <sup>40</sup> Srinivasa, G. R.; Abiraj, K.; Gowda, D. C. *Tetrahedron Lett.* **2003**, *44*, 5835.
- <sup>41</sup> Busch, M.; Schulz, K. *Chem. Ber.* **1929**, *62*, 1458-1466.
- <sup>42</sup> De Groot, H.; Van den Heuvel, E.; Barendrecht, E.; Janssen, L. J. J. Ger. Pat. 3,020,846, 1980; *Chem. Abstr.* **1981**, *94*, 54.
- <sup>43</sup> Galbraith, H. W.; Degering, E. F.; Hitch, E. F. *J. Am. Chem. Soc.* **1951**, *73*, 1323-1324.
- <sup>44</sup> Pasha, M. A.; Jayashankara, V. P.; *Ultrason. Sonochem.* **2005**, *12*, 433.
- <sup>45</sup> (a) Hudlicky, M. *ACS (Washington)* **1996**, 96-100. (b) Rylander, P. N. *Academic Press (New York)* **1985**. (c) Davies, R. R.; Hodgson, H. H. *J. Chem. Soc.* **1943**, 281-282. (d) Owsley, D. C.; Bloomfield, J. *J. Synthesis* **1977**, 118-120. (e) Figueras, F.; Coq, B. *J. Mol. Catal.* **2001**, *173*, 223-

- 
230. (f) Khurana, J. M.; Ray, A. *Bull. Chem. Soc.* **1996**, *69*, 407–410. (g) Laskar, D. D.; Prajapati, D.; Sandhu J. S. *J. Chem. Soc.* **2000**, 67–69.
- <sup>46</sup> Haber, F. *Z. Elektrochem. Angew. Phys. Chem.* **1898**, *22*, 506.
- <sup>47</sup> (a) Lee, G. H.; Choi, E. B.; Lee, E.; Pak, C. S. *Tetrahedron Lett.* **1995**, *36*, 5607. (b) Lee, G. H.; Choi, E. B.; Lee, E.; Pak, C. S. *Tetrahedron Lett.* **1994**, *35*, 2195. (c) Lee, G. H.; Choi, E. B.; Lee, E.; Pak, C. S. *Tetrahedron Lett.* **1993**, *34*, 4541.
- <sup>48</sup> McNaught A. D.; Wilkinson, A. *Blackwell Scientific Publications* (Oxford) **1997**.
- <sup>49</sup> Heinicke, G. *Crystal Research and Technology* **1984**, *19* (11), 1424–1424.
- <sup>50</sup> Thorwirth, R.; Bernhardt, F.; Stolle, A.; Ondruschka, B.; Asghari, J. *Chem.–Eur. J.* **2010**, *16*, 13236–13242.
- <sup>51</sup> Wada, S.; Urano, M.; Suzuki, H.; *J. Org. Chem.* **2002**, *67*, 8254.
- <sup>52</sup> Menuel, S.; Léger, B.; Addad, A.; Monflier, E.; Hapiot, F. *Green Chemistry* **2016**, *18* (20), 5500–5509.
- <sup>53</sup> Schmidt, R.; Fuhrmann, S.; Wondraczek, L.; Stolle, A. *Powder Technol.* **2016**, *288*, 123–131.
- <sup>54</sup> Rightmire, N.R.; Hanusa, T.P. *Dalton Trans.* **2016**, *45*, 2352–2362.
- <sup>55</sup> Margetić, D.; Štrukil, V. *Mechanochemical Organic Synthesis* **2016**, 1–54.
- <sup>56</sup> Stolle, A. *Ball Milling Towards Green Synthesis* **2014**, 241–276.
- <sup>57</sup> Ge´rad, E. M. C.; Sahin, H.; Encinas, A.; Bra´sse, S. *Synlett* **2008**, 7202–7204.
- <sup>58</sup> Schneider, F.; Stolle, A.; Ondruschka, B.; Hopf, H. *Org. Process Res. Dev.* **2009**, *13*, 44–48.
- <sup>59</sup> Schneider, F.; Szuppa, T.; Stolle, A.; Ondruschka, B.; Hopf, H. *Green Chem.* **2009**, *11*, 1894–1899.
- <sup>60</sup> Szuppa, T.; Stolle, A.; Ondruschka, B.; Hopfe, W.; *ChemSusChem* **2010**, *3*, 1288–1294.
- <sup>61</sup> Szuppa, T.; Stolle, A.; Ondruschka, B.; Hopfe, W.; *ChemSusChem* **2010**, *3*, 1181–1191.
- <sup>62</sup> Sopicka-Lizer, M. C. *High-Energy Ball Milling* **2010**, 1–5.
- <sup>63</sup> Paudert, R.; H. Harenz, R. Po´thig, G. Heinicke, L. Du¨nkel and H. Schumann, *Chem. Techn.* **1978**, *30*, 470.
- <sup>64</sup> Breitung-Faes, S.; Kwade, A. *Powder Technol.* **2011**, *212*, 383–389.
- <sup>65</sup> Thorwirth, R.; Stolle, A.; Ondruschka, B. *Green Chem.* **2010**, *12*, 985–991.
- <sup>66</sup> Wang, G.-W.; Liu, L.; *Chin. Chem. Lett.* **2004**, *15*, 587–590.
- <sup>67</sup> Komatsu, K.; Wang, G.-W.; Murata, Y.; Tanaka, T.; Fujiwara, K. *J. Org. Chem.* **1998**, *63*, 9358–9366.

- 
- <sup>68</sup> Becker, M.; Kwade, A.; Schwedes, J. *Int. J. Miner. Process.* **2001**, *61*, 189–208.
- <sup>69</sup> Kwade, A.; *Int. J. Miner. Process.* **2004**, *74*, 93–101.
- <sup>70</sup> Kakuk, G.; Zsoldos, I.; Csanady, A.; Oldal, I. *Rev. Adv. Mater. Sci.* **2009**, *22*, 21–38.
- <sup>71</sup> Stolle, A.; Szuppa, T.; Leonhardt, S. E.; Ondruschka, B. *Chem. Soc. Rev.* **2011**, *40*, 2317–2329.
- <sup>72</sup> Fulmer, D. A.; Shearhouse, W. C.; Mendonza, S. T.; Mack, J. *Green Chem.* **2009**, *11*, 1821–1825.
- <sup>73</sup> Naimi-Jamal, M. R.; Mokhtari, J.; Dekamin, M. G.; Kaupp, G. *Eur. J. Org. Chem.* **2009**, 3567–3572.
- <sup>74</sup> Rosenkranz, S.; Breitung-Faes, S.; Kwade, A.; *Powder Technol.* **2011**, *212*, 224–230.
- <sup>75</sup> Shan, N.; Toda, F.; Jones, W.; *Chem. Commun.* **2002**, 2372–2373.
- <sup>76</sup> Fernandez-Bertran, J.; Reguera, E.; *Solid State Ionics* **1997**, *93*, 139–146.
- <sup>77</sup> Bowmaker, G. A.; Hanna, J. V.; Hart, R. D.; Skelton, B. W.; White, A. H. *Dalton Trans.* **2008**, 5290–5292.
- <sup>78</sup> Bowmaker, G. A.; Chaichit, N.; Pakawatchai, C.; Skelton, B. W.; White, A. H. *Dalton Trans.* **2008**, 2926–2928.
- <sup>79</sup> Qiu, W.; Hirotsu, T.; *Macromol. Chem. Phys.* **2005**, *206*, 2470–2482.
- <sup>80</sup> Hammond, R. B.; Pencheva, K.; Roberts, K. J.; Auffret, T. J. *Pharm. Sci.* **2007**, *96*, 1967–1973.
- <sup>81</sup> Trotzki, R.; Hoffmann, M. M.; Ondruschka, B. *Green Chemistry* **2008**, *10* (7), 767–72.
- <sup>82</sup> Burmeister, C. F.; Stolle, A.; Schmidt, R.; Jacob, K.; Breitung-Faes, S.; Kwade, A. *Chem. Eng. Technol.* **2014**, *37*, 857–864.
- <sup>83</sup> Rodriguez, B.; Bruckmann, A.; Bolm, C. *Chem.–Eur. J.* **2007**, *13*, 4710–4722.
- <sup>84</sup> Schneider, F.; Ondruschka, B. *ChemSusChem* **2008**, *1*, 622–625.
- <sup>85</sup> Klingensmith, L. M.; Leadbeater, N. E. *Tetrahedron Lett.* **2003**, *44*, 765–768.
- <sup>86</sup> El-Sayed, T.; Aboelnaga, A.; Hagar, M. *Molecules* **2016**, *21* (9), 1111.
- <sup>87</sup> Feng, D.; Wang, K.; Wei, Z.; Chen, Y.-P.; Simon, C. M.; Arvapally, R. K.; Martin, R. L.; Bosch, M.; Liu, T.-F.; Fordham, S.; Yuan, D.; Omary, M. A.; Haranczyk, M.; Smit, B.; Zhou, H.-C. *Nature Communications* **2015**, *6*, 6106.
- <sup>88</sup> Palui, G.; Banerjee, A. *The Journal of Physical Chemistry* **2008**, *112* (33), 10107–10115.
- <sup>89</sup> Jia, X.; Chao, D.; He, L.; Liu, H.; Zheng, T.; Zhang, C.; Wang, C. *Macromolecular Research* **2011**, *19* (11), 1127–1133.
- <sup>90</sup> Bigelow, H. E., Robinson, D. B., *Organic Syntheses* **1955**, *3*, 103.

- 
- <sup>91</sup> Westphal, E.; Bechtold, I. H.; Gallardo, H. *Macromolecules* **2010**, *43* (3), 1319–1328.
- <sup>92</sup> Miller, S. R. *Chemical Communications* **2013** *49* (71), 7773-7775.
- <sup>93</sup> Wang, X.-S.; Ma, S.; Rauch, K.; Simmons, J. M.; Yuan, D.; Wang, X.; Yildirim, T.; Cole, W. C.; López, J. J.; Meijere, A. D.; Zhou, H.-C. *Chemistry of Materials* **2008**, *20* (9), 3145–3152.
- <sup>94</sup> Zhang, L.; Qu, Z. R. *Acta Crystallographica Section E: Structure Reports Online* **2008** *64* (11) o2202.
- <sup>95</sup> Chuang, L.; Ilana, F.; Elving, P. J. *Analytical Chemistry* **1965**, *37* (12), 1528-1533.
- <sup>96</sup> Blackadder, D. A.; Hinshelwood, C. *J. Chem. Soc.*, **1957**, 2898.
- <sup>97</sup> Shinkai, S.; Nakaji, T.; Ogawa, T.; Shigematsu, K.; Manabe, O. *J. Am. Chem. Soc.*, **1981**, *103*, 111.
- <sup>98</sup> Badger, G. M.; Lewis, G. E. *J. Chem. Soc.*, **1953**, 2147.

## APPENDIX

Single crystal measurements were performed by Manar Shoshani (Ph.D. candidate in Dr. S. Johnson's research group, University of Windsor). The single crystal data agrees with the literature values reported below.<sup>94</sup>

### Crystal data

$C_{16}H_{10}N_2O_8 \cdot 2C_3H_7NO$	$Z = 1$
$M_r = 504.45$	$F(000) = 264$
Triclinic, $P1$	$D_x = 1.386 \text{ Mg m}^{-3}$
Hall symbol: $-P 1$	Mo $K\alpha$ radiation, $\lambda = 0.71073 \text{ \AA}$
$a = 6.2926 (13) \text{ \AA}$	Cell parameters from 1381 reflections
$b = 7.2114 (13) \text{ \AA}$	$\theta = 2.9\text{--}27.4^\circ$
$c = 13.653 (4) \text{ \AA}$	$\mu = 0.11 \text{ mm}^{-1}$
$\alpha = 80.94 (4)^\circ$	$T = 293 \text{ K}$
$\beta = 85.30 (4)^\circ$	Cuboid
$\gamma = 81.72 (3)^\circ$	$0.20 \times 0.20 \times 0.20 \text{ mm}$
$V = 604.3 (3) \text{ \AA}^3$	

### Data collection

Rigaku SCXmini diffractometer	2363 independent reflections
Radiation source: fine-focus sealed tube	1607 reflections with $I > 2\sigma(I)$
Graphite monochromator	$R_{\text{int}} = 0.029$
Detector resolution: $13.6612 \text{ pixels mm}^{-1}$	$\theta_{\text{max}} = 26.0^\circ$ , $\theta_{\text{min}} = 2.9^\circ$
$\omega$ scans	$h = -7 \rightarrow 7$
Absorption correction: multi-scan ( <i>CrystalClear</i> ; Rigaku, 2005)	$k = -8 \rightarrow 8$
$T_{\text{min}} = 0.971$ , $T_{\text{max}} = 0.979$	$l = -16 \rightarrow 16$
5593 measured reflections	

### Refinement

Refinement on $F^2$	Primary atom site location: structure-invariant direct methods
Least-squares matrix: full	Secondary atom site location: difference Fourier map
$R[F^2 > 2\sigma(F^2)] = 0.052$	Hydrogen site location: inferred from neighbouring sites
$wR(F^2) = 0.154$	H-atom parameters constrained
$S = 1.04$	$w = 1/[\sigma^2(F_o^2) + (0.0869P)^2 + 0.0094P]$ where $P = (F_o^2 + 2F_c^2)/3$
2363 reflections	$(\Delta/\sigma)_{\text{max}} < 0.001$
167 parameters	$\Delta\rho_{\text{max}} = 0.20 \text{ e \AA}^{-3}$

0 restraints

$$\Delta\rho_{\min} = -0.19 \text{ e } \text{\AA}^{-3}$$

**Fractional atomic coordinates and isotropic or equivalent isotropic displacement parameters ( $\text{\AA}^2$ )**

	x	y	z	$U_{\text{iso}}^*/U_{\text{eq}}$
C1	1.2504 (3)	0.1247 (3)	0.53879 (14)	0.0368 (5)
C2	1.1485 (3)	0.1486 (3)	0.63147 (14)	0.0388 (5)
H2	1.2213	0.1037	0.6889	0.047*
C3	0.9387 (3)	0.2393 (3)	0.63829 (14)	0.0362 (4)
C4	0.8321 (3)	0.3072 (3)	0.55177 (14)	0.0361 (5)
H4	0.6909	0.3664	0.5558	0.043*
C5	0.9357 (3)	0.2870 (2)	0.45901 (13)	0.0340 (4)
C6	1.1450 (3)	0.1962 (2)	0.45217 (14)	0.0360 (4)
H6	1.2144	0.1830	0.3903	0.043*
C7	0.8248 (3)	0.3644 (3)	0.36581 (14)	0.0393 (5)
C8	0.8253 (3)	0.2634 (3)	0.73691 (14)	0.0429 (5)
C9	0.5021 (5)	0.1873 (5)	0.1616 (2)	0.0951 (10)
H9A	0.6554	0.1852	0.1536	0.143*
H9B	0.4689	0.0633	0.1894	0.143*
H9C	0.4427	0.2763	0.2052	0.143*
C10	0.1791 (4)	0.2888 (5)	0.0659 (2)	0.0897 (10)
H10A	0.1367	0.3194	-0.0013	0.135*
H10B	0.1337	0.3953	0.1003	0.135*
H10C	0.1133	0.1817	0.0988	0.135*
C11	0.5328 (4)	0.2465 (4)	-0.01670 (17)	0.0583 (6)
H11	0.4662	0.2823	-0.0764	0.070*
N1	1.4637 (2)	0.0230 (2)	0.54104 (12)	0.0396 (4)
N2	0.4107 (3)	0.2433 (3)	0.06578 (13)	0.0560 (5)
O1	0.9368 (2)	0.1852 (3)	0.81263 (10)	0.0609 (5)
H1	0.8628	0.1957	0.8643	0.091*
O2	0.6425 (2)	0.3456 (2)	0.74637 (11)	0.0587 (5)
O3	0.6225 (2)	0.4372 (2)	0.38429 (11)	0.0559 (5)
H3	0.5702	0.4880	0.3321	0.084*
O4	0.9084 (2)	0.3631 (3)	0.28388 (11)	0.0658 (5)
O5	0.7304 (3)	0.2054 (3)	-0.02061 (11)	0.0725 (6)

**Atomic displacement parameters ( $\text{\AA}^2$ )**

	$U^{11}$	$U^{22}$	$U^{33}$	$U^{12}$	$U^{13}$	$U^{23}$
C1	0.0248 (10)	0.0368 (10)	0.0480 (12)	-0.0002 (7)	0.0004 (8)	-0.0085 (9)
C2	0.0308 (10)	0.0441 (11)	0.0393 (10)	0.0020 (8)	-0.0022 (8)	-0.0062 (9)
C3	0.0287 (10)	0.0376 (10)	0.0404 (11)	0.0008 (7)	0.0016 (8)	-0.0067 (8)

C4	0.0256 (10)	0.0376 (10)	0.0428 (11)	0.0035 (7)	0.0003 (8)	-0.0074 (8)
C5	0.0280 (10)	0.0340 (9)	0.0390 (10)	0.0004 (7)	0.0000 (7)	-0.0077 (8)
C6	0.0313 (10)	0.0375 (10)	0.0383 (10)	-0.0012 (8)	0.0023 (8)	-0.0083 (8)
C7	0.0334 (11)	0.0427 (11)	0.0401 (11)	0.0018 (8)	0.0006 (8)	-0.0084 (8)
C8	0.0368 (11)	0.0525 (12)	0.0356 (11)	0.0035 (9)	-0.0004 (8)	-0.0042 (9)
C9	0.097 (2)	0.142 (3)	0.0424 (15)	-0.011 (2)	-0.0023 (14)	-0.0094 (17)
C10	0.0544 (18)	0.110 (2)	0.093 (2)	0.0092 (15)	0.0136 (15)	-0.0082 (19)
C11	0.0547 (15)	0.0755 (16)	0.0417 (12)	0.0016 (12)	-0.0043 (10)	-0.0081 (11)
N1	0.0257 (9)	0.0437 (9)	0.0473 (9)	0.0046 (7)	0.0009 (7)	-0.0097 (8)
N2	0.0496 (12)	0.0716 (13)	0.0446 (10)	-0.0024 (9)	0.0042 (8)	-0.0110 (9)
O1	0.0468 (9)	0.0897 (12)	0.0349 (8)	0.0200 (8)	-0.0010 (7)	-0.0018 (8)
O2	0.0395 (9)	0.0859 (11)	0.0401 (8)	0.0211 (8)	0.0030 (6)	-0.0069 (8)
O3	0.0372 (9)	0.0786 (11)	0.0427 (8)	0.0188 (7)	-0.0053 (6)	-0.0032 (8)
O4	0.0494 (10)	0.1019 (13)	0.0383 (9)	0.0144 (8)	0.0017 (7)	-0.0113 (9)
O5	0.0458 (10)	0.1218 (16)	0.0445 (10)	0.0002 (9)	0.0043 (7)	-0.0103 (10)

### Geometric parameters (Å, °)

C1—C6	1.394 (3)	C8—O1	1.304 (2)
C1—C2	1.395 (3)	C9—N2	1.447 (3)
C1—N1	1.434 (2)	C9—H9A	0.9600
C2—C3	1.389 (2)	C9—H9B	0.9600
C2—H2	0.9300	C9—H9C	0.9600
C3—C4	1.392 (3)	C10—N2	1.447 (3)
C3—C8	1.494 (3)	C10—H10A	0.9600
C4—C5	1.395 (3)	C10—H10B	0.9600
C4—H4	0.9300	C10—H10C	0.9600
C5—C6	1.387 (2)	C11—O5	1.235 (3)
C5—C7	1.492 (3)	C11—N2	1.309 (3)
C6—H6	0.9300	C11—H11	0.9300
C7—O4	1.197 (2)	N1—N1 <sup>i</sup>	1.251 (3)
C7—O3	1.325 (2)	O1—H1	0.8200
C8—O2	1.222 (2)	O3—H3	0.8200
C6—C1—C2	120.34 (17)	O1—C8—C3	114.04 (17)
C6—C1—N1	124.35 (17)	N2—C9—H9A	109.5
C2—C1—N1	115.31 (17)	N2—C9—H9B	109.5
C3—C2—C1	120.22 (18)	H9A—C9—H9B	109.5
C3—C2—H2	119.9	N2—C9—H9C	109.5
C1—C2—H2	119.9	H9A—C9—H9C	109.5
C2—C3—C4	119.34 (17)	H9B—C9—H9C	109.5
C2—C3—C8	121.08 (18)	N2—C10—H10A	109.5
C4—C3—C8	119.57 (17)	N2—C10—H10B	109.5
C3—C4—C5	120.42 (17)	H10A—C10—H10B	109.5
C3—C4—H4	119.8	N2—C10—H10C	109.5



C5—C4—H4	119.8	H10A—C10—H10C	109.5
C6—C5—C4	120.25 (17)	H10B—C10—H10C	109.5
C6—C5—C7	118.99 (17)	O5—C11—N2	124.4 (2)
C4—C5—C7	120.75 (16)	O5—C11—H11	117.8
C5—C6—C1	119.40 (18)	N2—C11—H11	117.8
C5—C6—H6	120.3	N1 <sup>i</sup> —N1—C1	113.5 (2)
C1—C6—H6	120.3	C11—N2—C10	122.1 (2)
O4—C7—O3	123.70 (19)	C11—N2—C9	121.0 (2)
O4—C7—C5	124.31 (18)	C10—N2—C9	116.8 (2)
O3—C7—C5	111.99 (17)	C8—O1—H1	109.5
O2—C8—O1	122.62 (18)	C7—O3—H3	109.5
O2—C8—C3	123.32 (18)		

Symmetry code: (i)  $-x+3, -y, -z+1$ .

---

## VITA AUCTORIS

### Personal information

Name: Sarah Salloum

Nationality: Canadian

### Education

B.Sc., Honours Chemistry, 2015

University of Windsor, Canada

M.Sc., Chemistry, 2017

University of Windsor, Canada

### Professional work experience

Graduate Teaching Assistant  
Chemistry & Biochemistry Department  
University of Windsor, Canada  
2015-present

Teacher Assistant  
Department of Languages & Literature  
University of Windsor, Canada  
2012-2014

### Publications

Sarah Salloum, Jonathan Yu, Omar Zghal, and S. Holger Eichhorn\*

“Synthesis of Unusually Stable Gold Nanoparticles Protected by Large Dithiol Ligands”  
(manuscript to be submitted)

Sarah Salloum, S. Holger Eichhorn\*

“Type of Organic Solvent Defines Size of AuNPs Prepared by a One-Phase Flow-Chemistry”  
(manuscript to be submitted)

Sarah Salloum, S. Holger Eichhorn\*

“Green and Low Cost Mechanochemical Synthesis of Azobenzene Tetracarboxylic Acid”  
(manuscript to be submitted)